

UC San Diego

UC San Diego Electronic Theses and Dissertations

Title

Mechanisms underlying the cardioprotective effects of tetracyclines in myocardial ischemic injury

Permalink

<https://escholarship.org/uc/item/0qc7q2mf>

Author

Griffin, Michael O.

Publication Date

2007

Peer reviewed|Thesis/dissertation

UNIVERSITY OF CALIFORNIA, SAN DIEGO

Mechanisms Underlying the Cardioprotective Effects of Tetracyclines in
Myocardial Ischemic Injury

A dissertation submitted in partial satisfaction

of the requirements for the degree

Doctor of Philosophy

in

Biomedical Sciences

by

Michael O. Griffin

Committee in charge:

Professor Francisco Villarreal, Chair
Professor Wolfgang Dillmann, Co-chair
Professor Kirk Knowlton
Professor Lindsey Miles
Professor Robert Ross
Professor Geert Schmid-Shoenbein

2007

Copyright

Michael O. Griffin, 2007

All rights reserved.

This dissertation of Michael O. Griffin is approved, and it is acceptable in
quality and form for publication on microfilm:

Co-Chair

Chair

University of California, San Diego

2007

DEDICATION

Dedicated to my wife, Danielle, and daughter, Ava

TABLE OF CONTENTS

Signature Page	iii
Dedication.....	iv
Table of Contents	v
List of Abbreviations.....	vii
List of Figures and Tables	x
Acknowledgements	xiv
Curriculum Vitae.....	xvi
Abstract of the Dissertation	xviii
Chapter 1. General Introduction.....	1
1.1. Scope of the Problem	1
1.2. Introduction to the Tetracyclines	3
1.3. Matrix Metalloproteinase Inhibition	8
1.4. Reactive Oxygen Species Scavenging	16
1.5. Anti-Apoptotic Effects	20
1.6. Objectives of the Dissertation.....	24
Chapter 2. Modulation of Post-Infarction Left Ventricular Remodeling via MMP Inhibition by Doxycycline, and Evaluation of New ZBGs for Development into novel MMP inhibitors	27
2.1. Abstract	27
2.2. Introduction	28
2.3. Experimental Methods	31

2.4. Results	35
2.5. Discussion.....	36
2.6. Acknowledgements.....	41
Chapter 3. Reduction of Myocardial Infarct Size via Plasmin Inhibition by Doxycycline.....	46
3.1. Abstract	46
3.2. Introduction	47
3.3. Experimental Methods	49
3.4. Results	60
3.5. Discussion.....	70
3.6. Acknowledgements.....	81
Chapter 4. Reduction of myocardial infarct size and stunning by minocycline	103
4.1. Abstract	103
4.2. Introduction	104
4.3. Experimental methods.....	107
4.4. Results	116
4.5. Discussion.....	122
Chapter 5. Summary and Future Directions	140
References.....	145

LIST OF ABBREVIATIONS

AHA	aceto hydroxamic acid
AIF	apoptosis inducing factor
ARVM	adult rat ventricular myocyte
CABG	coronary artery bypass graft
CHD	coronary heart disease
CK	creatine kinase
CMT	chemically-modified tetracycline
COX-2	cyclooxygenase-2
DOX	doxycycline
ECM	extracellular matrix
EGF	epidermal growth factor
GNFI	global no-flow ischemia
H ₂ O ₂	hydrogen peroxide
HOCl	hypochloride
IL-1	interleukin-1
iNOS	inducible nitric oxide synthase
IPC	ischemic preconditioning
I/R	ischemia/reperfusion
K-H	Krebs-Henseleit
LAD	left anterior descending coronary artery
LV	left ventricle

MI	myocardial infarction
MIN	minocycline
MPI	matrix metalloproteinase inhibitor
MPO	myeloperoxidase
MPTP	mitochondrial permeability transition pore
MT-MMP	membrane-type matrix metalloproteinase
MTT	methylthiazoletetrazolium
NO	nitric oxide
NRVF	neonatal rat ventricular fibroblast
NRVM	neonatal rat ventricular myocyte
$O_2^{\bullet -}$	superoxide
OH^{\bullet}	hydroxyl radical
$ONOO^-$	peroxynitrite
PDGF	platelet-derived growth factor
RFU	relative fluorescence units
ROS	reactive oxygen species
SOD	superoxide dismutase
TEA	tranexamic acid
TET	tetracycline
TIMP	tissue inhibitor of matrix metalloproteinases
TNF	tumor necrosis factor
TnI	troponin I

tPA	tissue-type plasminogen activator
TTC	triphenyl tetrazolium chloride
uPA	urokinase-type plasminogen activator
VEGF	vascular endothelial growth factor
ZBG	zinc-binding group

LIST OF FIGURES AND TABLES

Figure 1-1: Chemical structures of doxycycline, minocycline, and tetracycline...	26
Figure 2-1: Global and MMP-2/9 activity observed in ischemic/infarcted LV tissue 1 hour after coronary occlusion in either untreated or DOX-treated sham and MI rats.....	42
Figure 2-2: Global and MMP-2/9 activity observed in ischemic/infarcted LV tissue 24 hours after coronary occlusion in either untreated or DOX-treated MI rats	43
Figure 2-3: Representative gelatin zymogram of myocardial MMP-2 and MMP-9 levels in control and DOX-treated infarcted hearts 1 hour post-MI	44
Figure 2-4: Heterocyclic zinc-binding groups (ZBGs) proposed for use in MMP inhibitors.....	44
Figure 2-5: IC ₅₀ values for ZBGs against plasmin-activated MMPs produced by NRVFs.....	45
Figure 3-1: Langendorff perfusion protocol.....	83
Figure 3-2: Reduction of myocardial infarct size with DOX pretreatment.....	84
Figure 3-3: Reduction of 92 kDa MMP-9 levels in the ischemic region with DOX pretreatment	85
Figure 3-4: Myocardial global MMP activity in control and DOX-treated infarcted hearts and control and DOX-treated sham hearts	86
Figure 3-5: Myocardial myeloperoxidase (MPO) activity in control and DOX- treated ischemic hearts and control and DOX-treated sham hearts	87

Figure 3-6: Standard curve for the nitrotyrosine ELISA.....	88
Figure 3-7: Reduction of plasmin levels in the ischemic region with DOX pretreatment	89
Table 3-1: Hemodynamic data at 4 weeks post-I/R.....	90
Table 3-2: Histomorphometric data at 4 weeks post-I/R.....	90
Figure 3-8: Effects of DOX co-treatment on MMP activity and cell detachment in cultures of NRVMs stimulated with 83 kDa active MMP-9 for 48 hr	91
Figure 3-9: Effects of MMP stimulation on MMP activity and cell detachment in cultures of NRVMs	92
Figure 3-10: Effects of plasminogen treatment on plasmin activity in cultures of NRVMs and NRVMs as assessed by hydrolysis of a peptide substrate	93
Figure 3-11: NRVM detachment and death following 48 hr of plasminogen stimulation	94
Figure 3-12: Effects of DOX co-treatment on plasmin activity and cell detachment in cultures of NRVMs	95
Figure 3-13: Effects of plasminogen treatment on MMP activity in culture as assessed by hydrolysis of a peptide substrate.....	96
Figure 3-14: In vitro inhibition of human plasmin by the tetracyclines in the presence of divalent metals.....	97
Figure 3-15: In vitro inhibitory effects of DOX on plasmin in the presence of Ca ²⁺	98
Figure 3-16: Effects of tranexamic acid on isolated, perfused rat hearts subjected to 25 min of global, no-flow ischemia and 80 min of reperfusion .	99

Figure 3-17: Effects of plasmin on isolated, perfused rat hearts subjected to 20 min of global, no-flow ischemia and 75 min of reperfusion	100
Figure 3-18: Effects of plasmin treatment on plasmin and MMP activities in isolated, perfused rat hearts subjected to 20 min of global, no-flow ischemia and 75 min of reperfusion	101
Figure 3-19: Effects of plasmin treatment on β_{1D} -integrin levels in isolated, perfused rat hearts subjected to 20 min of global, no-flow ischemia and 75 min of reperfusion.....	102
Figure 4-1: Effects of MIN treatment on isolated, perfused rat hearts subjected to 35 min of global, no-flow ischemia and 120 min of reperfusion ...	130
Figure 4-2: Effects of DOX treatment on isolated, perfused rat hearts subjected to 30 min of global, no-flow ischemia and 120 min of reperfusion ...	131
Figure 4-3: Effects of DOX and MIN on mitochondrial swelling under conditions associated with permeability transition pore opening in diluted rat liver mitochondria	132
Figure 4-4: Effects of MIN on the recovery of mechanical function and coronary flow rate after 25 min of global, no-flow ischemia.....	133
Figure 4-5: MMP activity in heart homogenates from control and MIN-treated hearts after 25 min of global, no-flow ischemia and 30 min of reperfusion as assessed by hydrolysis of a peptide substrate	134
Figure 4-6: Effects of MIN on troponin I release following 25 min of global, no-flow ischemia.....	134

Figure 4-7: Protein carbonyl content in the homogenates of control and MIN-treated hearts following 25 min of global, no-flow ischemia and 30 min of reperfusion	135
Figure 4-8: Nitrotyrosine content in the homogenates of control and MIN-treated hearts following 25 min of global, no-flow ischemia and 30 min of reperfusion	135
Figure 4-9: Effects of DOX and MIN on neonatal rat ventricular myocyte survival following 12 hr of hypoxia and 24 hr reoxygenation.....	136
Figure 4-10: Effects of DOX and MIN on neonatal rat ventricular myocyte survival following 4 hr of chemical hypoxia and 24 hr of recovery	137
Figure 4-11: Effects of DOX and MIN on neonatal rat ventricular myocyte survival following incubation in 100 μ M H ₂ O ₂ for 24 hr	137
Figure 4-12: Increase in CK release upon reoxygenation in adult rat ventricular myocytes previously made hypoxic	138
Figure 4-13: Effects of DOX and MIN on adult rat ventricular myocyte survival following 1 hr of hypoxia and 2 hr of reoxygenation	139

ACKNOWLEDGEMENTS

I would like to thank the many people that have made important impacts on my work. I would like to thank my mentor Dr. Francisco Villarreal for his commitment to and support of my research, education, and future goals and opportunities. Additional thanks go to committee members Dr. Wolfgang Dillmann, Dr. Kirk Knowlton, Dr. Lindsey Miles, Dr. Bob Ross, and Dr. Geert Schmid-Schoenbein for all of their guidance and advice. Thank you to “the labbies”: Dr. Ricardo Garcia, Shirley Reynolds, Dr. Juan Asbun, and Dr. Sara Epperson for their helpful comments, suggestions, and advice on my project. Thanks to Dr. Yinhong Chen and Miki Jinno for training me on animal surgeries and for all of their help with the animal studies. A big thanks to Diego Romero-Perez for his help with collecting data from the isolated hearts. Thanks to Dr. Darrell Belke for his guidance in setting up and troubleshooting the isolated heart system. Thanks to Dr. Jorge Suarez for his help in culturing adult cardiomyocytes and to Dr. John Hollander for his help with using the hypoxia chambers. Thanks to Dr. Jason Yuan for use of his fluorescence microscope and to Dr. Jeff Omens for use of his pressure transducers and equipment. Finally, thank you Danielle for all of your support and understanding throughout graduate school.

Chapter 2, in part, has been published as it appears in Villarreal FJ, Griffin M, Omens J, Dillmann W, Nguyen J, Covell J. *Circulation* 2003;108(12):1487-1492, Lippincott Williams & Wilkins, 2003 and in Puerta DT, Griffin MO, Lewis JA, Romero-Perez D, Garcia R, Villarreal FJ, Cohen SM. *Journal of Biological Inorganic Chemistry* 2006;11(2):131-138, Springer Berlin Heidelberg, 2006. The dissertation

author was a co-investigator and co-author of these manuscripts. The dissertation author was the primary investigator and author of the portions of these manuscripts presented within Chapter 2.

Chapter 3, in part, has been published as it appears in Griffin MO, Jinno M, Miles LA, Villarreal FJ. *Molecular and Cellular Biochemistry* 2005;270(1-2):1-11, Springer US, 2005. The dissertation author was the primary investigator and author of this manuscript.

CURRICULUM VITAE

Education:

- 2005-present University of Wisconsin-Madison
School of Medicine and Public Health
Medical Student
- 2001-2007 University of California, San Diego
Department of Biomedical Sciences
Ph.D. in Biomedical Sciences
Thesis advisor: Dr. Francisco Villarreal
- 1996-2000 University of Wisconsin-Madison
College of Letters and Science
B.S. in Molecular Biology with Honors in the Major
Thesis advisor: Dr. Matthew Wolff

Awards, Honors, & Fellowships:

- 2003-2005 Physiology NIH Predoctoral Fellowship
- 2003 World Congress on Inflammation Young Investigator Travel Award
- 2002 American Heart Association New Investigator Travel Award
- 1996-2000 The West Bend Clinic Health Professions Scholarship
- 1996-2000 Robert C. Byrd Honors Scholarship
- 1999 Trewartha Honors Undergraduate Research Grant
- 1999 Golden Key National Honor Society
- 1999 Phi Kappa Phi National Honor Society

Publications:

1. Hacker TA, **Griffin MO**, Guttormsen B, Stoker S, Wolff MR. Platelet-derived growth factor inhibitor STI571 (imatinib mesylate) inhibits human vascular smooth muscle proliferation and migration in vitro but not in vivo. *J Invasive Cardiol.* 2007 Jun;19(6):269-74.

2. Puerta DT, **Griffin MO**, Lewis JA, Romero-Perez D, García R, Villarreal FJ, Cohen SM. Heterocyclic zinc-binding groups for use in next-generation matrix metalloproteinase inhibitors: potency, toxicity, and reactivity. *J Biol Inorg Chem*. 2006 Mar;11(2):131-8.
3. **Griffin MO**, Jinno M, Miles LA, Villarreal FJ. Reduction of infarct size by doxycycline: a role for plasmin inhibition. *Mol Cell Biochem*. 2005 Feb;270(1-2):1-11.
4. Villarreal FJ, **Griffin M**, Omens J, Dillmann W, Nguyen J, Covell J. Early short-term treatment with doxycycline modulates postinfarction left ventricular remodeling. *Circulation*. 2003 Sep 23;108(12):1487-92.
5. Torrealba JR, Lozano E, **Griffin M**, Stoker S, McDonald K, Greaser M, Wolff MR. Maximal ATPase activity and calcium sensitivity of reconstituted myofilaments are unaltered by the fetal troponin T re-expressed in human heart failure. *J Mol Cell Cardiol*. 2002 Jul;34(7):797-805.

Abstracts and Poster Presentations:

1. **Griffin MO**, Villarreal FJ. Reduction of infarct size by doxycycline: a role for plasmin inhibition. *J Mol Cell Cardiol*. 2004 Apr;36(4):609-40. (abstract)
2. Puerta D, Lewis J, **Griffin M**, García R, Villarreal F, Cohen S. Synthesis and evaluation of new chelators for use as MMP inhibitors using cardiac cell cultures. *J Mol Cell Cardiol*. 2004 Apr;36(4):609-40. (abstract)
3. Villarreal F, **Griffin M**. "Protective effects of doxycycline against protease-mediated cardiac cell injury." 6th World Congress on Inflammation, Vancouver, Canada; August 2-6, 2003. (poster)
4. **Griffin M**, Villarreal F. "In vitro activation of matrix metalloproteinases and effects on cardiac myocyte viability." American Heart Association Scientific Conference on Advances in the Molecular and Cellular Mechanisms of Heart Failure, Snowbird, UT; August 21-25, 2002. (poster)

ABSTRACT OF THE DISSERTATION

Mechanisms Underlying the Cardioprotective Effects of Tetracyclines in Myocardial
Ischemic Injury

by

Michael O. Griffin

Doctor of Philosophy in Biomedical Sciences

University of California, San Diego, 2007

Professor Francisco Villarreal, Chair

Professor Wolfgang Dillmann, Co-Chair

The tetracycline class of antibiotics, which include the members doxycycline (DOX) and minocycline (MIN), have additional biological effects independent of their antimicrobial actions, of which inhibition of matrix metalloproteinases (MMPs) is the best characterized. Tetracyclines are also capable of scavenging reactive oxygen species (ROS) and inhibiting apoptosis and likely possess other undescribed important biological properties. These non-antimicrobial actions of the tetracyclines promote cell survival in several models of neuronal cell injury. These biochemical processes targeted by the tetracyclines are also important in the pathogenesis of myocardial ischemia-reperfusion (I/R) injury and adverse ventricular remodeling following myocardial infarction (MI). Therefore, I hypothesized that tetracyclines would elicit cytoprotective and anti-remodeling effects following myocardial ischemic injury. The work described here explores the capacity of DOX and MIN to improve myocardial survival, structure, and function following injury and examines their underlying mechanisms. First, it was shown that DOX inhibited adverse remodeling post-MI by inhibiting MMP activation. Second, DOX reduced infarct size following I/R injury *in vivo* by a mechanism independent of MMP inhibition. Using myocyte cell cultures it was found that DOX improved myocyte survival by inhibiting plasmin-mediated proteolysis of β_{1D} -integrin, thereby preserving myocyte-matrix interactions. Third, MIN, but not DOX, reduced infarct size in isolated, perfused rat hearts subjected to I/R, potentially due to its ability to inhibit opening of mitochondrial permeability transition pore. Fourth, MIN attenuated myocardial stunning and improved coronary artery flow in isolated, perfused rat hearts independent of MMP inhibition. MIN

treatment was associated with increased peroxynitrite generation, suggesting that MIN promoted the formation of peroxynitrite-derived nitric oxide donor compounds capable of promoting vasodilation. Taken together, these studies demonstrate that DOX and MIN target different biochemical processes involved in the pathogenesis of myocardial I/R injury and remodeling. The lipophilic nature of MIN allows it to have greater impact on intracellular processes, such as inhibiting MPTP opening and increasing peroxynitrite generation. The less lipophilic nature of DOX confines its actions to the extracellular environment, with plasmin and MMP inhibition among its major effects.

Chapter 1. General Introduction

1.1 Scope of the Problem

Ischemic heart disease, also termed coronary heart disease (CHD), has fallen by 50% in the United States since its peak in 1963 (1). This reduction is likely due to the combination of improved preventative measures, such as smoking cessation and management of hyperlipidemia and hypertension, and improved therapeutics, such as coronary care units, thrombolysis, angioplasty, stenting, beta-blockers, and ACE inhibitors. Despite these advances, CHD remains the single leading cause of death in the United States among both men and women across all ethnicities. In 2003, CHD caused 1 of every 5 deaths, amounting to 1 death every minute and in 2006 amounted to an estimated direct and indirect cost of \$142.5 billion (2).

The etiology of CHD is primarily atherosclerosis in the epicardial coronary arteries. It is now believed that the majority of the more severe acute coronary syndromes associated with CHD, including acute myocardial infarction (MI), are the result of a catastrophic rupture of an unstable, lipid-rich atherosclerotic plaque (3, 4). Subsequent thrombus formation at the site of plaque rupture blocks blood flow to the myocardium, leading to myocardial ischemia. If the ischemia persists, myocardial necrosis and apoptosis ensue, ultimately leading to irreversible cell death (5).

Current strategies for treating an acute MI involve restoring the balance between myocardial oxygen supply and demand. Standard treatments to reduce oxygen demand include bedrest, pain management, beta-blockers, and nitrates.

However, it is the timely restoration of blood supply by reperfusion strategies developed within the last few decades that has had a profound effect on reducing infarct size and long term outcomes including mortality (6). Thrombolytic drugs, such as streptokinase and recombinant tissue-type plasminogen activator (tPA), and mechanical revascularization and stenting have been shown to reduce infarct size and improve left ventricular (LV) function and survival (7). Early reperfusion of the compromised myocardium is essential, as the size of the ensuing infarct is directly related to the length of time between the onset of ischemia and reperfusion (i.e., “time is muscle”) (8). Although reperfusion clearly reduces infarct size and mortality, its benefit is limited by reperfusion injury (9). Reperfusion injury is defined as the death of additional myocytes after blood flow is restored and is distinct from and additional to the injury associated with the initial ischemic event. Reperfusion injury is an intensely studied but incompletely understood phenomenon that likely involves the generation of reactive oxygen species (ROS), intracellular calcium overload, activation of proteases, and numerous other factors which ultimately lead to the dysfunction and death of cells that were still viable at the time of restoration of blood flow (9).

In many patients who experience an MI, both the infarcted region and the remote myocardium are subjected to altered mechanical stresses that can promote adverse ventricular remodeling (10). Remodeling of the heart post-MI can result in infarct expansion, chamber dilatation, and compensatory hypertrophy and fibrosis of the non-infarcted myocardium. These changes can have profound effects on the

functional status of the heart and, thus, the patient's prognosis. The process of remodeling is influenced by infarct size, infarct healing, and ventricular wall stress and involves alterations in myocyte structural, contractile, and signaling proteins as well as alterations in the extracellular matrix (ECM). Clearly, the best way to address adverse remodeling is by reducing infarct size in the first place. However, for those patients who are at risk for post-MI remodeling, preserving or improving the mechanical properties of the heart is an appealing strategy for improving patient outcomes.

Thus, the management of reperfusion injury and the attenuation of adverse post-MI ventricular remodeling are currently two important goals. The identification and characterization of novel therapeutics to target these processes is an important step toward improving patient outcomes. This dissertation presents data demonstrating the potential utility of the tetracyclines in managing both myocardial reperfusion injury and remodeling.

1.2. Introduction to the Tetracyclines

1.2.1. Bacteriologic Uses

The tetracyclines are an aging family of broad-spectrum antibiotics. The parent compound, aureomycin, was first isolated from *Streptomyces aureofaciens* in 1947 (11). Soon after, other natural tetracyclines were isolated, including tetracycline (TET), for which the family of molecules is named. Since then, the modification of naturally-occurring tetracyclines and the total synthesis of novel compounds within

the tetracycline family have generated thousands of compounds. Two of the more common semi-synthetic tetracyclines used clinically as antibiotics are doxycycline (DOX) and minocycline (MIN). Due to its broad-spectrum antibiotic efficacy, DOX is indicated for the treatment of a variety of infections, including anthrax, Chlamydial infections, community-acquired pneumonia, Lyme disease, malaria, cholera, syphilis, *Yersinia pestis* (plague), periodontal infections, and others. MIN also displays broad-spectrum efficacy and is most often used clinically in the treatment of severe acne, but it is also indicated for many of the same infections as DOX.

The tetracyclines exert their antibiotic effect primarily by binding to the bacterial ribosome and halting protein synthesis (12). Bacterial ribosomes have a high-affinity binding site located on the 30S subunit and multiple low-affinity sites on both the 30S and 50S subunits (13). Upon binding the ribosome, the tetracyclines allosterically inhibit binding of the amino acyl-tRNA at the acceptor site (A-site). Following inhibition of the A-site, the peptidyltransferase site (P-site) lacks the tRNA-amino acid substrate needed for the amino acyl transfer reaction, and protein synthesis ceases (14).

The use of tetracyclines has declined in recent decades due to the emergence of resistant strains of bacteria. The primary mechanism of resistance is mediated by increased drug efflux out of the cell by a family of Tet proteins located on the cytoplasmic surface of the cell membrane (15). The Tet protein is encoded by a transposon and functions as an antiporter, extruding a tetracycline-magnesium complex, $[TC-Mg]^+$, in exchange for a proton (16). Expression of the Tet protein is

tightly regulated by the tetracycline repressor (TetR) (17). In the absence of tetracycline, the TetR binds to its operator site and inhibits the expression of the Tet protein. Upon binding $[\text{TC-Mg}]^+$, the TetR undergoes a conformational change and dissociates from its operator, thereby allowing expression of the Tet protein. While an understanding of the mechanisms of bacterial resistance to the tetracyclines is important clinically, it also has led to the development of the Tet regulatory system, an important transcriptional regulation tool that is used extensively for targeted gene regulation in eukaryotes (18).

1.2.2. Chemical Properties

While the complex chemistry of the tetracyclines is beyond the scope of this dissertation, a basic understanding of the important features of these compounds is necessary to appreciate their ability to interact with such a wide variety of biomolecules. TET, DOX, and MIN are all composed of a four ring core to which are attached various side groups (Figure 1-1). The dimethylamino group at the C4 carbon on the upper half of the molecule has been shown to be necessary for antimicrobial activity. 4-*dedimethylamino* tetracyclines, also called chemically modified tetracyclines (CMTs), lack antimicrobial activity *in vivo* presumably due to the inability of the molecule to adapt a zwitterionic form necessary for activity (19). However, CMTs do retain the ability to bind other nonmicrobial targets, such as matrix metalloproteinases (MMPs), facilitating their use in the treatment of other disease processes (20).

The oxygen-rich lower half of the molecule is critical for binding to both prokaryotic and eukaryotic targets, and interference with this region reduces or eliminates the effectiveness of the drug (21). One reason this region is important for binding is that it is an important site for metal ion chelation. It has been shown that binding of tetracyclines to proteins, including TetR, may be greatly enhanced when the tetracycline is complexed with divalent metal ions such as Ca^{2+} and Mg^{2+} (22). The binding of the tetracyclines to MMPs is thought to be mediated by the chelation of structural and catalytic Zn^{2+} ions within the enzyme (21, 23). In addition, binding to the bacterial ribosome involves binding to RNA-bound Mg^{2+} (24). The strength of tetracycline-metal interaction is dependent on both the tetracycline and the metal ion present. In general, the affinity of the tetracyclines for different divalent metals is, in order of decreasing affinity: $\text{Cu}^{2+} > \text{Co}^{2+} = \text{Fe}^{2+} > \text{Zn}^{2+} > \text{Mn}^{2+} > \text{Mg}^{2+} > \text{Ca}^{2+}$ (25). The relative affinities of different tetracyclines for a given metal also differ and are highly dependent on pH and the presence of other metal ions (26-28). It is believed that the relative superiority of DOX as an MMP inhibitor is due to its increased affinity for Zn^{2+} compared with TET or MIN (29).

Tetracyclines also show varying degrees of lipophilicity. In general, there is a direct relationship between lipophilicity and activity against Gram-positive bacteria. The lipophilicity of TET, DOX, and MIN, as determined by partitioning between octanol and aqueous buffer, has been determined to be 0.025, 0.600, and 1.1, respectively (30), and the minimum inhibitory concentration against *Staphylococcus aureus* is 0.21, 0.19, and 0.10 $\mu\text{g/ml}$, respectively (31). This difference in lipophilicity

also affects tissue distribution. MIN is able to cross the blood-brain barrier much more readily than DOX or TET. MIN attains levels in the brain nearly 3-fold higher than DOX, and TET is undetectable in the brain (32).

Interestingly, tetracyclines have also been shown to actively accumulate within certain tissues. One study found that cultured gingival fibroblasts accumulated MIN to a concentration >60-fold above the extracellular concentration within minutes despite a relatively low affinity of transport, with a K_m and V_{max} of 219 μM and 14.2 ng/min/ μg protein, respectively (33). DOX and TET were also found to accumulate, however much more slowly, with a V_{max} of 2.5 and 1.8 ng/min/ μg protein, respectively (33). A subsequent study found that the rate of transport of MIN, DOX, and TET into gingival fibroblasts increased following incubation with various growth factors and cytokines, including FGF-2, PDGF, TNF- α , IL-1 β , and phorbol myristate acetate (34). Recently, accumulation of tetracyclines into cultured quiescent neutrophils was also demonstrated (35). MIN, DOX, and TET accumulated to levels 64, 7.5, and 1.8-fold above the extracellular concentration, respectively (35). Thus, these studies suggest that tetracyclines may actively accumulate in tissues at sites of inflammation, thereby enhancing both the antimicrobial and non-antimicrobial actions of these drugs at these sites and also serving as reservoirs for drug release.

TET has also been found to accumulate within myocardial infarcts, and this property was exploited in the 1960s and 1970s by utilizing technetium-labeled TET ($^{99\text{m}}\text{Tc}$ -TET) for localizing and sizing MIs radiologically. $^{99\text{m}}\text{Tc}$ -TET achieved levels 5- to 8-fold higher within the infarct region compared with the uninfarcted

region in dogs subjected to permanent coronary occlusion for 24 hours (36). Using an organ culture of intact beating mouse hearts, it was shown that ^{99m}Tc-TET accumulated in irreversibly injured hearts but not reversibly injured hearts (37). Taken together, these studies suggest that TET accumulates in infarcted myocardium but only following disruption of the cell membrane and the onset of irreversible injury. The mechanism for accumulation is uncertain but may involve chelation of intracellular calcium and calcium-binding proteins. Whether the more lipophilic DOX and MIN also concentrate at sites of infarction has not been reported.

1.3 Matrix Metalloproteinase Inhibition

As already alluded to, the tetracyclines have been shown to have effects on numerous biological processes by mechanisms independent of their antimicrobial properties. Probably the best characterized non-antimicrobial property of the tetracyclines is their ability to inhibit members of the MMP family of endopeptidases.

1.3.1. Introduction to the Matrix Metalloproteinases

The MMPs are a family of zinc-dependent extracellular proteases that are involved in many physiological and pathophysiological processes including embryogenesis, tissue remodeling, inflammation, and tumor invasion (38). MMPs can be subdivided based on crude substrate specificities into the collagenases, gelatinases, stromelysins, and membrane-type MMPs (MT-MMPs) (39). The collagenase group includes MMP-1 (interstitial collagenase), MMP-8 (neutrophil collagenase), and MMP-13 (collagenase-3), all of which possess the ability to cleave fibrillar collagens

(types I, II, and III). The collagenases cleave the triple-helical fibrillar collagens at a recognition site located $\frac{3}{4}$ of the length of the molecule from the N-terminus, producing $\frac{3}{4}$ and $\frac{1}{4}$ fragments. These triple-helical fragments subsequently denature into single α -chains, termed gelatins. The gelatinases, which include MMP-2 (gelatinase A) and MMP-9 (gelatinase B), proteolyze the gelatins into smaller fragments. The gelatinases also degrade basement membrane collagen (type IV) directly. The stromelysin group includes MMP-3 (stromelysin-1), MMP-7 (matrilysin), MMP-10 (stromelysin-2), and MMP-11 (stromelysin-3). The stromelysins have a broad substrate specificity and are capable of degrading many ECM components, including proteoglycans, laminin, fibronectin, collagen type IV, and others. The MT-MMPs include 6 different MMPs, of which MMP-14 (MT1-MMP) is the best characterized, that contain either a transmembrane domain or GPI anchor that localizes them to the cell membrane. They are capable of activating other MMPs in addition to proteolyzing several ECM components (40). It is important to note that these categories are based on crude substrate specificities, and it is becoming increasingly apparent that there is considerable overlap in substrate specificity between different MMPs. This has made the investigation of specific MMP activities in the physiological mix of MMPs present both *in vivo* and in cell culture quite difficult, in part due to the inability to generate substrate probes with adequate specificity for a single MMP.

MMP activity is tightly controlled at the level of transcription, activation of the latent enzyme, and by endogenous MMP inhibitors. MMP transcription is modulated

by a range of cytokines, pro-inflammatory mediators, growth factors, and hormones, such as IL-1, IL-6, TNF- α , EGF, PDGF, TGF- β , IFN- γ , and bFGF (41, 42). The effect of these factors on MMP transcription, either induction or inhibition, appears to be cell type specific and also differs depending upon the MMP. MMPs are secreted as inactive zymogens (pro-MMPs), and they generally contain an autoinhibitory pro-domain, a catalytic zinc-binding domain, and a substrate-binding hemopexin domain (38). They also contain additional structural zinc and calcium ions distinct from the active site which serve to stabilize tertiary structure. Coordination of the active site zinc by a cysteine moiety in the pro-domain blocks access of substrates to the active site cleft (43). Activation of the latent enzyme can occur by proteolytic removal of the pro-domain by other proteases, such as the serine protease plasmin (38). Proteolytic activation may also be mediated by MT-MMPs and trypsin (38, 43). Non-proteolytic activation can also occur by sulfhydryl-group oxidation of the pro-domain cysteine moiety under conditions of oxidative stress (43). Upon release of the catalytic zinc by the pro-domain, the active site is unmasked, followed by autocleavage of the pro-peptide and generation of a fully active MMP (43).

It is interesting that, while serine proteases such as plasmin and trypsin can activate MMPs, MMP activity can also lead to increased serine protease activity. MMPs are able to proteolytically inactivate serine protease inhibitors, such as α_1 -antitrypsin and α_1 -antichymotrypsin, thereby disinhibiting the active serine proteases (44, 45). Thus, there may exist a positive feedback loop in which serine proteases activate MMPs and MMPs further increase serine protease activity.

The MMPs are inhibited endogenously by the tissue inhibitors of MMPs (TIMPs) and by nonspecific serum proteinase inhibitors such as α_2 -macroglobulin (46). The TIMPs, which include TIMPs-1, -2, -3, and -4, act by non-covalently binding MMPs with 1:1 stoichiometry. In general, the TIMPs can inhibit all MMPs except MT1-MMP. An interesting exception is that binding of TIMP-2 to MT1-MMP may actually facilitate MMP-2 activation (38).

1.3.2 Mechanisms of Matrix Metalloproteinase Inhibition by Tetracyclines

Inhibition of MMPs has been shown to be beneficial in many pathological conditions in which MMP-mediated proteolysis of the extracellular matrix (ECM) contributes to the pathogenesis, such as heart remodeling, tumor invasion, and inflammation (38, 47). MMP inhibitor development was, for a considerable period of time, an intense area of investigation (48). Since the initiation of MMP inhibitor development in the 1980s, numerous synthetic compounds with potent and specific *in vitro* MMP inhibitory activities have been developed, and many have entered clinical trials, including Marimastat (British Biotech), Prinomastat (Agouron), Rebimastat (Bristol-Myers Squibb), Tanomastat (Bayer), MMI-270 (Novartis), RS-130830 (Hoffman-La Roche), and others (48). However, due to lack of efficacy and serious musculoskeletal side effects, none of these MMP inhibitors have been developed past phase III clinical trials.

Currently, the only clinically available MMP inhibitor is doxycycline, which is marketed as Periostat (CollaGenex Pharmaceuticals), and it is indicated only for the treatment of periodontitis (48). Following the seminal experiment by Golub et al.

showing that MIN inhibited collagenase derived from rat gingiva (49), the tetracyclines became increasingly studied for their ability to inhibit MMPs.

The mechanism by which tetracyclines inhibit MMPs has not been completely elucidated. It is believed that they exert their anti-proteolytic effects by both direct inhibition of MMPs and by inhibiting MMP expression. The direct inhibition of MMPs appears to be mediated by an interaction between the tetracycline molecule and the metal ions within the MMP. MMP inhibition can be reversed by the addition of millimolar amounts of Ca^{2+} (49) or micromolar amounts of Zn^{2+} (50). In addition, CMT-5, a pyrazole derivative of tetracycline with reduced affinity for Ca^{2+} and Zn^{2+} due to removal of the carbonyl oxygen at C11 and hydroxyl group at C12, does not effectively inhibit MMP activity (21). Interestingly, it appears that the mechanism of inhibition is dependent on chelation of the structural metals rather than chelation of the active site Zn^{2+} . The catalytic domain of recombinant MMP-8 was shown to be less sensitive to inhibition by DOX than the full-length MMP-8 (51), suggesting regions of the MMP other than the catalytic site are important for inhibition by tetracyclines. In addition, it was recently shown by deuterium exchange mass spectrometry that DOX binds to MMP-7 near the structural Zn^{2+} and Ca^{2+} ions and does not bind to the catalytic Zn^{2+} (52).

The effectiveness of tetracycline inhibition against various MMPs depends on the tetracycline species, MMP species, and the pH. It has been shown that DOX is more potent than MIN or TET against collagenases purified from rabbit corneas, with IC_{50} values of 15 μM , 190 μM , and 350 μM , respectively, and this trend may be

explained by the relatively high affinity of DOX and low affinity of TET for Zn^{2+} (29). The IC_{50} values for DOX against the collagenases MMP-8, MMP-13, and MMP-1 is 1-10 μM , 5-30 μM , and $>200 \mu M$, respectively (53-55); the reasons for the differences in inhibition of the various MMPs are not clear. The pH of the system also affects inhibition as evidenced by the ability of DOX to inhibit MMP-8 at $pH > 7.1$ and inability to inhibit at $pH < 7.1$ (56).

In addition to inhibiting MMPs directly, tetracyclines also inhibit MMP activity by inhibiting MMP synthesis. DOX inhibited TNF- α -induced MMP-8 RNA and protein accumulation in cultured rat synovial fibroblasts (57). In addition, in cultured human skin fibroblasts, TET inhibited IL-1 β -induced MMP-3 expression (58). By using an MMP-3 promoter coupled to a CAT reporter construct, these authors demonstrated that the inhibition was at the level of MMP-3 transcription and had an IC_{50} of 1 μM . The mechanisms by which the tetracyclines inhibit MMP expression are not entirely understood. Since MMP transcription is induced by a host of pro-inflammatory cytokines and other growth factors, including IL-1, IL-6, TNF- α , PDGF, EGF, VEGF, and others (59), it is likely that these upstream signaling cascades leading to MMP expression are important targets of tetracyclines.

An interesting consequence of MMP inhibition is the indirect inhibition of serine proteases. As previously mentioned, MMPs can inactivate serine protease inhibitors (44, 45). Accordingly, MMP inhibition with DOX or CMTs has been shown to preserve serine protease inhibitors, thereby inhibiting serine proteases activity (60-64).

1.3.3 Matrix Metalloproteinase Inhibition in Myocardial Infarction and Ischemia/Reperfusion Injury

MMP activity is upregulated early following an MI, suggesting an important role in mediating the acute healing and remodeling processes of the heart, including inflammation, angiogenesis, and scar formation and remodeling. However, early MMP activity may be a double-edged sword, leading also to early damage of the cardiac ECM. It has been shown that MMP activity increases within minutes of ischemia, reflecting activation of pre-formed latent MMPs within the myocardium (65-67). The simultaneous appearance of type I collagen fragments in serum indicates that this early MMP activity contributes to significant collagen proteolysis (68). This early damage may set the stage for long term adverse remodeling. The role of MMP activity during these early time periods have been addressed primarily using genetically engineered mice. These studies have demonstrated that reduced MMP activity attenuates adverse remodeling post-MI but also inhibits healing of the infarct. Thus, controversy exists in the literature about whether early MMP inhibition exerts a beneficial or detrimental effect on long term cardiac structure and function.

Using a genetic approach, Heymans et al. showed that MMP-9-deficient mice but not MMP-3- or MMP-12-deficient mice showed reduced LV rupture post-MI as did TIMP-1-overexpressing mice (69). This suggests that MMP-9 and possibly other MMPs play a role in compromising the early structural integrity of the heart. However, MMP-9-deficient mice also displayed impaired wound healing, with reduced leukocyte infiltration into the infarct region and larger residual necrotic areas

(69). In a similar study, Ducharme et al. showed that MMP-9-deficient mice had reduced LV dilation post-MI but also reduced macrophage infiltration into the infarct region and reduced collagen content within the developing scar (70). MMP-2-deficient mice also showed reduced LV dilation and incidence of cardiac rupture post-MI but also inhibited phagocytic removal of necrotic debris from the infarct (71, 72).

In addition to their role in mediating post-MI healing and remodeling, there is emerging evidence that the MMPs may actually contribute to myocyte death and dysfunction following ischemia/reperfusion (I/R) injury. MMP-2 activity is increased in isolated, perfused rat hearts following I/R, and treatment with an MMP-2 neutralizing antibody or with DOX attenuated the increase in MMP-2 activity upon reperfusion and improved the recovery of contractile function (73). In follow-up studies this group showed that MMP-2 activation following I/R resulted in proteolysis of troponin I and myosin light chain, and that inhibition of MMP-2 activity with DOX prevented their proteolysis (74, 75). In an *in vivo* mouse model, Romanic et al. showed that MMP-9-deficient mice subjected to I/R had reduced infarct sizes and reduced neutrophil infiltration into the infarct region compared with wild-type controls (76). These studies suggest that MMPs may contribute to I/R injury, but the mechanisms underlying the injury are not entirely clear. It is also possible that MMP-mediated disruption of the normal myocyte-matrix architecture leads to myocyte cell death, since disruption of normal cell-ECM interactions has been shown to contribute to the induction of myocyte apoptosis both *in vitro* (77) and *in vivo* (78).

These previous studies demonstrate that inhibition of MMP activity holds promise for salvaging myocytes and preserving cardiac structure and function post-MI. However, for pharmacologic MMP inhibition to be beneficial, the timing of MMP inhibition will likely be important. For example, early short-term MMP inhibition post-MI (<48 hours) may block the early damage to the ECM while still allowing later events (>48 hours), such as inflammation and wound healing, to proceed normally. However, it remains to be determined whether the potentially beneficial and detrimental effects of MMP inhibition can be separated by the appropriate timing of pharmacologic MMP inhibition.

1.4 Reactive Oxygen Species Scavenging

1.4.1 Mechanisms of Reactive Oxygen Species Scavenging by Tetracyclines

Another well-characterized non-antimicrobial property of the tetracyclines is their ability to scavenge reactive oxygen species (ROS). ROS are produced under many pathological conditions, including myocardial I/R injury and inflammatory processes, and can lead to the oxidative destruction or dysfunction of many cellular constituents. ROS are highly reactive and include the free radicals superoxide ($O_2^{\bullet-}$) and hydroxyl radical (OH^{\bullet}) and the non-free radicals hydrogen peroxide (H_2O_2) and hypochloride ($HOCl$) (9). Superoxide ($O_2^{\bullet-}$) can be formed by several cellular processes, including the xanthine oxidase-catalyzed reduction of molecular oxygen (O_2), NADPH oxidase during the oxidative burst in activated neutrophils, and as byproducts of lipoxygenase/cyclooxygenase and mitochondrial electron transport (79,

80). $O_2^{\cdot -}$ can be converted to H_2O_2 by superoxide dismutase (SOD). H_2O_2 can then suffer one of three fates: 1) react with Fe^{2+} to form $OH^{\cdot} + OH^-$ via the Fenton reaction, 2) react with another molecule of $O_2^{\cdot -}$ to form $H_2O + OH^{\cdot} + OH^-$ via the Haber-Weiss reaction, or 3) be detoxified to $H_2O + O_2$ by catalase or glutathione peroxidase. In the neutrophil, myeloperoxidase (MPO) generates HOCl from the reaction H_2O_2 with Cl^- . $O_2^{\cdot -}$ can also react with nitric oxide (NO) to form the reactive nitrogen species peroxynitrite ($ONOO^-$) (9, 81).

Regardless of the source or ROS species, ROS can cause cellular injury when they overwhelm cellular antioxidant systems, such as SOD, catalase, glutathione peroxidase, and antioxidant vitamins, such as E and C. ROS mediate injury by formation of lipid peroxides and protein carbonyls and by causing DNA and RNA strand breaks. This can lead to compromised cell membrane integrity and necrosis, or it can activate apoptotic cascades.

DOX, MIN, and TET all have a multiply-substituted phenol ring, similar to vitamin E. The phenol ring is key to the ROS-scavenging abilities of these compounds. The reaction of the phenol ring with a free radical generates a phenolic radical that becomes relatively stable and unreactive due to resonance stabilization and steric hindrance by the phenol ring side groups (82). MIN was recently shown to directly scavenge ROS in several cell-free mixed-radical assays with a potency comparable to vitamin E, and its scavenging ability was not dependent on chelation of Fe^{2+} (i.e., inhibition of the Fenton reaction) (82). Depending on the assay used, MIN had an IC_{50} of 3-40 μM and was 9-250 times more potent of a scavenger than DOX

and 200-300 times more potent than TET. The authors concluded that the superior scavenging ability of MIN is likely due to the presence of the diethylamino group on the phenolic carbon, which is unique to MIN and provides improved steric hindrance (82). Other groups have shown DOX to be an effective ROS scavenger. DOX was shown to inhibit both HOCl and a mixture of neutrophil-derived ROS *in vitro*, with an IC₅₀ of ~2 μM (83). In addition, DOX was shown to inhibit HOCl-mediated activation of MMP-1 from osteosarcoma cells, with an IC₅₀ of ~50 μM (84).

1.4.2 Reactive Oxygen Species Scavenging in Myocardial Ischemia/Reperfusion Injury

The generation of ROS upon reperfusion of ischemic myocardium is thought to be one of the primary mediators of reperfusion injury. A major source of ROS generation during reperfusion is the myocyte respiratory chain. During ischemia, redox components of the respiratory chain are reduced and inappropriately donate electrons to O₂ to form O₂^{•-} (85). While residual oxygen can generate some O₂^{•-} during ischemia, the reintroduction of O₂ during reperfusion leads to a burst of O₂^{•-} (and other ROS) within seconds (86). Another potential source of ROS in the heart is xanthine oxidase, present primarily in the cytosol of endothelial cells (87). Xanthine oxidase is an important enzyme in purine metabolism, catalyzing the conversion of hypoxanthine or xanthine and O₂ to uric acid and generating O₂^{•-} in the process. During ischemia, the degradation of ATP to adenosine and finally hypoxanthine provides a rich substrate for xanthine oxidase; however, the lack of O₂ limits the activity of the enzyme. Upon restoration of O₂ during reperfusion, xanthine

oxidase activity resumes, and $O_2^{\bullet-}$ is formed (88). A third potential source of ROS in the reperfused heart is infiltrating neutrophils (80). In activated neutrophils, NADPH oxidase reduces O_2 to $O_2^{\bullet-}$, and MPO can convert H_2O_2 to HOCl. Given the time course of neutrophil infiltration into the reperfused myocardium, it is unlikely that they constitute a significant source of early ROS. However, neutrophils likely constitute a continual source of oxidative stress during the inflammatory response.

Several studies have investigated the protective effects of scavenging ROS or inhibiting ROS production in myocardial I/R injury using both genetic and pharmacologic approaches. Overexpression of SOD or glutathione peroxidase in mice has been shown to reduce infarct size and improve recovery of function following I/R in isolated, perfused hearts (89-91) and *in vivo* (89). It has also been shown that administration of exogenous SOD and/or catalase reduces the extent of I/R injury in canine (92, 93) and porcine (94) models. Several pharmacological antioxidants have also been shown to attenuate I/R injury. N-2-mercaptopyrionyl glycine (MPG) (95), edaravone (96), tempol (97), and vitamin E (98) are examples of antioxidants that have been shown to reduce the extent of myocardial I/R injury in animal models.

While antioxidant treatment has been shown to be beneficial in animal models of I/R, clinical use of antioxidants have given mixed results. Administration of exogenous SOD to patients undergoing angioplasty for an acute MI did not reduce the degree of myocardial stunning (99). On one study, vitamin E was found to improve contractile function and reduce cardiac enzyme release following coronary artery bypass graft (CABG) surgery (100). However, in another study vitamin E had no

effect on the extent of myocardial injury following CABG or valve repair (101). The reasons for the discrepancy between animal and human studies may be related to species difference or to the fact that animal studies are generally performed with healthy hearts while human studies generally involve diseased hearts.

1.5 Anti-Apoptotic Effects

1.5.1 Introduction to the Apoptotic Cascade

A key event in the execution of apoptotic cascade is the activation of caspases, a family of cysteine proteases. Caspases can be divided into upstream “initiator” caspases, which function to activate downstream caspases, and the downstream “executioner” caspases that are responsible for the proteolytic destruction of the cell (102). Caspases may be activated by either the extrinsic (death receptor) pathway or the intrinsic (mitochondrial) pathway. In the extrinsic pathway (reviewed in (103)), death signal proteins such as TNF- α and Fas ligand bind to their cell surface receptors and, through signal transduction cascades, lead to the activation of an initiator caspase, caspase-8. Caspase-8 in turn activates downstream caspases, such as caspases-3.

In the intrinsic pathway (reviewed in (104)), a variety of extracellular and intracellular stress stimuli converge on the mitochondria to destabilize it and cause the release of pro-apoptotic factors into the cytosol. A key factor mediating mitochondrial destabilization is opening of the mitochondrial permeability transition pore (MPTP), a large, high-conductance pore that spans both the inner and outer mitochondrial membranes. Opening of the MPTP occurs in response to Ca^{2+} , ROS, inorganic

phosphate, and alkaline pH (105). Once the MPTP opens, there is an influx of water, which leads to swelling of the mitochondrial matrix and eventually rupture of the outer mitochondrial membrane. Cytochrome c and other pro-apoptotic proteins, such as Smac/DIABLO and apoptosis-inducing factor (AIF) are released from the intermembrane space into the cytosol. Cytochrome c binds the cytosolic adapter protein Apaf-1 which allows the recruitment and activation of an initiator caspase, caspase-9, which then activates downstream caspases (106). Smac/DIABLO binds and inhibits caspase inhibitor proteins thereby disinhibiting caspase activity (107). AIF translocates to the nucleus and induces chromatin condensation and DNA fragmentation in a caspase-independent manner (108).

The mitochondrial apoptosis pathway is also partly regulated by the Bcl-2 family of proteins (109). Bcl-2 family members may be pro-apoptotic (Bax, Bad, Bid) or anti-apoptotic (Bcl-2, Bcl-xL). In response to apoptotic stimuli, the pro-apoptotic Bcl-2 proteins undergo a conformational change, translocate from the cytosol to the mitochondria, insert into the outer mitochondrial membrane, and trigger the release of cytochrome c. The anti-apoptotic Bcl-2 proteins are localized to the outer mitochondrial membrane and inhibit cytochrome c release by sequestering pro-apoptotic Bcl-2 proteins.

1.5.2 Mechanisms Underlying the Anti-Apoptotic Effects of Tetracyclines

There is an increasing body of evidence that the tetracyclines possess anti-apoptotic properties. In a seminal study by Yrjanheikki et al., it was found that MIN and DOX increased the survival of hippocampal neurons following global brain

ischemia in gerbils, and this protection was associated with reduced caspase-1 expression (110). MIN was subsequently evaluated in several other models of neuronal injury and found to also be protective against Huntington disease (111), traumatic brain injury (112), and Parkinson's disease (113). In each of these cases, the neuroprotection by MIN was associated with a reduction in caspase-1 and/or caspase-3 expression, suggesting MIN was protective by inhibiting the expression of key factors within the apoptotic cascade.

In addition to inhibiting caspase expression, MIN has also been shown to inhibit caspase activity by blocking activation. Zhu et al. demonstrated that MIN inhibits cytochrome c release and caspase-3 activation in mice with amyotrophic lateral sclerosis (114). Using isolated mitochondria, they also showed that MIN inhibited Ca^{2+} - and Bid-induced mitochondrial swelling and cytochrome c release, indicating that the mitochondria, and perhaps the MPTP, were direct targets of MIN (114). In a follow-up study, the same group showed that MIN inhibited mitochondrial release of cytochrome c, Smac/DIABLO, and apoptosis-inducing factor (AIF) in both a culture model and an *in vivo* mouse model of Huntington disease, indicating MIN inhibits both caspase-dependent (cytochrome c and Smac/DIABLO) and caspase-independent (AIF) mitochondrial death pathways (115). MIN also protected cultured renal epithelial cells from I/R injury and inhibited mitochondrial cytochrome c release (116). Interestingly, this group found that protection by MIN was dependent on MIN-induced upregulation of Bcl-2, as antisense-mediated downregulation of Bcl-2 abolished the protective effects of MIN (116). Taken together, these studies

demonstrate that MIN, and possibly also DOX, possess anti-apoptotic effects mediated by inhibition of caspase expression and by mitochondrial stabilization.

1.5.3 Inhibition of the Apoptotic Cascade in Myocardial Ischemia/Reperfusion

Injury

Both necrosis and apoptosis have been observed in the heart the settings of MI and I/R injury, and strategies aimed at reducing the extent of apoptosis or necrosis have been shown to reduce infarct size. In both humans and rodents, up to 30% of the myocytes within the infarct region and border zone display evidence of apoptosis following MI (117-120). It is thought that apoptosis may predominate early after the onset of ischemia (<6 hours), while necrosis may predominate later (> 6 hours) (118). In culture, myocytes undergo apoptosis in response to a variety of stimuli, including hypoxia (121), hypoxia followed by reoxygenation (122), acidosis (123), oxidative stress (124), stretch (125), disruption of cell-matrix interactions (77, 78, 126), TNF- α (127), and Fas ligand (128).

Given the complexity of the apoptotic process and the multiple potential initiating factors, it is not surprising that numerous strategies aimed at attenuating apoptosis have been investigated. One strategy is to inhibit the downstream players in the apoptotic cascade, the caspases, and indeed, caspase inhibition with tetrapeptide-based competitive inhibitors has been shown to attenuate apoptosis and reduce infarct size in rats *in vivo* (129, 130). Other strategies have focused on inhibiting the release of pro-apoptotic factors from the mitochondria. Cyclosporin A, a direct inhibitor of MPTP opening, was found to improve the functional recovery of isolated, perfused rat

hearts subjected to I/R (131) and to reduce infarct size in mice *in vivo* (132). It has also been postulated that the cardioprotective effects of Na⁺/H⁺ exchanger inhibitors, such as amiloride and cariporide, are mediated by reducing calcium loading during ischemia and slowing the return of the intracellular pH to normal during reperfusion, thereby inhibiting MPTP opening (105). Overexpression of Bcl-2 in mice also inhibits apoptosis and reduces infarct size *in vivo* (133). In addition, MIN has recently been shown to improve myocyte survival and reduce infarct size, and this was correlated with reduced caspase expression and reduced mitochondrial release of cytochrome c and Smac/DIABLO (134).

These previous studies demonstrate that blocking apoptosis by directly inhibiting factors within the apoptotic cascade can salvage myocytes and reduce infarct size. MIN has been shown to effectively block apoptosis in models of neuronal injury, and there is at least preliminary evidence that MIN can reduce infarct size by blocking apoptosis in the heart. Additional studies are needed to clarify this potentially important role of tetracyclines in the heart.

1.6 Objectives of the Dissertation

As described above, the tetracyclines have remarkably diverse non-antimicrobial properties. They have been shown to inhibit MMPs, scavenge ROS, and inhibit apoptosis in various disease states. Since these same processes have all previously been shown to contribute to the pathogenesis of MI, myocardial I/R injury,

and adverse cardiac remodeling, the tetracyclines appear to potentially be an attractive tool for the treatment of myocardial ischemic injury and warrant further investigation.

The goals at the outset of the work presented in this dissertation are to 1) assess the ability of DOX to inhibit MMPs post-MI and attenuate adverse ventricular remodeling (described in Chapter 2), 2) determine whether MMPs contribute to I/R injury and the potential for MMP inhibition by DOX to improve myocyte survival (described in Chapter 3), and 3) explore the antioxidant and anti-apoptotic capacity of DOX and MIN in the settings of myocardial I/R and myocardial stunning (described in Chapter 4). A summary and discussion of the data is presented in Chapter 5.

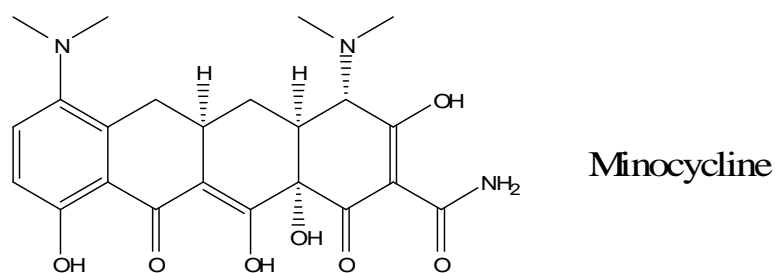
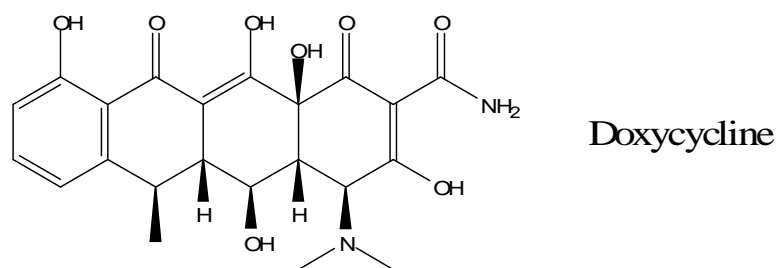
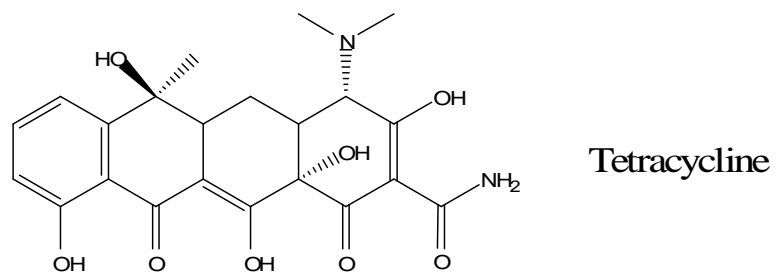


Figure 1-1. Chemical structures of doxycycline, minocycline, and tetracycline.

Chapter 2. Modulation of post-infarction left ventricular remodeling via MMP inhibition by doxycycline, and evaluation of new ZBGs for development into novel MMP inhibitors

2.1. Abstract

MI is associated with early MMP activation and ECM degradation. It was previously shown that early short-term DOX treatment preserves cardiac structure and function. In this study, the effect of DOX on myocardial MMP activity was investigated to assess whether the observed anti-remodeling effects of DOX were due inhibition of MMPs. Rats treated daily with or without DOX beginning 48 hours prior to experimentation were subjected to coronary occlusion for either 1 hour or 24 hours. Using nonspecific and MMP-2/9-specific fluorogenic MMP peptide substrates, it was found that DOX treatment preserved tissue MMP levels at both 1 hour and 24 hours post-MI in rats. Assessment of MMP-2 and MMP-9 activity by zymography revealed only MMP-2 activity, indicating that the results obtained with the MMP-2/9 substrate likely reflected only MMP-2 activity. When DOX was supplemented to the samples to a concentration expected 4 hours after treatment *in vivo* (35 μ M), MMP activity was reduced by 25%. These results suggest that early, short-term treatment with DOX inhibits MMP activation and release in the setting of MI. In an effort to develop improved MMP inhibitors (MPIs) over DOX and hydroxamate-based MPIs, recently developed new zinc-binding groups (ZBGs) were investigated for their capacity to inhibit MMPs in culture. MMPs secreted by cultured neonatal rat ventricular

fibroblasts (NRVFs) were activated by the addition of plasminogen to the culture, and the MMP activity was assessed in the presence of various concentrations of new ZBGs. All of the new ZBGs showed greater potency toward inhibiting MMP activity than acetohydroxamic acid (AHA), with IC_{50} values ranging from 86 μ M to 3.2 mM compared with 8.7 mM for AHA. These results demonstrate that potent, nontoxic, and biocompatible alternatives to the hydroxamic acid zinc chelator are available for use in MPIs, with the potential to generate inhibitors more potent and specific than DOX and hydroxamic acid-based MPIs.

2.2. Introduction

Many patients who experience a MI may undergo cardiac remodeling (10). Post-MI remodeling can result in chamber dilatation as well as hypertrophy and fibrosis of noninfarcted myocardium. Severe degrees of cardiac remodeling are associated with increased risk for the development of heart failure.

Accompanying cardiac myocyte cell death in the setting of MI is damage to the existing ECM of the heart, in particular to collagens (135, 136). The cardiac ECM provides structural support and integrity to the myocardium (137) and facilitates the conversion of myocyte contraction into pump function. The integrity of the original ECM is thought to play an important role in determining the extent of remodeling after MI (138). It has been shown that physically restricting the heart during the development of MI attenuates remodeling and improves cardiac function (139). These

results support the concept that preserving the original ECM reduces the degree of remodeling and improves the function of the scar region and normal myocardium.

Degradation of ECM follows the activation of MMPs. MMPs are a family of zinc-binding endoproteinases that are secreted as zymogens (38). Reports have documented the time-dependent activation of MMPs after ischemia or MI. MMP activation can occur within minutes after ischemia, with significant increases occurring as early as 15 minutes and peaking 1 to 2 days after MI (65, 66, 140). It is believed that early (<48-hour) MMP activation is associated with zymogen activation, whereas subsequent (>48-hour) increases are associated with inflammation (65, 66). Chronic inflammation is largely derived from macrophage infiltration (141) and is associated with enhanced expression and activity of MMPs (66). Macrophages modulate wound healing, including the activation of fibroblasts and angiogenesis (142, 143). Angiogenesis is dependent on MMP activity (69, 144). Indeed, the inhibition of macrophage function in the setting of postinjury chronic inflammation can compromise wound healing (143). The sequence described above of early events after ischemic injury suggest that early, short-term pharmacological inhibition of MMP activity (<48 hours) may preserve the original ECM matrix without compromising chronic inflammation-associated wound healing and scarring.

DOX, a member of the tetracyclines, has been shown to attenuate MMP expression and activity (145-148). Results from my laboratory demonstrated that rats treated with DOX from 48 hours before MI to 36 hours post-MI show significantly preserved wall thickness in the infarct region and increased LV compliance compared

with untreated control rats at 2 weeks post-MI (149). At 4 weeks post-MI, DOX-treated rats continued to show significantly preserved infarct wall thickness and increased LV compliance, in addition to reduced heart weight to body weight ratio, inner LV diameter, and myocyte cross-sectional area (149). Analysis of 2D epicardial LV strains showed that DOX-treated animals had epicardial strain patterns more closely resembling that of a normal LV wall compared with untreated animals (149). These results demonstrate that DOX treatment attenuates ventricular remodeling by preserving wall thickness and decreasing compensatory hypertrophy and dilatation.

In addition to inhibiting MMPs, DOX can also inhibit a wider range of other proteases, including cysteine and serine proteases (64). DOX has also been shown to inhibit the activity and/or expression of iNOS (150), phospholipase A₂ (151), and TNF- α (152), in addition to scavenging reactive oxygen species (153). DOX has also been shown to upregulate COX-2 expression and prostaglandin E₂ levels (154). Because of these pleiotropic effects of DOX, it remains to be determined whether the attenuation of post-MI LV remodeling by DOX is due to its MMP inhibitory properties.

DOX is currently the only available clinically-approved MMP inhibitor (MPI) and is marketed under the name Periostat (Collagenex Pharmaceuticals) for treatment of periodontitis (48). Given the pleiotropic effects of DOX *in vivo*, the development of biocompatible MPIs with increased specificity would provide a valuable research tool for investigation of MMP-dependent processes and pathologies. However, the development of more specific MPIs for clinical use and *in vivo* research use has

proven disappointing. Most MPIs have been developed around a peptidomimetic backbone designed to interact with the MMP active site combined with a hydroxamic acid-based zinc binding group (ZBG) designed to coordinate with the catalytic zinc ion, thereby inactivating the MMP (155). These hydroxamic acid-based MPIs have failed in clinical trials due to poor bioavailability and musculoskeletal-related side effects (48). Recently, novel ZBGs based on hydroxypyridinones, hydroxypyridinethiones, pyrones, and thiopyrones been developed for incorporation into MPIs (156). These new ZBGs have shown improved potency and stability *in vitro* compared with hydroxamate. However, the biocompatibility and efficacy of these ZBGs in a more physiologic environment are unknown and must be examined prior to their development into MPIs.

The purpose of the current study was twofold: 1) To investigate the effects of DOX treatment on early myocardial MMP activity in the setting of MI, and 2) To assess the potency of new ZBGs in cultured cardiac fibroblasts.

2.3. Experimental Methods

2.3.1. *In vivo* experiments

2.3.1.1. Doxycycline treatment

Male Sprague-Dawley rats (Harlan, Indianapolis, IN) were used. DOX (Sigma, St. Louis, MO) was administered orally in 2 doses at 30 mg/kg per day, a dose known to attain an effective *in vivo* inhibition of MMP activity (148). Treatment began 48 hr before thoracotomy and continued until the animal was sacrificed. All

procedures were approved by the Institutional Animal Care and Use Committee and conform to published NIH guidelines for animal research.

2.3.1.2. Surgery

Animals were anesthetized with ketamine (100 mg/kg) and xylazine (5 mg/kg) intramuscularly, intubated, and positive-pressure ventilated with room air (Kent Scientific, Torrington, CT). A left thoracotomy was performed, the pericardium opened, the heart exposed, and the left anterior descending coronary artery occluded. Sham animals were treated identically, except the ligature was not tightened. In one set of experiments, after 1 hour of ischemia the heart was rapidly excised, rinsed in PBS, flash frozen, and stored at -80°C. In another set of experiments, the chest was closed in layers, and the animal was extubated and allowed to recover. After 24 hours the animal was anesthetized as before, the chest reopened, and the heart excised as described above.

2.3.1.3. Tissue processing

Flash-frozen ischemic or infarcted LV (excluding septum) and RV tissue was homogenized on ice in 100 volumes of buffer (50 mM Tris pH 7.4, 150 mM NaCl, 5 mM CaCl₂, 0.2 mM NaN₃, 0.1% Triton X-100), yielding a 100X diluted sample. Lysates were cleared by centrifugation at 12,000 g for 10 min at 4°C. Protein concentrations of the tissue extracts were determined using the Bio-Rad Protein Assay (Bio-Rad, Hercules, CA).

2.3.1.4. MMP activity

2.3.1.4.1. Fluorogenic substrates

Fluorescence-quenched peptide substrate probes were used. Cleavage of the peptide results in release of the quencher and an increase in fluorescence. To assess global MMP activity, lysate was reacted with 10 μ M OmniMMP substrate (Mca-Pro-Leu-Gly-Leu-Dpa-Ala-Arg, BIOMOL Research Laboratories, Plymouth Meeting, PA). To assess MMP-2 activity, Mca-Pro-Leu-Ala-Nva-DAP[DNP]-Ala-Arg (Sigma) was used. Fluorescence (340 nm excitation, 405 nm emission) was kinetically assessed using a fluorescence microplate reader (Bio-Tek Instruments, Winooski, VT). The MMP inhibitor phenanthroline was used to confirm that substrate cleavage was attributable to MMPs.

2.3.1.4.2. Gelatin zymography

Gelatin zymography was performed as previously described (157). The samples were diluted 1:1 in 2X non-reducing sample buffer (125 mM Tris pH 6.8, 4% SDS, 20% glycerol) and electrophoresed on 7.5% poly-acrylamide gels copolymerized with 0.1% gelatin. An internal control (purified human MMP-2/MMP-9, Chemicon, Temecula, CA) was loaded to normalize activities between gels. Gels were washed in renaturation buffer (2.5% Triton X-100) and then in developing buffer (50 mM Tris pH 7.4, 200 mM NaCl, 5 mM CaCl₂, 0.02% Brij 35) for 30 min each. Gels were then incubated in fresh developing buffer overnight at 37°C with shaking. Following incubation, the gels were stained with 0.1% Coomassie Blue G-250, and bands of gelatinolytic activity were digitally quantified using Kodak 1D (Eastman-Kodak, Rochester, NY).

2.3.2. Cell culture experiments

2.3.2.1. Neonatal rat ventricular fibroblast (NRVF) isolation and culture

NRVFs were prepared as previously described (158). The hearts of 1-2 day old Sprague-Dawley rats were excised, minced, and digested with collagenase type 2 (80 U/ml, Worthington, Lakewood, NJ) and pancreatin (0.6 mg/ml, Sigma). The dispersed cells were applied to a discontinuous percoll density gradient, and the myocytes and NRVFs were separated. The NRVFs were plated on tissue culture dishes in media (DMEM + 10% FBS). After 30 min the dishes were washed with media to remove non-adherent cells, and the remaining adherent NRVFs were incubated in fresh media at 37°C in a 5% CO₂ humidified environment. Cells were passaged upon reaching 90% confluence. Cells from the first or second passages were used in the experiments. The NRVFs were serum starved by replacing the media with serum-free DMEM for 24 hours prior to experimentation.

2.3.2.2. Inhibition of NRVF-derived MMPs by ZBGs

To activate NRVF MMPs, cells were treated with plasminogen (60 µg/ml, Sigma) for 16 hours. MMP activity was determined by reacting culture media with 10 µM OmniMMP substrate as described above in the presence of ZBGs. Aprotinin (8 µg/ml) was also included to neutralize residual plasmin activity. The data were fit to the sigmoidal Hill equation: $Y = \frac{[DOX]^n}{([DOX]^n + k^n)}$ (Prism, GraphPad Software, San Diego, CA). Y is the rate of substrate hydrolysis as a fraction of maximal substrate hydrolysis, n is the Hill coefficient, and k is the DOX concentration at which activity is half maximal (IC₅₀).

2.4 Results

2.4.1. Doxycycline preserved LV MMP activity post-MI

Global MMP activity was significantly preserved at 1 hour post-MI in the ischemic or infarcted tissue in rats treated with DOX (Figure 2-1A). The use of the MMP-2/9 substrate yielded comparable results (Figure 2-1B). Addition of 2 mM phenanthroline to homogenates eliminated any detectable MMP activity.

Measurement of global MMP activity at 24 hours post-MI revealed an even greater loss of MMP activity in the control MI group compared with the 1 hour post-MI data, and DOX treatment significantly preserved global MMP activity (Figure 2-2A). MMP-2/9 activity was also reduced at 24 hours post-MI. DOX treatment tended toward preserved MMP-2/9 activity, but this did not reach statistical significance given the small sample size ($p = 0.17$, $n = 2$ per group) (Figure 2-2B).

Supplementation of DOX (35 μ M) to tissue homogenates (given the 100X dilution after homogenization) of animals treated with the drug resulted in ~25% inhibition of MMP activity (749 \pm 60 RFU/min control vs. 562 \pm 109 RFU/min DOX, $p \leq 0.05$), indicating the actual MMP activity *in vivo* was suppressed by DOX treatment.

Gelatin zymography experiments of 1 hour post-MI hearts yielded only MMP-2 activity and no detectable MMP-9 activity (Figure 2-3), indicating that the results obtained with the MMP-2/9 substrate likely reflect only MMP-2 activity. No differences in MMP-2 zymographic activity were observed between control and DOX treated hearts.

2.4.2. ZBG potency against NRVE-derived MMPs

New ZBGs (Figure 2-4) were analyzed for the ability to inhibit plasmin-activated MMPs produced by NRVFs in culture. All of the ZBGs showed greater potency than acetohydroxamic acid (AHA), with 9 demonstrating the strongest inhibition ($IC_{50} = 86 \mu M$) (Figure 2-5A). Compound 3 had not been tested due to poor aqueous solubility.

2.5. Discussion

The capacity of MMP inhibition to preserve post-MI heart structure as well as passive and contractile function is an emerging area of research (39, 59). Cheung et al. (73) demonstrated using isolated perfused hearts that after 20 min of no-flow ischemia, there was an early increase in MMP-2 activity in the coronary effluent after reperfusion. MMP-2 release was enhanced with longer ischemia and reduced recovery of mechanical function during reperfusion. The authors noted that use of DOX improved recovery of mechanical function during reperfusion, supporting the concept that myocardial ischemia can induce activation of MMPs. In addition, their data support the idea that MMP activation is associated with induction of contractile dysfunction. Another report showed an inverse correlation between the release of MMP-2 into the coronary effluent and LV MMP activity in the setting of ischemia (140). In this study, preconditioning of the ischemic heart preserved LV function, leading to decreased MMP-2 release into the coronary effluent while increasing LV MMP activity by ~18%. These results compare favorably with my observations that MMP activity was reduced by 1 hour post-MI and that DOX treatment preserved LV

MMP activity (16% greater versus control MI) to levels similar in shams. Taken together, these results suggest that activation of MMPs during ischemia causes their release from the myocardium, leading to increased MMP activity in the coronary effluent and decreased activity in the myocardium. Blocking MMP activity prevents their release.

During homogenization of the tissue, the samples were diluted 100X in homogenization buffer. To determine if this 100X dilution resulted in reduced MMP inhibition by DOX, DOX was supplemented to the tissue samples to levels anticipated 4 hours after treatment *in vivo* (35 μ M). DOX supplementation yielded ~25% inhibition in global MMP activity. Therefore, the actual MMP activity *in vivo* was reduced by DOX treatment, and the preservation of MMP activity seen in the substrate hydrolysis assays reflected a preservation of MMP enzyme levels in the tissue.

Analysis of MMP activity using a MMP-2/9 substrate probe gave similar results to the nonspecific OmniMMP probe. When the samples were assayed by zymography, the lack of any detectable MMP-9 suggested that the activity detected with the MMP-2/9 probed was due to MMP-2 activity. However, no difference in MMP-2 activity between control MI and MI+DOX was seen by gelatin zymography. One possible explanation for this discrepancy is that zymography lacked sufficient sensitivity to detect the ~10% loss in MMP-2/9 activity detected with the peptide substrate in MI rats. Analysis of MMP activity with the substrate probe is a kinetic assay in which degradation of substrate is monitored in real time. Gelatin zymography is an older technique in which the gel must be developed for an empirically

determined amount of time to provide desirable resolution of the bands. Therefore, the MMP-2/9 substrate probe data showing a change in MMP activity are likely more accurate and reliable than the gelatin zymography data showing no change. Another possibility for the discrepancy is that the MMP-2/9 substrate probe is amenable to cleavage by another MMP not detected by zymography. This could be investigated by determining whether MMP-2/9 activity is diminished by an MMP-2 neutralizing antibody, but these experiments were not done in this study.

Interestingly, in the rats treated with DOX from 48 hours before MI to 36 hours post-MI, DOX treatment did not alter the ratio of muscle to scar in the infarct region compared with untreated rats (149). Therefore, given that the DOX-treated rats also had thicker LV walls, DOX treatment actually resulted in a net preservation of both muscle and scar compared with untreated rats. Whether this apparent preservation of muscle (i.e., myocyte salvage) was due to the MMP inhibitory effects of DOX or some other mechanism is unclear. Further investigation into the cardioprotective (i.e., myocyte salvage) actions of DOX was subsequently studied in a model of myocardial I/R, and the results are presented in Chapter 3.

My results show that short-term MMP inhibition by DOX was correlated with attenuated ventricular remodeling seen at 2 and 4 weeks post-MI and with myocyte salvage. However, although DOX reduced MMP activation and release, the possibility remains that DOX elicited these effects by some other mechanism independent of MMP inhibition. In light of the pleiotropic effects of DOX, I investigated the potency of new ZBGs as an initial step in screening these compounds

for development into more specific MPIs. MPI design and synthesis have yielded a vast number of compounds with a variety of backbone substituents that are designed to interact with specific MMP subsites. In comparison, little progress has been made on improving the ZBG of the inhibitor that binds directly to the ubiquitous active-site Zn^{2+} ion. With the limitations of hydroxamic acids as a ZBG clearly established, it is increasingly apparent that improved ligands must be developed for second-generation MPIs (159, 160). The promising inhibitory potential of these new ZBGs against recombinant MMPs (155, 156) led us to examine their activities in a cellular assay. NRVF cultures were selected for evaluating new ZBGs on the basis of two primary reasons. First, cardiac fibroblasts have a well documented capacity to produce and secrete a variety of MMPs into culture media in zymogen form, including MMP-2 and MMP-9 (161). The fibroblast-secreted MMPs are amenable to activation by several mechanisms, including protease-mediated cleavage by enzymes such as plasminogen (162). Addition of plasminogen activates MMPs by first itself being cleaved by urokinase plasminogen activator present on the cell surface and then cleaving the prodomain of the MMP (163). The second reason for using NRVFs was to select a system that would secrete a mixture of MMPs that was representative of the MMPs present in the heart *in vivo*.

The new ZBGs showed greater potency than AHA, and the order of potency largely paralleled that seen *in vitro* using purified MMPs (155). Of notable exception, 5 demonstrated significantly greater potency, while 7 showed markedly reduced potency in NRVF culture. These discrepancies may be due to interactions of these

compounds with other components of the cellular media. At the concentrations of ZBG used to inhibit these enzymes these compounds will complex loosely bound metal ions in the culture medium and may inhibit metalloenzymes other than MMPs, which might perturb the observed efficacy in this assay. Therefore, assessing the MMP inhibitory capacity of the new compounds in culture provides additional information regarding the efficacy toward a “physiological” mix of MMPs that might remain concealed by *in vitro* assessment alone. Subsequent experiments demonstrated that the ZBGs inhibited cell invasion of HT1080 fibrosarcoma cells, and that the ability to inhibit invasion correlated well with their ability to inhibit MMPs (155). In addition, all of the ZBGs showed low toxicity at concentrations up to 100 μ M (with the exception of 7), and compounds 1-6 were comparable to AHA (155). These results demonstrate that potent, nontoxic, and biocompatible alternatives to the hydroxamic acid chelator are available for use in MPIs, with the potential to generate inhibitors more potent and specific than DOX.

In conclusion, I provide correlative evidence that the attenuation of ventricular remodeling and myocyte salvage seen with DOX treatment was due to MMP inhibition. However, given the pleiotropic nature of the DOX, other actions of the drug may have contributed to its observed effects by mechanisms that were not investigated in this study. The screening and development of new ZBGs into MPIs may provide more specific and useful tools for investigation of MMP-dependent processes, such as remodeling, and for treatment of MMP-dependent pathologies.

2.7. Acknowledgements

Chapter 2, in part, has been published as it appears in Villarreal FJ, Griffin M, Omens J, Dillmann W, Nguyen J, Covell J. *Circulation* 2003;108(12):1487-1492, Lippincott Williams & Wilkins, 2003 and in Puerta DT, Griffin MO, Lewis JA, Romero-Perez D, Garcia R, Villarreal FJ, Cohen SM. *Journal of Biological Inorganic Chemistry* 2006;11(2):131-138, Springer Berlin Heidelberg, 2006. The dissertation author was a co-investigator and co-author of these manuscripts. The dissertation author was the primary investigator and author of the portions of these manuscripts presented in Chapter 2.

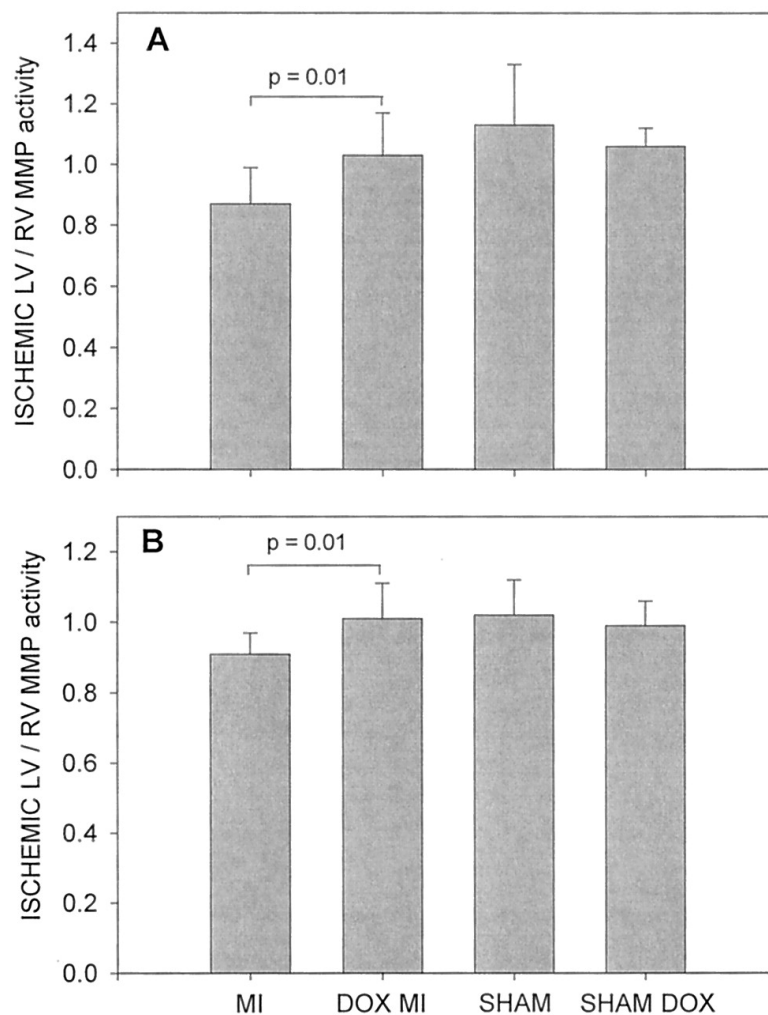


Figure 2-1. Global (A) and MMP-2/9 (B) activity observed in ischemic/infarcted LV tissue 1 hour after coronary occlusion in either untreated (n = 5 per group) or DOX-treated (n = 10 per group) sham and MI rats. MMP activity was assessed using fluorogenic substrates. LV values (RFU/min) were normalized to those of the right ventricle. Significant preservations of MMP activity were observed in ischemic and infarcted tissue of infarcted DOX rats versus those of MI controls.

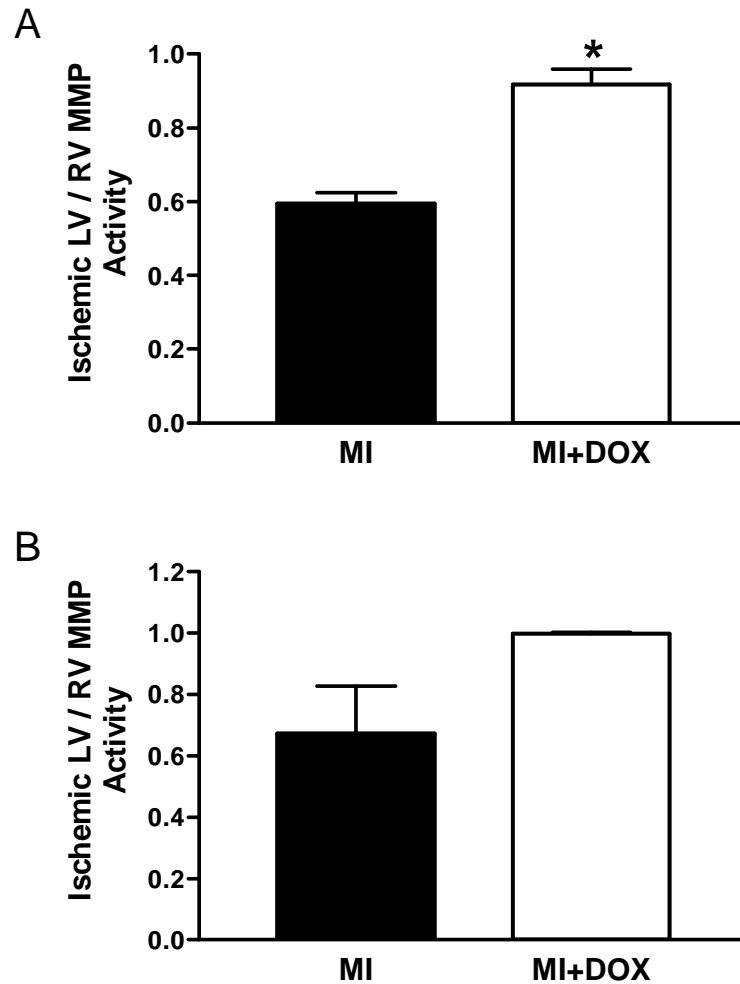


Figure 2-2. Global (A) and MMP-2/9 (B) activity observed in ischemic/infarcted LV tissue 24 hours after coronary occlusion in either untreated ($n = 2$) or DOX-treated ($n = 2$) MI rats. MMP activity was assessed using fluorogenic substrates. LV values (RFU/min) were normalized to those of the right ventricle. Significant preservation of global MMP activity was observed in ischemic/infarcted tissue of MI+DOX rats versus those of MI controls. MMP-2/9 activity also tended toward preservation with DOX treatment, but this did not reach statistical significance ($p = 0.17$). * $p \leq 0.05$.

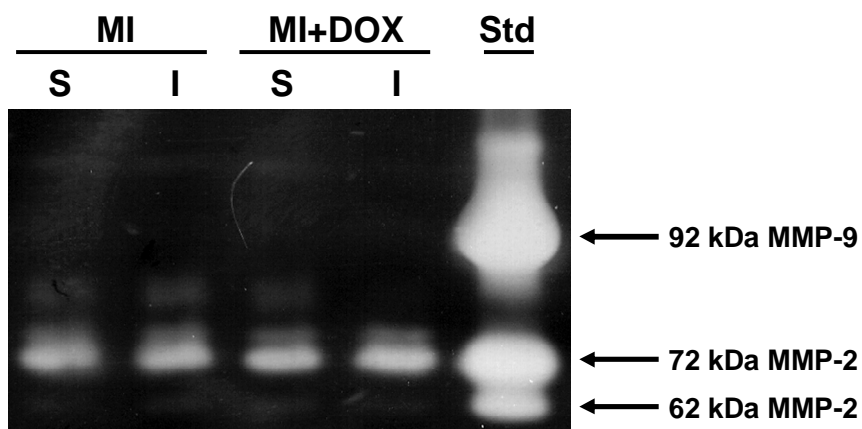


Figure 2-3. Representative gelatin zymogram of myocardial MMP-2 and MMP-9 levels in control (MI) and DOX-treated (MI+DOX) infarcted hearts 1 hour post-MI. 'I' and 'S' indicate ischemic/infarcted region and septum, respectively. 'Std' indicates human MMP-2/MMP-9 standard.

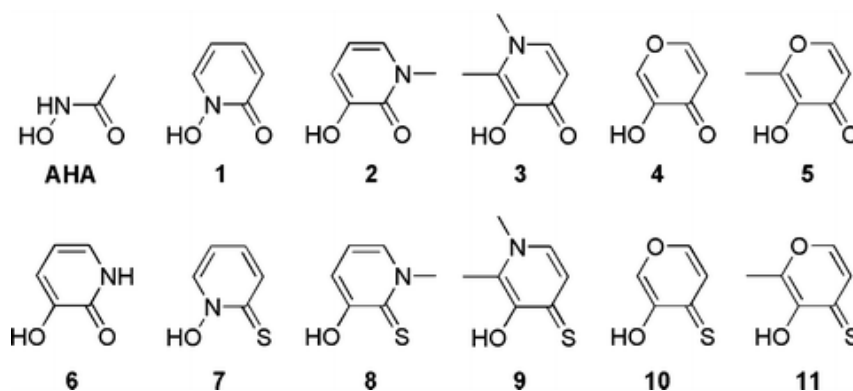


Figure 2-4. Heterocyclic zinc-binding groups (ZBGs) proposed for use in MMP inhibitors. Hydroxypyridinones (**1-3**, **6**), pyrones (**4**, **5**), hydroxypyridinethiones (**7-9**), and thiopyrones (**10**, **11**) were tested. Acetohydroxamic acid (AHA) was utilized as a benchmark in the experiments described herein.

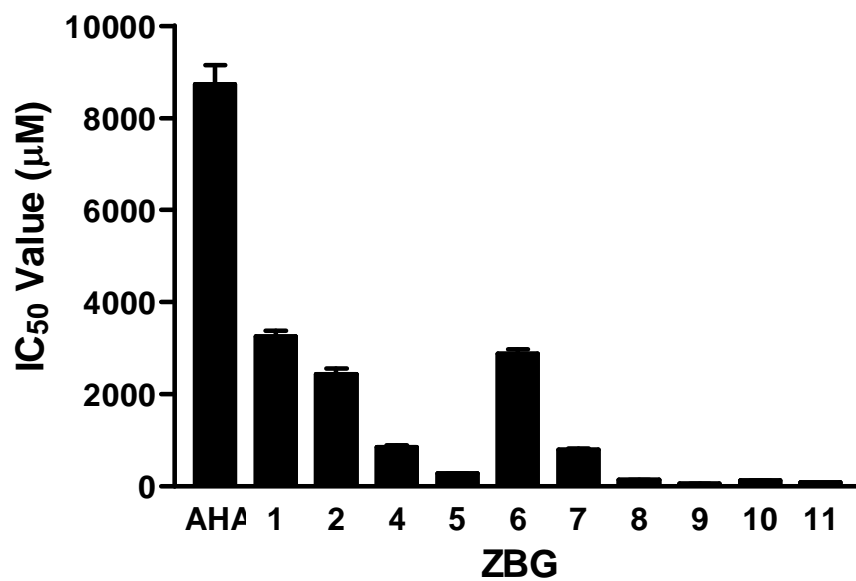


Figure 2-5. IC₅₀ values for ZBGs against plasmin-activated MMPs produced by NRVEs. Data are mean±SEM from experiments performed in triplicate from two different cell preparations.

Chapter 3. Reduction of myocardial infarct size via plasmin inhibition by doxycycline

3.1. Abstract

Myocardial I/R injury is associated with the activation of MMPs and serine proteases. I hypothesized that activation of MMPs and the serine protease plasmin contribute to early cardiac myocyte death following I/R and that broad-spectrum protease inhibition with DOX preserves myocyte viability. DOX pretreatment reduced infarct size by 37% in rats subjected to 30 min of coronary occlusion and 2 days of reperfusion. DOX attenuated increases in MMP-9 and plasmin levels as determined by gelatin zymography and immunoblot, respectively. Neutrophil extravasation was unaltered by DOX as assessed by myeloperoxidase activity. Hemodynamic and morphometric analyses after 4 weeks of reperfusion showed that DOX pretreatment did not compromise left ventricular structure or function and did not alter scar size. To examine the contribution of MMPs and plasmin to myocyte injury, cultures of neonatal rat ventricular myocytes (NRVMs) were treated for 48 hours with MMP-2, -3, or -9 or plasminogen in the presence or absence of DOX. MMP treatment did not affect myocyte viability. Plasminogen treatment led to increased plasmin activity, resulting in loss of β_{1D} -integrin, NRVM detachment, and apoptosis. DOX co-treatment inhibited plasmin activity and preserved NRVM attachment, whereas co-treatment with the broad-spectrum MMP inhibitor GM6001 had no effect. Enzyme activity assays showed DOX directly inhibited plasmin *in vitro*

in the presence of calcium. Infusion of the plasmin inhibitor tranexamic acid into isolated, perfused hearts subjected to I/R did not affect the recovery of function likely due to the absence of plasminogen in the perfusate. Infusion of purified plasmin into isolated perfused hearts did not exacerbate I/R injury, however the concentration of plasmin infused was sub-physiological. These results indicate that plasmin causes disruption of myocyte attachment and viability independently of MMP activation *in vitro* and that inhibition of plasmin by DOX may reduce I/R-induced myocyte death *in vivo* through the inhibition of plasmin.

3.2. Introduction

Reperfusion of the myocardium following acute coronary occlusion has been shown to salvage myocytes and reduce infarct size (7); however, its benefit is limited due to reperfusion injury (9). Upon reperfusion, the extravasation of neutrophils and monocytes, release of inflammatory cytokines, generation of reactive oxygen species, and release of proteolytic enzymes contribute to additional myocyte dysfunction and death beyond that generated by ischemia alone (9). Reperfusion injury consists of both necrotic and apoptotic forms of cell death (118), and strategies aimed at reducing the extent of apoptosis or necrosis have been demonstrated to reduce infarct size (164-166). In adherent cell types, apoptotic cell death can be induced by disrupting interactions with the underlying ECM. Disruption of normal cell-ECM interactions has been shown to contribute to the induction of myocyte apoptosis both *in vitro* (77) and *in vivo* (78).

It has been demonstrated that ECM degradation occurs within minutes of myocardial ischemia and may be mediated in part by the early activation of MMPs (65, 68). MMPs are a family of zinc-dependent endopeptidases that are expressed as inactive zymogens and activated through proteolytic processing by other proteases (38). In studies using isolated perfused rat hearts, MMP inhibition reduces I/R-induced troponin I degradation and improves recovery of mechanical function (73). However, other ECM-degrading proteases are activated within the ischemic myocardium, including serine proteases of the plasminogen/plasmin system (167). In addition to its well-known role in clot lysis, plasmin also mediates pericellular proteolysis of ECM proteins both directly and through the activation of MMPs (167). Increased plasmin levels have been observed following coronary occlusion (69). The inactive plasminogen zymogen is proteolytically activated to plasmin by plasminogen activators. Urokinase-type plasminogen activator is upregulated following coronary occlusion in the pig (168) and in the mouse predisposes the heart to rupture following coronary occlusion (69). Broad-spectrum serine protease inhibition with aprotinin attenuates creatine kinase release following I/R and improves recovery of mechanical function in the rat (169) and dog (170). While these results suggest that MMPs and/or plasmin may have a role in mediating early myocardial ischemic injury, their effects on myocardial infarct size following I/R have not been investigated *in vivo*.

DOX, a member of the tetracycline family of antibiotics, has been shown to inhibit MMP expression and activity (145) and to preserve cardiac function following I/R injury (73). However, recent reports indicate DOX also directly inhibits cysteine

protease activity (171) and indirectly inhibits serine protease activity via inhibition of MMP-mediated degradation of endogenous serine protease inhibitors (60, 64).

In this study I hypothesized that DOX reduces infarct size *in vivo* following I/R injury by inhibiting MMPs or plasmin. The results presented here show that DOX treatment attenuated increases in plasmin and MMP-9 activities following myocardial I/R injury and reduced infarct size *in vivo*. Using a myocyte culture system, plasmin but not MMP-9 induced myocyte death by detachment, and this was inhibited by DOX. *In vitro* enzyme activity assays showed a specific and direct inhibition of plasmin by DOX. These results suggest that DOX may reduce myocyte death *in vivo*, at least in part, through the inhibition of plasmin.

3.3. Experimental Methods

3.3.1. *In vivo* rat study

3.3.1.1. Doxycycline treatment

Adult male Sprague-Dawley rats (Harlan, Indianapolis, IN) weighing 250-300 g were used. DOX (30 mg/kg per day; Sigma, St. Louis, MO) or water was administered orally beginning 48 hours before surgery and continuing 48 hours post-surgery. This DOX dose effectively blocks MMP activity in models of tissue injury and healing in the rat (172, 173). All procedures were approved by the Institutional Animal Care and Use Committee and conform to published NIH guidelines for animal research.

3.3.1.2. Surgery

Animals were anesthetized by intraperitoneal injection of ketamine (100 mg/kg) and xylazine (10 mg/kg), intubated, and positive-pressure ventilated with room air using a pressure-controlled ventilator (Kent Scientific, Torrington, CT). Following a left thoracotomy, the pericardium was opened. The left anterior descending coronary artery (LAD) was ligated by silk suture for 30 min, released, and the suture left in place as a point of reference. The chest was closed in layers, and the animal was extubated and allowed to recover. Successful occlusion and reperfusion were verified by visual inspection of left ventricle (LV) color. Sham animals were treated identically, except the ligature was not tightened.

3.3.1.3. Determination of infarct size

At 48 hours post-I/R, the animals were anesthetized as described above. The carotid artery was cannulated, and cold cardioplegia (4.0 g/L NaCl, 4.48 g/L KCl, 1.0 g/L NaHCO₃, 2.0 g/L glucose) was infused to induce cardiac arrest. A median sternotomy was performed, and the LAD was re-occluded in the same location as before. Trypan blue (0.4%) was infused via the carotid artery cannula to delineate the area-at-risk. The heart was then excised, sliced into 2-mm short-axis rings, and stained with triphenyltetrazolium chloride (TTC, 1.0%) to identify viable myocardium within the area-at-risk. Apical and basal surfaces of each slice were photographed. The areas-at-risk and infarct areas were determined by a blinded observer using computer-assisted planimetry (NIH Image).

3.3.1.4. Tissue collection

At 48 hours post-I/R, the hearts were rapidly excised and perfused with cold cardioplegia to remove blood. LV freewall (ischemic region) and septum (non-ischemic region) were separated, flash frozen, and stored at -80°C until assayed. Except where noted otherwise, tissue samples were homogenized on ice in lysis buffer (50 mM Tris pH 7.4, 150 mM NaCl, 5 mM CaCl_2 , 0.2 mM NaN_3 , 0.1% Triton X-100). Lysates were cleared by centrifugation at 12,000 g for 10 min at 4°C . Protein concentrations of the tissue extracts were determined using the Bio-Rad Protein Assay (Bio-Rad, Hercules, CA) or the BCA Assay (Pierce, Rockford, IL) with a BSA standard.

3.3.1.5. Myeloperoxidase (MPO) assay

The MPO assay was performed as previously described (76) with modifications. Tissue samples were homogenized in MPO lysis buffer (50 mM KH_2PO_4 pH 6.0, 0.5% hexadecyltrimethylammonium bromide (Sigma) and incubated on ice for 30 min. Lysates were cleared by centrifugation at 12,000 g for 10 min at 4°C and the supernatants reacted with 0.4 mM tetramethylbenzidine (Sigma) and 0.006% H_2O_2 in 50 mM KH_2PO_4 at pH 6.0. Absorbance at 655 nm was continuously monitored.

3.3.1.6. Nitrotyrosine quantification

Nitrotyrosine content in the heart samples was determined using the Nitrotyrosine ELISA kit per manufacturer instructions (Hycult Biotechnology, Uden, The Netherlands) with modifications. A nitrotyrosine standard curve was generated per manufacturer instructions. Tissue samples were homogenized in “Dilution Buffer”

and cleared by centrifugation at 12,000 g for 10 min at 4°C. To each well of the ELISA plate was added 200 µl sample, and the plate was incubated overnight at 4°C. After washing 4 times with “Wash Buffer”, biotinylated anti-nitrotyrosine antibody tracer was added and the plate incubated for 2 hours at room temperature. After washing 4 times, streptavidin-peroxidase was added for 1 hour at room temperature. After washing 4 times, TMB substrate was added and the plate incubated for 1 hour at room temperature. “Stop solution” was then added and the absorbance at 405 nm was determined.

3.3.1.7. Hemodynamics

Hemodynamic measurements were performed as previously described (68). LV and aortic pressures were measured at 4 weeks post-I/R in anesthetized, closed-chest rats using a Millar pressure transducer (Millar Instruments, Houston, TX) inserted via the carotid artery. Data were digitally recorded (DataQ Instruments, Akron, OH).

3.3.1.8. LV morphology

LV morphology was assessed as previously described (68). At 4 weeks post-I/R, the hearts were rapidly excised and perfused with cold cardioplegia to remove blood. The LV was fixed in formalin, embedded in wax, and sectioned (10 µm) from the base of the LV, spanning the length of the scar. Sections that most clearly transversed the infarct region were stained with Milligan’s trichrome. Measurements included scar size, internal and external LV diameters, and LV freewall and septal wall thicknesses. Ventricular diameters were derived from exterior and interior LV

circumferences, whereas wall thickness measurements at the center of the infarct and opposing (septal) wall were made in triplicate. Hearts with scar sizes of less than 5% of the LV were not included in the analysis.

3.3.2. Neonatal rat ventricular myocyte (NRVM) and fibroblast (NRVF) cultures

3.3.2.1. NRVM and NRVF isolation and culture

NRVMs were prepared as previously described (174). The hearts of 1-2 day old Sprague-Dawley rats were excised, minced, and digested with collagenase type 2 (80 U/ml, Worthington, Lakewood, NJ) and pancreatin (0.6 mg/ml, Sigma). The dispersed cells were applied to a discontinuous percoll density gradient, and the NRVMs and NRVFs were separated.

The NRVMs were plated on 1% gelatin-coated tissue culture dishes to a density of 2.5×10^5 cells/cm² in plating media (68% DMEM, 17% M199, 10% horse serum, 5% FBS) and incubated at 37°C in a 5% CO₂ humidified environment. The NRVMs were cultured for 2 days in plating media, by which time the cells were spontaneously contracting. This purification protocol resulted in cultures of >95% myocytes as assessed by visual inspection of beating cells and morphological characteristics. The media was then replaced with serum-free maintenance media (80% DMEM, 20% M199) until experimentation (1-2 days).

The NRVFs were plated on tissue culture dishes in plating media. After 1 hour the dishes were washed with plating media to remove non-adherent cells, and the remaining adherent NRVFs were incubated in fresh plating media at 37°C in a 5%

CO₂ humidified environment. Upon reaching 80% confluence the media was replaced with serum-free maintenance media for 24 hours prior to experimentation.

3.3.2.2. Plasminogen and MMP treatments

NRVMs or NRVMs were stimulated with bovine plasminogen (Sigma), porcine or human plasmin (Sigma), human recombinant active MMP-9 (Calbiochem, La Jolla, CA), human recombinant proMMP-3 (Calbiochem), or human fibroblast-derived proMMP-2/active MMP-2 mix (Sigma) for 16-48 hours in the presence or absence of protease inhibitors.

In studies involving DOX, the broad-spectrum hydroxamate-based MMP inhibitors GM6001 (Sigma) and MMP Inhibitor III (Calbiochem), or the serine protease inhibitor aprotinin (Calbiochem), the drug was added 1 hour prior to stimulation with plasminogen or MMPs.

3.3.2.3. Cell detachment assay

Cell detachment was assessed as previously described (175). Following treatment, the wells were rinsed with PBS, and the remaining viable adherent cells were assessed using a methylthiazolotetrazolium (MTT)-based *in vitro* toxicology assay kit (Sigma) per manufacturer instructions.

3.3.2.4. Annexin V labeling

NRVMs were grown on gelatin-coated coverslips. Annexin V and propidium iodide labeling were performed using the BD ApoAlert Annexin V kit per manufacturer instructions (BD Biosciences, San Diego, CA). The cells were then

fixed with 3.4% formaldehyde and counterstained with 4',6-diamidino-2-phenylindole dihydrochloride (DAPI, Sigma).

3.3.3. Isolated, perfused rat hearts

3.3.3.1. Langendorff method

Male Sprague-Dawley rats (Harlan) weighing 200-225 g were used. The animals were anesthetized by intraperitoneal injection of ketamine (100 mg/kg) and xylazine (10 mg/kg) coadministered with heparin (1000 U/kg), intubated, and positive-pressure ventilated with room air using a pressure-controlled ventilator (Kent Scientific). The heart was quickly excised and placed into a dish of ice-cold Krebs-Henseleit (K-H) buffer (118 mM NaCl, 4.7 mM KCl, 1.2 mM KH₂PO₄, 1.2 mM MgSO₄, 2.5 mM CaCl₂, 0.5 mM EDTA, 11 mM glucose, 25 mM NaHCO₃). The aorta was quickly cannulated to a 14-gauge IV catheter connected to a Langendorff perfusion system. After cannulation, the heart was retrogradely perfused at a constant pressure of 80 mmHg with K-H buffer. The K-H buffer was prefiltered to 0.22 μm, continuously bubbled with 95% O₂/5% CO₂, and maintained at 37°C. The time from removal of the heart to perfusion was 1-2 min.

The left atrium was removed, and a water-filled balloon connected to a pressure transducer (Grass-Telefactor, West Warwick, RI) was inserted into the LV through the mitral valve. The balloon volume was adjusted to achieve an end-diastolic pressure of 8-12 mmHg. Pacing leads attached to an electrical stimulator (Grass-Telefactor) were placed on the right atrium, and the heart was paced at 300 beats/min. Pacing was stopped during ischemia and resumed during reperfusion. LV pressure

was digitally acquired (DataQ Instruments) throughout the experiment. At various times coronary effluent was collected for 1 min for determination of coronary flow rate. At the end of the protocol the hearts were removed, flash frozen, and stored at -80°C.

3.3.3.2. Ischemia-reperfusion protocol

3.3.3.2.1. Tranexamic acid (TEA) treatment

After 45 min of aerobic perfusion, hearts were subjected to 25 min of global, no-flow ischemia (GNFI) by clamping the perfusion line. The clamp was then released and the hearts reperfused for 80 min. After 15 min of aerobic perfusion, the plasmin inhibitor TEA (200 mg/L, Sigma) or vehicle (water) was infused into hearts for the remainder of the experiment (Figure 3-1A).

3.3.3.2.2. Plasmin treatment

After 25 min of aerobic perfusion, hearts were subjected to 20 min of GNFI and 75 min reperfusion. After 20 min of aerobic perfusion, human plasmin (2.1 µg/ml; Sigma) or vehicle (water) was infused into hearts for the last 5 min of aerobic perfusion and the first 10 min of reperfusion (Figure 3-1B).

3.3.3.3. Creatine kinase (CK) release

Coronary effluent was collected on ice for measurement of CK activity before ischemia and during reperfusion. To each well of a microtiter plate was added 100 µl of coronary effluent and 200 µl of CK reagent (Pointe Scientific, Canton, MI). The rate of change in absorbance of NADH was determined spectrophotometrically at 340

nm for 15 min at 25°C. The enzyme activity was calculated using the molar extinction coefficient of NADH ($\epsilon = 6.22$).

3.3.4. Plasmin activity

3.3.4.1. Plasmin peptide substrate hydrolysis

A chromogenic peptide substrate was used to assess plasmin activity. The sample was reacted with 0.5 mM N-p-tosyl-gly-pro-lys-pNA (Sigma) in Tris buffer (50 mM, pH 7.5). The rate of change in absorbance at 405 nm was continuously monitored.

3.3.4.2. Fibrin zymography

Fibrin zymography was performed as previous described (176). The samples were diluted 1:1 in 2X non-reducing sample buffer (125 mM Tris pH 6.8, 4% SDS, 20% glycerol) and electrophoresed on 10% poly-acrylamide gels copolymerized with 1.2 mg/ml fibrinogen (Sigma) and 0.01 NIH units/ml thrombin (Sigma). Gels were washed in renaturation buffer (2.5% Triton X-100) and then in developing buffer (50 mM Tris pH 7.4, 200 mM NaCl, 5 mM CaCl₂, 0.02% Brij 35) for 30 min each. Gels were then incubated in fresh developing buffer overnight at 37°C with shaking. Following incubation, the gels were stained with 0.1% Coomassie Blue G-250, and bands of gelatinolytic activity were digitally quantified using Kodak 1D (Eastman Kodak, Rochester, NY).

3.3.5. MMP activity

3.3.5.1. Gelatin zymography

Gelatin zymography was performed as previously described (157). The samples were diluted 1:1 in 2X non-reducing sample buffer (125 mM Tris pH 6.8, 4% SDS, 20% glycerol) and electrophoresed on 7.5% poly-acrylamide gels copolymerized with 0.1% gelatin. An internal control (purified human MMP-2/MMP-9, Chemicon, Temecula, CA) was loaded to normalize activities between gels. Gels were washed in renaturation buffer (2.5% Triton X-100) and then in developing buffer (50 mM Tris pH 7.4, 200 mM NaCl, 5 mM CaCl₂, 0.02% Brij 35) for 30 min each. Gels were then incubated in fresh developing buffer overnight at 37°C with shaking. Following incubation, the gels were stained with 0.1% Coomassie Blue G-250, and bands of gelatinolytic activity were digitally quantified (Kodak 1D).

3.3.5.2. OmniMMP assay

A fluorescence-quenched peptide substrate probe was used to assess global MMP activity. Cleavage of the peptide results in release of the quencher and an increase in fluorescence. The samples were reacted with 10 μM OmniMMP substrate (Mca-Pro-Leu-Gly-Leu-Dpa-Ala-Arg, BIOMOL Research Laboratories, Plymouth Meeting, PA) in assay buffer (50 mM Tris pH 7.5, 150 mM NaCl, 5 mM CaCl₂). Fluorescence (335 nm excitation, 405 nm emission) was monitored continuously at 37°C for 30 min using a fluorescence microplate reader (Bio-Tek Instruments, Winooski, VT).

3.3.6. Immunoblots

Immunoblotting was performed as previously described (76). The samples were diluted 1:1 with 2X reducing sample buffer (17% glycerol, 8.7% β-ME, 5.2%

SDS, 109 mM Tris pH 6.8), electrophoresed on 7.5% poly-acrylamide gels, and transferred to PVDF membranes (Millipore, Bedford, MA). Blots were probed with a rabbit polyclonal anti-plasminogen antibody (1:250, Biogenesis Ltd., Kingston, NH), a mouse monoclonal anti-plasminogen antibody (177) (1:200), a mouse monoclonal anti- α -actinin antibody (1:400, Upstate U.S.A., Charlottesville, VA), or a rabbit polyclonal anti- β_{1D} -integrin antibody (178) (1:10,000) followed by appropriate horseradish peroxidase-conjugated secondary antibodies (1:5000, Santa Cruz Biotechnology, Santa Cruz, CA or Chemicon). The immunoreactive proteins were detected using an enhanced chemiluminescence reaction kit (Amersham Biosciences, Piscataway, NJ). Blots were digitally scanned and band intensities were quantified (Kodak 1D).

3.3.7. *In vitro* plasmin inhibition by DOX

Human plasmin (100 nM; Sigma) was incubated with various concentrations of DOX in assay buffer (50 mM Tris pH 7.5, 150 mM NaCl, 5 mM CaCl₂) for 1 hour at room temperature. N-p-tosyl-gly-pro-lys-pNA was then added to a final concentration of 0.5 mM and the increase in absorbance at 405 nm was continuously monitored. The data were fit to the sigmoidal Hill equation: $Y = \frac{[DOX]^n}{[DOX]^n + k^n}$ (Prism, GraphPad Software, San Diego, CA). Y is the rate of substrate hydrolysis as a fraction of maximal substrate hydrolysis, n is the Hill coefficient, and k is the DOX concentration at which activity is half maximal (IC₅₀).

To assess the mode of inhibition of plasmin by DOX, plasmin (100 nM) was incubated with various concentrations of DOX in assay buffer for 1 hour at room

temperature. N-p-tosyl-gly-pro-lys-pNA was then added to a final concentration of 20 μ M to 1 mM. Data were analyzed using the Lineweaver-Burk model with linear regression.

To assess the calcium-dependence of the inhibition of plasmin by DOX, plasmin (100 nM) was incubated with 100 μ M DOX, 100 μ M minocycline (Sigma), or 100 μ M tetracycline (Sigma) in buffer (50 mM Tris pH 7.5, 150 mM NaCl) containing 5 mM CaCl₂, 5 mM MgSO₄, 5 mM Ba(OH)₂, or 5 mM ZnCl₂ for 1 hour at room temperature. Plasmin activity was then determined using N-p-tosyl-gly-pro-lys-pNA as described above.

3.3.8. Statistical analysis

Results are expressed as mean \pm SEM except where noted. Comparisons between means were analyzed, as appropriate, by student's t-test or one-way ANOVA followed by Bonferroni t-test. A value of $p \leq 0.05$ was considered statistically significant.

3.4. Results

3.4.1. *In vivo* rat study

3.4.1.1. Doxycycline reduced infarct size

To assess the effects of DOX on infarct size following myocardial I/R injury, rats were subjected to 30 min of coronary occlusion followed by 48 hours of reperfusion. In the vehicle group, the mean area at risk was 46.0 \pm 1.6% of the LV, and the infarct area was 39.9 \pm 5.0% of the area at risk. In the DOX-treated group, the

mean area at risk was comparable ($50.0 \pm 3.1\%$ of LV), but the infarct area was significantly reduced to $25.2 \pm 4.9\%$ of the area at risk (Figure 3-2).

3.4.1.2. Doxycycline attenuated MMP-9 upregulation in the ischemic region

Gelatin zymography of 48 hours post-I/R tissue homogenates from the ischemic region and septum revealed bands corresponding to 92 kDa MMP-9 and 72 and 75 kDa MMP-2 (Figure 3-3A). Densitometric analysis revealed MMP-9 levels were increased 3-fold in the ischemic region of the I/R group compared with Sham, and this increase was attenuated in the I/R+DOX group (Figure 3-3B). MMP-9 levels in the septum remained unchanged between groups; no differences in MMP-2 levels were observed in any group.

3.4.1.3. Doxycycline had no effect on global MMP activity in the ischemic region

Since gelatin zymography allows only the detection of MMP-2 and MMP-9, MMP activity was measured using a broad-spectrum MMP peptide substrate to assess the global MMP activity present in the hearts at 48 hours post-I/R. MMP activity was significantly higher in the ischemic region of the I/R group compared to the Sham group (Figure 3-4). DOX treatment did not reduce MMP activity in the ischemic region of I/R+DOX compared with I/R. Although the Sham+DOX group also had higher MMP activity compared with Sham, it did not reach statistical significance. No significant differences in MMP activity were observed between groups in the septum.

3.4.1.4. Doxycycline did not inhibit the inflammatory response

Since MMP-9 is associated with neutrophil infiltration in other models of MI (76, 179), I assessed the capacity of DOX to inhibit neutrophil accumulation in the

myocardium by measuring MPO activity. MPO is an enzyme located within the primary granules of neutrophils and has commonly been used as a marker of tissue neutrophil content (180). At 48 hours post-I/R, MPO activity in the ischemic region in both the I/R and I/R+DOX groups was significantly higher compared to septum, indicating infiltration of neutrophils into the ischemic region (Figure 3-5). No significant difference in MPO activity in the ischemic region was observed between the I/R and I/R+DOX groups, indicating DOX treatment did not inhibit neutrophil infiltration into the ischemic region.

3.4.1.5. I/R did not generate nitrotyrosine

Peroxynitrite formed under conditions of oxidative stress can react with tyrosine residues on proteins to form nitrotyrosine. Therefore, nitrotyrosine was assayed at 48 hours post-I/R using a commercially available ELISA kit as a marker of oxidative stress. The reliable limit of detection of this kit was found to be ~25 nM (Figure 3-6). However, in all heart samples the measured concentration of nitrotyrosine was below this limit, suggesting a lack of peroxynitrite generation.

3.4.1.6. Doxycycline reduced plasmin levels in the ischemic region

Since DOX has inhibitory effects on proteases other than MMPs, I assessed the effects of DOX on plasminogen and plasmin levels in the I/R hearts. Immunoblots revealed a significant increase in plasminogen in the ischemic region compared to septum in both the I/R group and the I/R+DOX group (Figures 3-7A and B). DOX treatment tended toward reduced plasminogen levels in the ischemic region compared

with the untreated I/R group, but this did not reach statistical significance (Figure 3-7B).

An immunoreactive band of 68 kDa also appeared in the ischemic region of the I/R and I/R+DOX groups, consistent with the active plasmin form of the protease (Figure 3-7A). Plasmin levels were significantly increased in the ischemic region compared to septum in I/R and I/R+DOX. DOX treatment significantly reduced plasmin levels in the ischemic region of I/R+DOX compared with I/R (Figure 3-7C).

3.4.1.7. Hemodynamic function was not compromised by I/R

Hemodynamic function was measured at 4 weeks post-I/R. The results are summarized in Table 3-1. No significant differences were observed between Sham and I/R or among any groups in left ventricular end-diastolic pressure, peak systolic pressure, developed pressure, or max \pm dP/dt. In addition, no differences were observed among any groups in aortic systolic pressure, diastolic pressure, or mean arterial pressure.

3.4.1.8. LV dimensions and scar size were not affected by I/R

LV morphometry was performed at 4 weeks post-I/R. The results are summarized in Table 3-2. Heart weights and heart weight to body weight ratios were similar for all groups. A significant increase in the LV weight to body weight ratio was observed in the I/R+DOX group compared with the I/R group. The Sham+DOX group also showed a slight increase in the LV weight to body weight ratio compared with the Sham group, but this did not reach statistical significance. No significant differences were observed between Sham and I/R rats in outer or inner LV diameters,

and DOX treatment did not result in a significant change in LV diameters. No significant differences were observed between Sham and I/R rats in ischemic and septal wall thicknesses, and DOX treatment did not result in a significant change in wall thicknesses. In addition, no significant difference in scar area was observed between I/R and I/R+DOX.

3.4.2. NRVM & NRVF cultures

3.4.2.1. MMPs did not cause NRVM detachment or death

Given the enhanced levels of MMP-9 observed with I/R injury *in vivo*, I investigated the effects of recombinant, 83 kDa active MMP-9 on NRVMs *in vitro*. MMP-9 was added to NRVMs up to a concentration of 2 nM, which corresponds to serum concentrations of MMP-9 reported in humans post-MI (181). DOX co-treatment resulted in a dose-dependent inhibition of MMP activity, and the broad-spectrum MMP inhibitor GM6001 completely inhibited MMP activity by 1 μ M (Figures 3-8A and B). Interestingly, media from DOX-treated cells showed a dose-dependent loss of MMP zymographic activity, whereas GM6001-treated cells retained MMP zymographic activity (Figure 3-8B).

MMP-9 did not cause cell detachment nor induce cell death at any concentration tested (Figure 3-8C). A slight but significant decrease in the number of viable adherent cells was observed with 25 and 50 μ M GM6001, likely due to cytotoxicity at high concentrations. The small increase in the number of viable adherent cells with 50 and 100 μ M DOX compared to controls (Figure 3-8C) suggests

that DOX may reduce NRVM detachment that occurs under normal, untreated culture conditions.

The effects of stimulation of NRVMs with proMMP-3 and a proMMP-2/active MMP-2 mixture for 48 hours were also assessed (Figure 3-9). Addition of proMMP-3 (20 nM) did not lead to increased MMP activity in the culture as assessed by hydrolysis of a peptide substrate. However, the co-administration of a low, catalytic concentration of plasminogen (5 µg/ml) with proMMP-3 resulted in a 51% increase in MMP activity. Addition of a mixture of proMMP-2 and active MMP-2 (20 nM) resulted in a 45% increase in MMP activity in the culture, and co-administration of 5 µg/ml plasminogen with this MMP-2 mixture resulted in a 108% increase in MMP activity (Figure 3-9A). Although addition of MMP-2 or MMP-3 with plasminogen for 48 hours resulted in increased MMP activity, no NRVM detachment was noted when the cells were observed by microscopy (Figure 3-9B). In contrast, 60 µg/ml plasminogen led to an obvious loss of NRVM attachment and viability (Figure 3-9B).

3.4.2.2. NRVMs and NRVMs convert plasminogen to plasmin

Addition of plasminogen to NRVMs for 48 hours led to a dose-dependent and time-dependent increase in plasmin activity as assessed by hydrolysis of a plasmin-specific peptide substrate (Figures 3-10A and B). Addition of plasminogen to NRVMs also led to a time-dependent increase in plasmin activity (Figure 3-10B).

3.4.2.3. Plasmin induced NRVM, but not NRVM, detachment and death

The addition of 60 µg/ml plasminogen to NRVMs for 48 hours resulted in cell rounding and a loss of cell-cell and cell-matrix interactions (Figure 3-11A). MTT

assay results showed that ~50% of the NRVMs were detached by 48 hours of stimulation with 60 $\mu\text{g/ml}$ plasminogen (Figures 3-11B and C). Interestingly, 60 $\mu\text{g/ml}$ plasminogen did not result in NRVF detachment and death (Figure 3-11C). To verify that NRVM detachment was due to plasmin activity, the cells were stimulated with 60 $\mu\text{g/ml}$ purified plasmin. Cell detachment occurred more rapidly with plasmin than plasminogen, as 92% of the NRVMs were detached by 16 hours of stimulation. Immunoblots of cell lysate against β_{1D} -integrin revealed an immunoreactive doublet of ~125 kDa, corresponding to the mature and precursor forms of the protein as previously described (178). Plasmin stimulation resulted in the loss of mature β_{1D} -integrin (Figure 3-11D), the primary β_1 -integrin isoform expressed in the postnatal heart (182).

Plasminogen-treated NRVMs showed increased membrane staining with annexin V and increased nuclear fragmentation (Figure 3-11E). The cells did not stain with propidium iodide, indicating maintenance of membrane integrity. Surprisingly, many of the detached NRVMs continued to spontaneously beat, also indicating membrane integrity. Thus, these data are consistent with early apoptotic cell death.

3.4.2.4. Doxycycline inhibited plasmin activity in culture and preserved NRVM attachment

I assessed the effects of DOX on plasminogen-treated NRVMs. DOX co-treatment resulted in a dose-dependent decrease in plasmin activity as assessed by hydrolysis of a peptide substrate, with an apparent IC_{50} of ~36 μM (Figure 3-12A). DOX also resulted in a time-dependent decrease in plasmin activity as assessed by

fibrin zymography (Figure 3-12B). DOX preserved NRVM attachment in the presence of 60 $\mu\text{g/ml}$ plasminogen in a dose-dependent manner, with 50 μM completely preserving attachment (Figure 3-12C). However, the broad-spectrum MMP inhibitor GM6001 did not inhibit plasmin activity (Figure 3-12A) nor did it preserve myocyte attachment (Figure 3-12C). DOX also completely preserved levels of mature β_{1D} -integrin while GM6001 did so to a much lesser extent (Figure 3-11D).

To verify that the reduction in plasmin activity by DOX was due to the direct inhibition of plasmin rather than inhibition of the conversion of plasminogen to plasmin, NRVMs were stimulated with purified plasmin (60 $\mu\text{g/ml}$) for 16 hours in the presence or absence of DOX. 100 μM DOX inhibited plasmin activity by 72% (Figure 3-12A), demonstrating plasmin to be a direct target of DOX.

Media from NRVMs treated for 16 hours with 60 $\mu\text{g/ml}$ plasmin or plasminogen revealed a diffuse immunoreactive doublet at the approximate molecular weight of pure plasmin (Figure 3-12D). Interestingly, DOX co-treatment reduced plasmin levels in the media of both the plasmin-treated (lane 3) and plasminogen-treated cells (lane 5).

3.4.2.5. Plasmin did not activate myocyte-derived MMPs but did activate co-culture-derived MMPs

Since plasmin is a known activator of MMPs, I also measured MMP activity following 48 hours of plasminogen (60 $\mu\text{g/ml}$) stimulation using the OmniMMP substrate. No increase in MMP activity was observed in NRVMs (Figure 3-13A). However, treatment of NRVM and NRVF co-cultures with plasminogen yielded a 2.2-

fold increase in MMP activity (Figure 3-13B), implicating fibroblasts as the primary source of plasmin-activated MMPs in the heart. Co-treatment with DOX, the plasmin inhibitor aprotinin, or the broad-spectrum MMP inhibitors GM6001 and Inhibitor III attenuated the increase in MMP activity induced by plasminogen (Figure 3-13B).

3.4.3. *In vitro* plasmin inhibition

The addition of DOX to plasmin (100 nM) in buffer containing 5 mM Ca^{2+} resulted in a dose-dependent inhibition of plasmin activity with an IC_{50} of 18.4 μM as determined by hydrolysis of a peptide substrate (Figure 3-14A).

The presence of Ca^{2+} in the buffer was necessary for inhibition of plasmin by DOX. To determine whether other divalent metal ions would allow for the inhibition of plasmin by DOX, I assayed plasmin activity in the presence of Mg^{2+} or Ba^{2+} . DOX did not inhibit plasmin in the presence of Mg^{2+} or Ba^{2+} (Figure 3-14B). Inhibition of plasmin was specific to DOX, as neither MIN nor TET inhibited plasmin in the presence of Ca^{2+} , Mg^{2+} , or Ba^{2+} (Figure 3-14B). The addition of Zn^{2+} completely eliminated plasmin activity even in the absence of any of the tetracyclines, likely due to a toxic fixative effect of Zn^{2+} on the protease.

The mode of inhibition of plasmin by DOX (ie, competitive, noncompetitive, uncompetitive, or mixed) was assessed by holding the concentration of DOX constant at a series of fixed values and measuring the effect of increasing the substrate on the initial reaction rate in the presence of Ca^{2+} . Sigmoidal enzyme kinetic plots showed that V_{max} decreased with increasing concentrations of DOX, suggesting either a

noncompetitive or uncompetitive mode of inhibition (Figure 3-15A). A Lineweaver-Burk plot yielded straight lines for DOX that did not intersect on either the X-axis or Y-axis, indicating the inhibition of plasmin by DOX was likely mixed inhibition (Figure 3-15B).

3.4.4. Isolated hearts

3.4.4.1. Plasmin inhibition did not protect against I/R injury

To more specifically investigate the role for plasmin inhibition in protection against I/R injury, the plasmin inhibitor tranexamic acid (TEA, 1.3 mM) was tested in isolated, perfused rat hearts subjected to 25 min of global, no-flow ischemia and 80 min of reperfusion. TEA has an affinity for the lysine binding sites of plasmin(ogen) and prevents plasmin(ogen) binding to lysine-containing substrates, with an IC_{50} of 20 μ M (183). Therefore, TEA was infused into hearts at a concentration higher than its IC_{50} to ensure adequate inhibition of plasmin in this system. The recovery of mechanical function, as measured by LV developed pressure, was similar in both the control and TEA-treated groups (Figure 3-16A). In addition, the release of creatine kinase (CK) was similar in both groups (Figure 3-16B), as were the coronary flow rates (Figure 3-16C).

3.4.4.2. Plasmin addition did not worsen I/R injury

Since the crystalloid perfusion buffer lacked the plasminogen that would be found in blood, I examined the effects of adding plasmin to the perfusion buffer in isolated, perfused rat hearts subjected to 20 min of GNFI and 75 min of reperfusion.

Hearts were infused with plasmin (2.1 $\mu\text{g/ml}$) during the last 5 min of aerobic perfusion and the first 10 min of reperfusion. No differences were seen between control and plasmin-treated hearts in LV developed pressure (Figure 3-17A), CK release (Figure 3-17B), or coronary flow rate (Figure 3-17C). The infusion of plasmin resulted in a measurable increase in plasmin activity in the effluent during the time of infusion (Figure 3-18A). MMP activity in the effluent increased ~6-fold immediately upon reperfusion. However, plasmin treatment did not result in a further increase in MMP activity compared with control hearts (Figure 3-18B). Plasmin treatment also did not increase MMP activity in the heart homogenates at the end of the experiment (Figure 3-18C).

Since plasmin treatment resulted in the loss of mature β_{1D} -integrin in cultured NRVMs (Figure 3-11D), β_{1D} -integrin levels were also assessed in the isolated, perfused rat hearts treated with plasmin. Immunoblots of heart homogenates against β_{1D} -integrin revealed an immunoreactive doublet of ~125 kDa, corresponding to the mature and precursor forms of the protein as previously described (178). Plasmin treatment tended toward reduced mature β_{1D} -integrin levels in the plasmin-treated group (Figure 3-19), but this did not reach statistical significance ($p = 0.13$).

3.5. Discussion

The unique observations from this study were that DOX pretreatment significantly reduced infarct size 2 days post-I/R in the rat heart *in vivo*. The smaller infarct size correlated with reduced MMP-9 and plasmin levels in the ischemic region,

suggesting a possible role for these proteases in mediating I/R injury. The assessment of MMPs and plasmin effects on cultured NRVMs demonstrated that physiological concentrations of plasmin, but not MMPs, were capable of inducing cell death by detachment. DOX inhibited plasmin activity in culture and preserved NRVM attachment, suggesting that DOX may reduce myocyte death *in vivo*, at least in part, through the inhibition of plasmin.

Previous studies demonstrated latent (92 kDa) and active (83 kDa) MMP-9 are upregulated within hours of I/R and are primarily derived from neutrophils (76, 179). I observed increases in 92 kDa MMP-9 in the ischemic region 48 hours post-I/R correlating with increased neutrophil content. However, increases in 83 kDa active MMP-9 were not observed. A plausible explanation for lack of increased 83 kDa MMP-9 is that MMP-9 activation and subsequent clearance from the myocardium may occur within the first 48 hours following I/R, since neutrophil accumulation peaks within the first 24 hours of reperfusion in the rat (184).

I found that pretreatment of rats with DOX reduced tissue levels of 92 kDa MMP-9 within the ischemic region but did not alter neutrophil content, suggesting that MMP-9 levels may not necessarily follow neutrophil infiltration. Reductions in MMP-9 levels without a concomitant reduction in inflammatory cell infiltrate have also been reported with DOX treatment in a mouse model of abdominal aortic aneurysm (185). Furthermore, MMP-9-deficient mice subjected to I/R showed only slight reductions in neutrophil infiltration into the I/R region (69). Thus, my results

indicate that although DOX reduced 92 kDa MMP-9 levels, it did not appear to affect the acute inflammatory response following I/R.

Although DOX treatment reduced 92 kDa MMP-9 levels, global MMP activity within the ischemic region was not reduced by DOX as assessed by OmniMMP substrate hydrolysis. Since the 92 kDa form of MMP-9 is the inactive zymogen form of the protease, the increase in 92 kDa MMP-9 with I/R and attenuation by DOX may not affect global MMP activity within the heart. Gelatin zymography detects only MMP-2 and MMP-9, and it is likely that the changes in MMP activity within the hearts post-I/R reflect changes in the activities of other MMPs. MMP-1, -3, -13, and -14 have also been identified within the mammalian myocardium (39) and may account for the observed changes in activity. However, it is difficult to quantify the activity of a given MMP isoform due to overlapping substrate specificities and a lack of isoform-specific substrate probes.

Since DOX has been shown to have antioxidant properties (153), I assessed its ability to reduce oxidative stress in the I/R hearts. Under conditions of oxidative stress, including inflammation and reperfusion injury, peroxynitrite can form when superoxide reacts with nitric oxide (186). Peroxynitrite can modify proteins by interacting with and nitrating tyrosine residues to form nitrotyrosine (187). Increased nitrotyrosine levels have been observed with I/R in isolated, perfused rat hearts (81) and after 5 hours reperfusion in an *in vivo* rat model (188). In contrast to these previous studies (81, 188), I did not observe an increase in nitrotyrosine levels above the limit of detection for the ELISA assay. However, detection of nitrotyrosine may

depend on the model of I/R used and the length of reperfusion. In my study nitrotyrosine levels were assayed in an *in vivo* model after 48 hours reperfusion, much later than in previous studies (81, 188). It is possible that nitrotyrosine levels were increased before 48 hours of reperfusion, but earlier time points were not tested in this study.

To determine whether the protective effects of DOX seen at 48 hours post-I/R translated into long-term benefits in myocardial structure and function, I assessed contractile function and LV structure at 4 weeks post-I/R. LV function was comparable between Sham and I/R groups in all parameters measured, suggesting that 30 min of ischemia did not cause sufficient injury to compromise function after 4 weeks of reperfusion in the rat. Nonetheless, it is important to note that no differences were seen in DOX-treated versus untreated animals, indicating DOX treatment did not compromise contractile function at 4 weeks. Likewise, analysis of heart sizes and dimensions revealed no significant differences between Sham and I/R groups. The I/R+DOX group revealed a small, but significant, increase in the LV wt/BW ratio compared with I/R. However, the difference in LV wt/BW ratios between I/R+DOX and I/R is likely of little importance given the similar LV diameters and wall thicknesses between these groups and the comparable dimensions between Sham and I/R groups. The lack of a reduction in scar size with DOX treatment was surprising in light of the reduced infarct size at 48 hours post-I/R and our previously published studies using a permanent occlusion model of MI (149). Thus, although DOX exerted an early cardioprotective effect, it may only delay myocyte death and the pathogenic

processes involved in I/R injury. Whether DOX treatment beyond 48 hours post-I/R would confer protection at later time points remains to be determined.

The integrity of cell-matrix interactions is necessary for myocyte survival both *in vitro* (77, 126) and *in vivo* (78). To investigate whether reduced infarct size was due to reduced MMP-9 activity with DOX, I investigated the effects of MMP-9 on cell survival in cultures of NRVMs. Addition of physiological concentrations of MMP-9 did not alter NRVM attachment or viability, suggesting MMP-9 alone is not sufficient to directly disrupt myocyte-matrix interactions. DOX and GM6001 both effectively inhibited global MMP activity. Interestingly, whereas GM6001 did not inhibit MMP-2 or MMP-9 zymographic activity due to dissociation of the inhibitor during electrophoresis, DOX reduced MMP-2 and MMP-9 zymographic activity. This suggests DOX treatment causes a loss of functional MMP-2 and MMP-9 protein or that DOX does not dissociate from the MMP during zymography. Therefore, MMP inhibition by DOX appears to occur by different mechanisms than GM6001.

The effects of additional MMPs on NRVMs were also explored. Although the addition of MMP-2 and MMP-3 with a small, catalytic amount of plasminogen increased MMP activity in the NRVM cultures, it did not cause cell detachment. These results in combination with the MMP-9 results provide evidence against a cytotoxic role of MMPs against myocytes in culture. However, it is possible that MMPs contribute to myocardial injury under the vastly different conditions present *in vivo* during I/R.

Increases in the serine protease plasmin and its zymogen, plasminogen, were also noted within the ischemic region 2 days following I/R. A study by Heymans et al. (69) showed similar increases in plasminogen and plasmin levels within the infarct region of mice. Plasminogen is produced primarily by the liver and is maintained in plasma at a high concentration of ~220 µg/ml in rats (189). The increased plasminogen levels observed following I/R suggest leakage of plasminogen into the myocardium due to increased microvascular permeability. uPA expression has been shown to be increased in the ischemic heart (168), likely promoting activation of extravasated and endogenous plasminogen and increasing plasmin levels within the myocardium

Studies using knockout mice have suggested a central role for plasmin in mediating inflammatory, wound healing, and remodeling processes post-MI either directly or by activation of MMPs (69, 190). uPA knockout mice subjected to MI show reduced plasmin levels and impaired leukocyte infiltration, reduced incidence of cardiac rupture, reduced MMP-2 and MMP-9 activities, and impaired healing and scar formation (69). These observations suggest that plasmin activation may mediate ECM degradation, allowing infiltration of inflammatory and wound-healing cells, but also potentially reducing the tensile strength of the infarcted myocardium. Myocyte death occurs *in vivo* as a result of disruption of normal myocyte anchorage (78), suggesting ECM proteolysis by plasmin or subsequent activation of MMPs could disrupt myocyte-matrix interactions and lead to cell death.

To determine whether plasmin could degrade myocyte-matrix attachments and whether DOX had any effect on this process, I assessed the effects of plasmin with or without DOX co-treatment on cultured NRVMs. Plasmin is a serine protease with trypsin-like specificity capable of degrading various adhesive glycoproteins, such as fibronectin, laminin, and vitronectin (175, 191), and indirectly degrading collagen via activation of MMPs (167). Previous studies have demonstrated plasmin-mediated disruption of cell-matrix interactions in several adherent cell types: cultured vascular smooth muscle cells convert plasminogen to plasmin, resulting in fibronectin proteolysis and cell detachment and death (175), and plasminogen stimulation of CHO cells causes fibronectin and laminin degradation, inducing detachment and death (192). In addition, stimulation of human keratinocytes with plasminogen results in proteolysis of vitronectin and cell detachment (191).

In agreement with previous studies (175, 191, 192), I observed that stimulation of NRVMs or NRVFs with plasminogen led to dose- and time-dependent increases in plasmin activity and that the conversion of plasminogen to plasmin occurred via endogenous plasminogen activators. In NRVMs, increased plasmin activity yielded morphological changes, such as cell rounding and loss of intercellular contacts, and loss of β_{1D} -integrin leading to cell detachment. Interestingly, NRVFs did not detach in the presence of plasminogen despite a high level of plasmin activity, suggesting a myocyte-specific phenomenon. Evidence of nuclear fragmentation and annexin V labeling in NRVMs confirmed an apoptotic mode of cell death. I did not observe MMP activation in NRVMs stimulated with plasminogen, suggesting that MMPs did

not contribute to NRVM detachment. This was further supported by the inability of the broad-spectrum MMP inhibitor GM6001 to preserve β_{1D} -integrin and cell attachment. These data suggest that the direct proteolytic degradation of cell-matrix attachments by plasmin induces NRVM detachment and apoptosis.

Pretreatment of the NRVM cultures with DOX prior to plasminogen stimulation preserved NRVM attachment and resulted in a dose-dependent inhibition of plasmin activity, with an IC_{50} of $\sim 36 \mu M$. The inhibition of plasmin activity upon stimulation with purified plasmin (as opposed to plasminogen) demonstrated the inhibitory effect of DOX was subsequent to plasminogen activation, however inhibition of plasminogen activators by DOX was not tested. Similar to the gelatin zymography results, fibrin zymography also showed a time-dependent reduction in fibrinolytic activity in NRVMs co-treated with DOX. Again it was surprising that DOX reduced zymographic activity since it was expected that DOX would dissociate from plasmin during electrophoresis. Sorsa et al. (60) suggest an indirect inhibition of serine proteases by DOX via inhibition of MMP-mediated degradation of the serine protease inhibitor α_1 -antitrypsin. Grenier et al. (64) showed DOX preserves α_1 -antitrypsin levels and inhibits the trypsin-like activity of periodontal pathogen *T. denticola*. Contrary to these previous studies (60, 64), I showed that MMP inhibition by DOX played no role in inhibiting plasmin activity in culture since GM6001 treatment had no effect on plasmin activity despite complete inhibition of MMP activity. Therefore, the ability of DOX to inhibit plasmin and preserve NRVM attachment was specific and independent of MMP inhibition.

Similar to my zymography data showing that DOX co-treatment reduced MMP protein levels in NRVMs stimulated with MMP-9, immunoblot analysis showed DOX co-treatment also reduced the amount of plasmin in NRVMs stimulated with plasminogen or plasmin. The mechanism by which DOX exerts this effect is uncertain. Autoproteolysis of plasmin is known to occur (193), and it is possible that DOX accelerates this process. Also, cellular uptake and degradation of plasmin is known to be mediated by LDL receptor-related proteins (194), and it is possible that DOX may promote this process. The reduction in plasmin levels in culture by DOX correlates well with my observations of a 76% reduction in plasmin levels with DOX treatment in the rat post-IR. Whether the mechanism by which plasmin is eliminated in culture contributes to the loss of plasmin *in vivo* post-I/R remains to be determined. These unique, and as of yet undescribed, capabilities of DOX offer tempting possibilities for treatment of pathologies where protease activation underlies the disease process.

Enzyme kinetic assays *in vitro* showed that DOX directly inhibited plasmin, and the mode of inhibition was mixed. The current paradigm for inhibition of MMPs by DOX involves chelation of the catalytic and/or structural zinc ions within the MMP (48). However, since plasminogen lacks any known metal binding sites, the mechanism of inhibition by DOX must be different than for the MMPs. All of the tetracyclines contain a large hydrophobic core formed by the aromatic groups with a number of hydrophilic sidegroups giving the molecules amphiphilic character. They have been shown to bind proteins through combined hydrophobic and electrostatic

interactions and induce conformational changes in the protein (195, 196). This amphiphilic nature of DOX may facilitate its binding to plasmin and disruption of the protein structure.

Interestingly, the inhibition of plasmin by DOX was dependent on the presence of Ca^{2+} . This finding is interesting given a previous study showing divalent metal ions are required for binding of tetracycline to the TET repressor protein (22). In that study, binding was greatest in the presence of Mg^{2+} , followed by Ca^{2+} and then Ba^{2+} . My finding that Ca^{2+} and not Ba^{2+} or Mg^{2+} facilitated plasmin inhibition by DOX indicates that, although divalent metal ions are required, the specific metal needed for formation of the tetracycline-cation-protein complex depends on both the tetracycline species and the protein species present. Since TET and MIN did not inhibit plasmin in the presence of any of the divalent cations, the inhibition was specific to DOX and not a broad effect of the tetracycline class of drugs.

To further investigate the role of plasmin in I/R injury, isolated rat hearts were subjected to I/R in the presence plasmin or the plasmin inhibitor TEA. The finding that TEA did not reduce injury was not unexpected, as the crystalloid perfusion buffer lacked the plasminogen that would be found in blood. Indeed, assessment of plasmin activity in untreated hearts subjected to I/R revealed no plasmin activity in the coronary effluent. It was more unexpected that plasmin addition did not exacerbate I/R injury, as assessed by the recovery of contractile function and CK release. The plasmin-treated hearts tended toward a reduction in mature β_{1D} -integrin levels, but this was not statistically significant. Although the plasma concentration of plasminogen is

~220 $\mu\text{g/ml}$ in rats (189), I exposed the isolated, perfused hearts to 2.1 $\mu\text{g/ml}$ plasmin from 5 min before ischemia to 10 min after the onset of reperfusion due to the cost and availability of commercial plasmin. Based on the intensities of the plasmin and plasminogen bands in the immunoblots from the *in vivo* I/R hearts, the ratio of plasmin to plasminogen was ~1:3 at 48 hours post-I/R. Using the normal circulating concentration of 220 $\mu\text{g/ml}$ plasminogen in rats, the calculated plasmin concentration in the *in vivo* I/R hearts was ~55 $\mu\text{g/ml}$. Therefore, the concentration of plasmin infused into the isolated hearts was much lower than would be expected *in vivo* post-I/R. Incubation of papillary muscles in 0.64 U/ml plasmin (~ 213 $\mu\text{g/ml}$ assuming 3 U/mg) for 4 hours was shown to increase MMP activity, disrupt the collagen ECM, and decrease systolic performance (197), demonstrating that higher levels of plasmin are detrimental to myocardial structure and contractile function. It is likely that the addition of 55 $\mu\text{g/ml}$ plasmin, rather than 2.1 $\mu\text{g/ml}$ plasmin, to the isolated, perfused hearts throughout reperfusion would exacerbate I/R injury, but this remains to be determined.

Although I demonstrated that plasmin induced NRVM detachment and apoptosis *in vitro*, one limitation of this study is that I have not directly demonstrated that this occurs *in vivo* following I/R injury. My determination of infarct size using TTC only discriminates between viable and nonviable tissue irrespective of whether cell death occurred by apoptosis or necrosis. However, given the high levels of plasminogen present in the bloodstream and tissue, it is reasonable to expect that plasmin activation plays an important role in inducing cell death during I/R.

Secondly, the reduction of plasmin levels by DOX and reduced infarct size *in vivo* coupled with the potent inhibition of plasmin by DOX *in vitro* suggest that the inhibition of plasmin by DOX contributed to the reduction in infarct size. However, it is also possible that the reduced plasmin levels occurred secondarily to reduced infarct size via an alternate cardioprotective mechanism of DOX that was not explored in this study. Thirdly, the response of neonatal myocytes to plasmin may not completely parallel the response of adult myocytes *in vivo*. NRVMs were selected as the model of choice rather than adult myocytes due to the relative stability of NRVMs in culture over several days. Whereas adult myocyte cultures are fraught with loss of cylindrical morphology and detachment of calcium-intolerant cells early in primary culture, NRVMs are routinely cultured for days to weeks for investigation of myocyte morphology, function, and viability and the effects of experimental agents on these parameters. Therefore, NRVMs are a robust and suitable model to study the effects of protease-induced myocyte injury.

In conclusion, DOX treatment reduced infarct size *in vivo*, possibly by inhibiting plasmin, a serine protease capable of degrading myocyte-matrix attachments. Further exploration of the pathophysiological role of plasmin in mediating myocardial I/R injury is thus warranted.

3.7. Acknowledgements

Chapter 3, in part, has been published as it appears in Griffin MO, Jinno M, Miles LA, Villarreal FJ. *Molecular and Cellular Biochemistry* 2005;270(1-2):1-11, Springer

US, 2005. The dissertation author was the primary investigator and author of this paper.

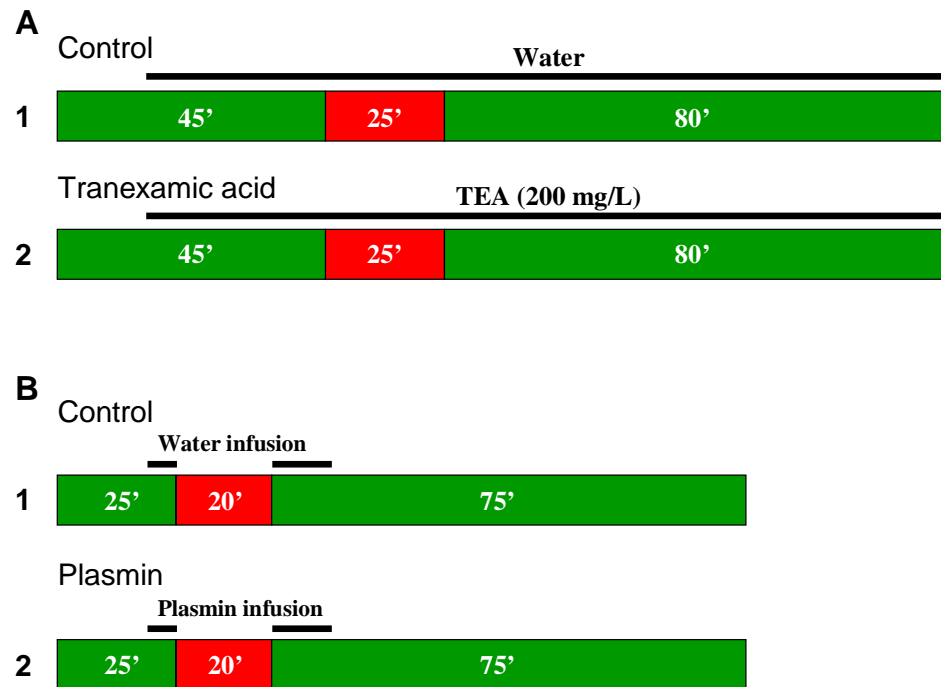


Figure 3-1. Langendorff perfusion protocol. Green depicts time of aerobic perfusion, and red depicts time of global, no-flow ischemia.

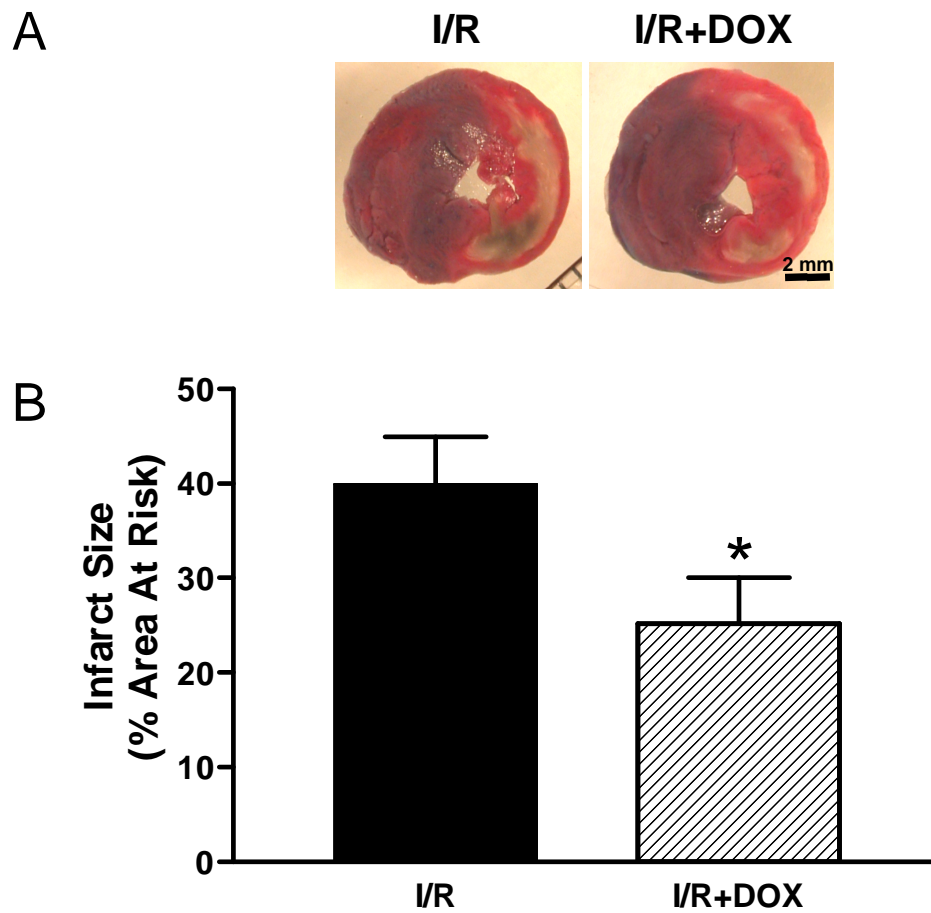


Figure 3-2. Reduction of myocardial infarct size with DOX pretreatment. **A**, Representative control (I/R) and DOX-treated (I/R+DOX) infarcted hearts stained with trypan blue and triphenyltetrazolium chloride for infarct size determination. **B**, Morphometric analysis of infarct size in I/R (n = 8) and I/R+DOX (n = 8). Values are mean±SEM. * $p \leq 0.05$.

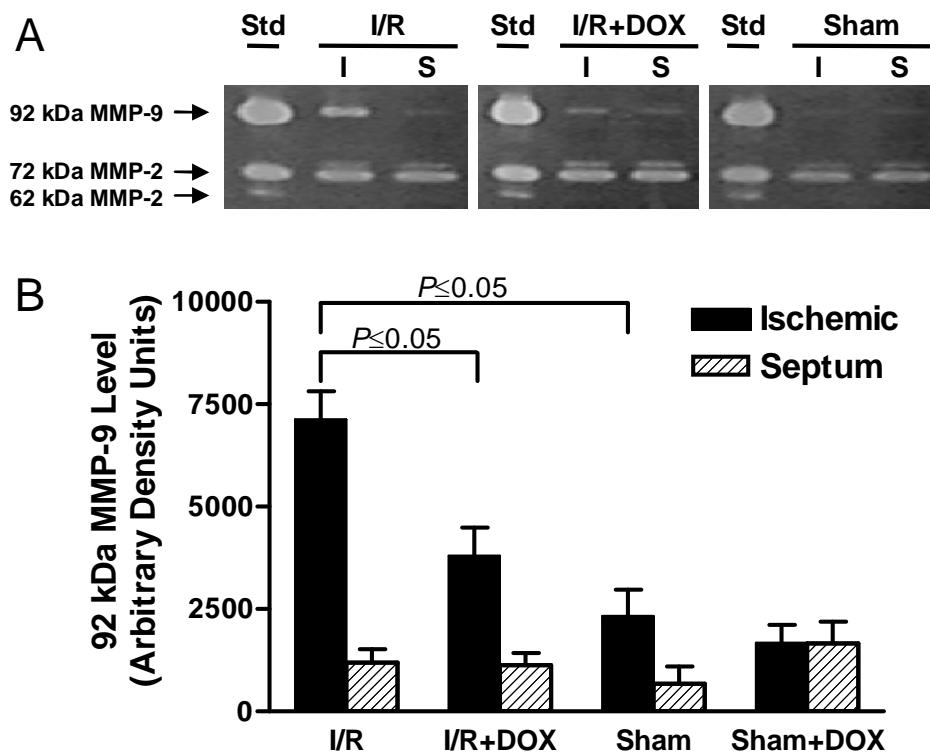


Figure 3-3. Reduction of 92 kDa MMP-9 levels in the ischemic region with DOX pretreatment. **A**, Representative gelatin zymograms of myocardial MMP-2 and MMP-9 levels in control (I/R) and DOX-treated (I/R+DOX) infarcted hearts and sham hearts. 'I' and 'S' indicate ischemic region and septum, respectively. 'Std' indicates human MMP-2/MMP-9 standard. **B**, Densitometric analysis of 92 kDa MMP-9 zymographic activity in I/R (n = 11), I/R+DOX (n = 12), Sham (n = 5), and Sham+DOX (n = 5). Values are mean±SEM.

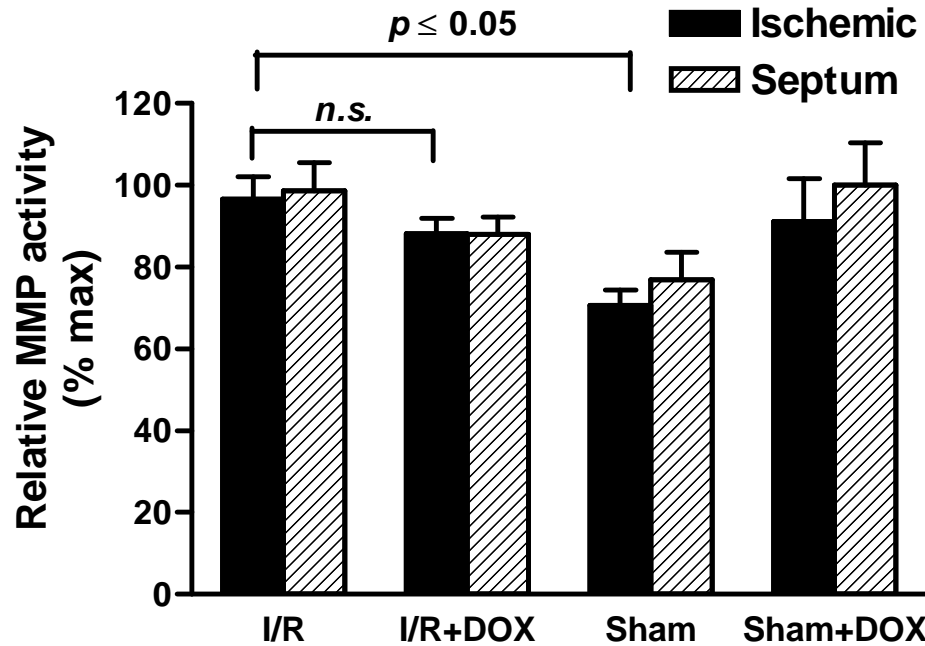


Figure 3-4. Myocardial global MMP activity in control (I/R, $n = 11$) and DOX-treated (I/R+DOX, $n = 12$) infarcted hearts and control (Sham, $n = 5$) and DOX-treated (Sham+DOX, $n = 5$) sham hearts. MMP activity was assessed by hydrolysis of a peptide substrate. Activities are expressed as the percentage of maximal activity. Values are mean \pm SEM. *n.s.* = not significant.

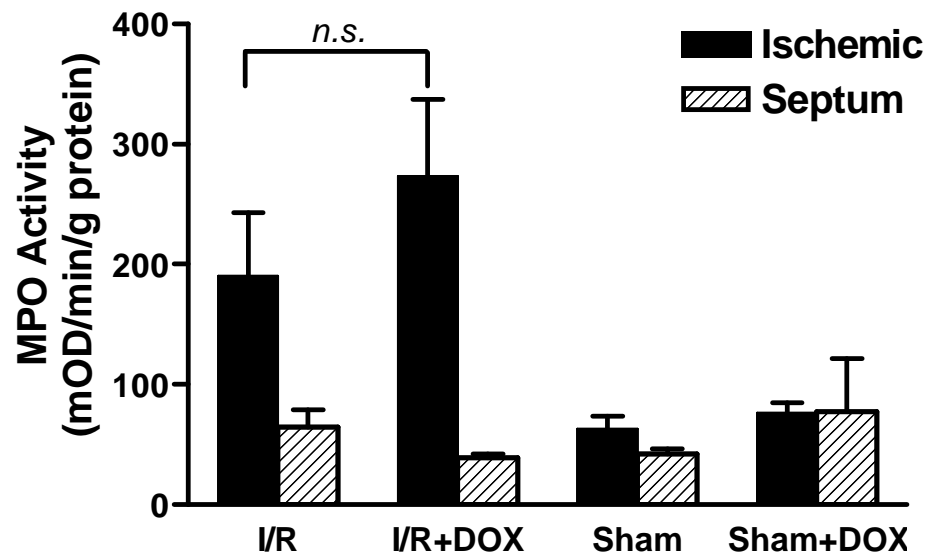


Figure 3-5. Myocardial myeloperoxidase (MPO) activity in control (I/R, $n = 11$) and DOX-treated (I/R+DOX, $n = 12$) ischemic hearts and control (Sham, $n = 5$) and DOX-treated (Sham+DOX, $n = 5$) sham hearts. No significant difference was observed between I/R and I/R+DOX ischemic regions. Values are mean \pm SEM. *n.s.* = not significant.

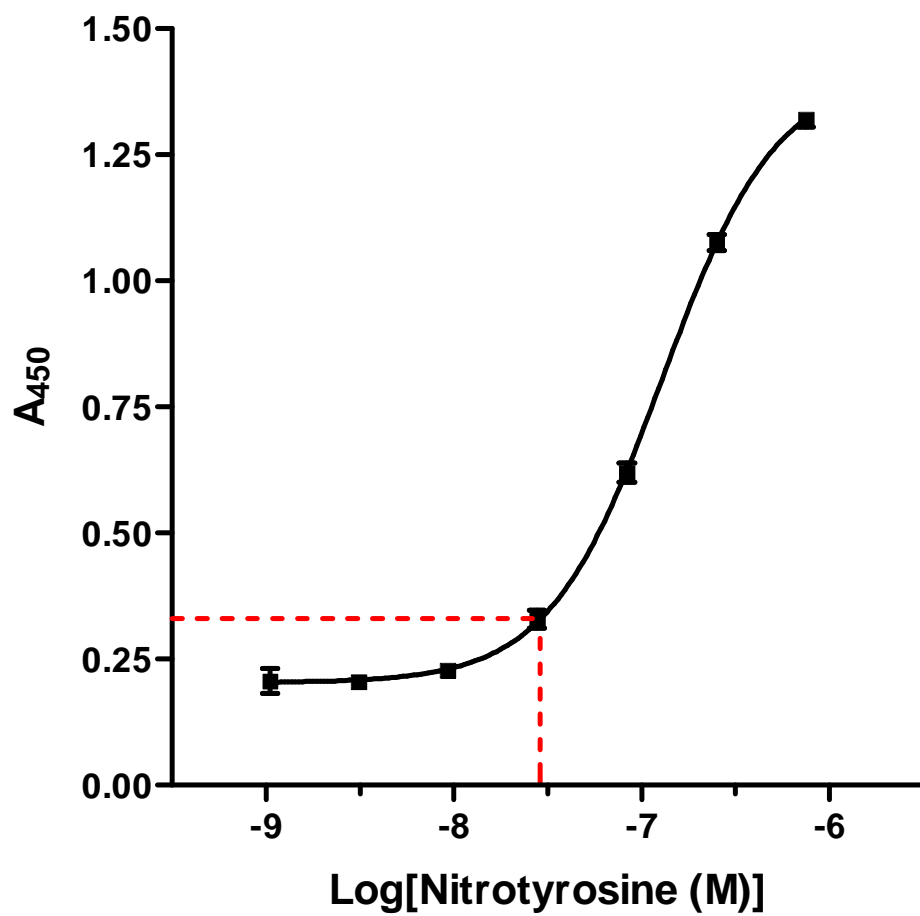


Figure 3-6. Standard curve for the nitrotyrosine ELISA. The reliable limit of detection was determined to be ~25 nM as indicated by the dashed red line. In all heart samples the measured concentration of nitrotyrosine was below this limit.

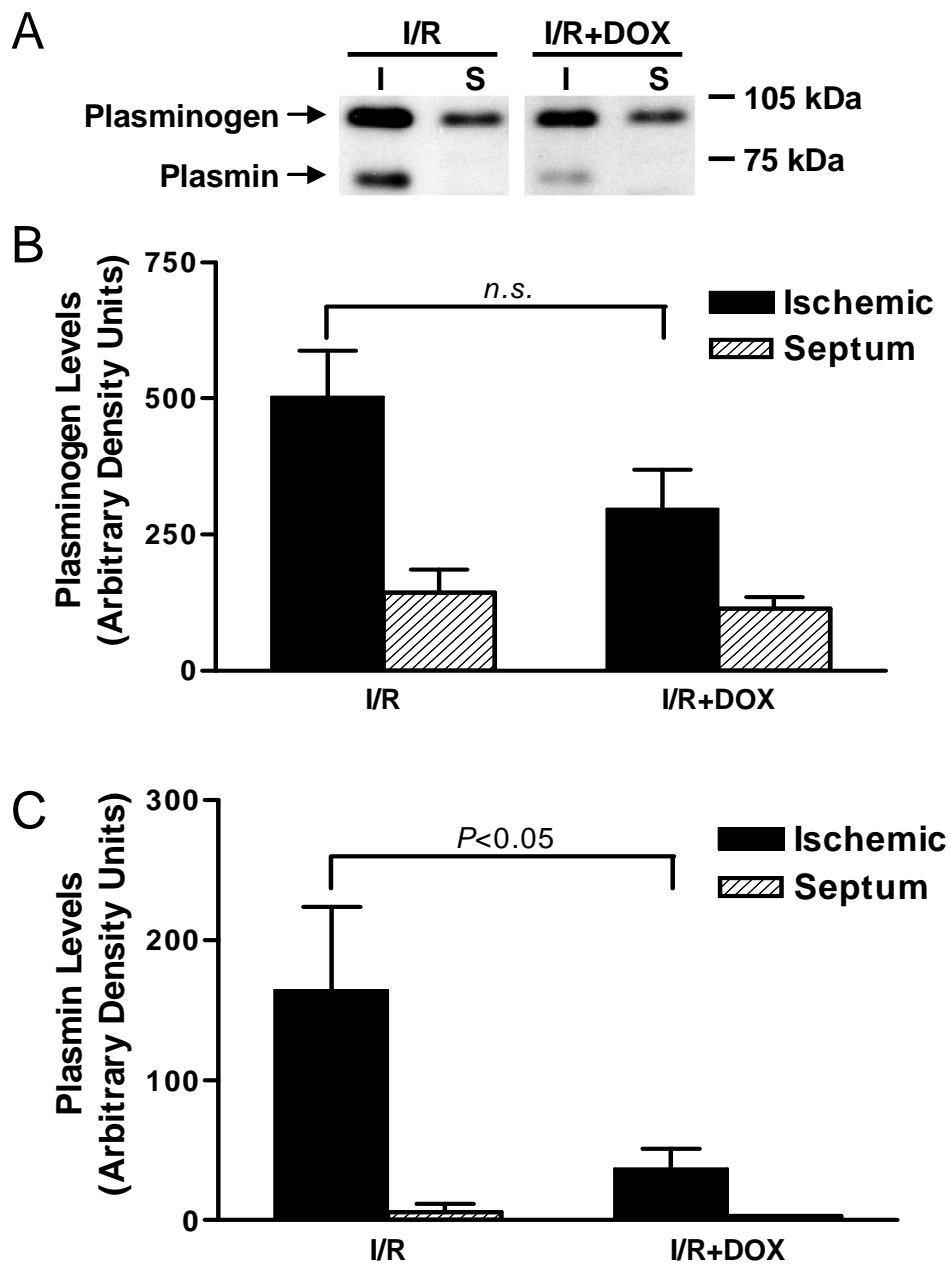


Figure 3-7. Reduction of plasmin levels in the ischemic region with DOX pre-treatment. **A**, Representative immunoblots of myocardial plasminogen and plasmin levels in control (I/R) and DOX-treated (I/R+DOX) infarcted hearts. 'I' and 'S' indicate ischemic region and septum, respectively. **B** and **C**, Densitometric analysis of plasminogen and plasmin levels in I/R (n = 11) and I/R+DOX (n = 12). Values are mean±SEM. *n.s.* = not significant.

Table 3-1. Hemodynamic data at 4 weeks post-I/R. EDP = end-diastolic pressure, PSP = peak systolic pressure, ΔP = developed pressure, MAP = mean arterial pressure. Data are mean \pm SD.

	Sham	Sham+DOX	I/R	I/R+DOX
n	6	6	6	4
Heart Rate, bpm	305 \pm 41	331 \pm 47	299 \pm 45	288 \pm 33
LV				
EDP, mmHg	3.3 \pm 1.3	3.0 \pm 2.8	4.8 \pm 4.4	3.8 \pm 1.3
PSP, mmHg	116 \pm 26	95 \pm 12	108 \pm 27	113 \pm 5.6
ΔP , mmHg	112 \pm 26	92 \pm 11	103 \pm 24	109 \pm 5.2
Max +dP/dt, mmHg/s	7725 \pm 2362	6547 \pm 1737	6283 \pm 2692	6859 \pm 555
Max -dP/dt, mmHg/s	-5851 \pm 2087	-4314 \pm 1051	-4817 \pm 1999	-4670 \pm 463
Aorta				
n	6	6	6	5
Systolic, mmHg	117 \pm 24	94 \pm 12	107 \pm 23	104 \pm 23
Diastolic, mmHg	83 \pm 22	66 \pm 10	77 \pm 22	75 \pm 22
MAP, mmHg	94 \pm 22	76 \pm 11	87 \pm 23	84 \pm 22

Table 3-2. Histomorphometric data at 4 weeks post-I/R. BW = body weight, HW = heart weight. Data are mean \pm SD. * $p \leq 0.05$ between I/R and I/R+DOX.

	Sham	Sham+DOX	I/R	I/R+DOX
n	6	6	6	5
BW, g	392 \pm 18	388 \pm 38	382 \pm 14	383 \pm 20
HW/BW, mg/g	3.68 \pm 0.16	3.75 \pm 0.12	3.67 \pm 0.29	4.08 \pm 0.40
LV wt/BW, mg/g	2.60 \pm 0.21	2.81 \pm 0.12	2.56 \pm 0.27*	3.09 \pm 0.28*
LV outer dia, mm	7.72 \pm 0.33	7.96 \pm 0.29	7.84 \pm 0.69	8.18 \pm 0.37
LV inner dia, mm	4.08 \pm 0.52	4.19 \pm 0.55	4.93 \pm 0.79	5.02 \pm 0.60
Wall thickness, mm				
Ischemic	1.57 \pm 0.05	1.80 \pm 0.23	1.12 \pm 0.61	1.23 \pm 0.34
Septum	1.77 \pm 0.23	1.74 \pm 0.11	1.69 \pm 0.23	1.77 \pm 0.12
Scar area, %LV	---	---	16.1 \pm 8.6	23.0 \pm 10.0

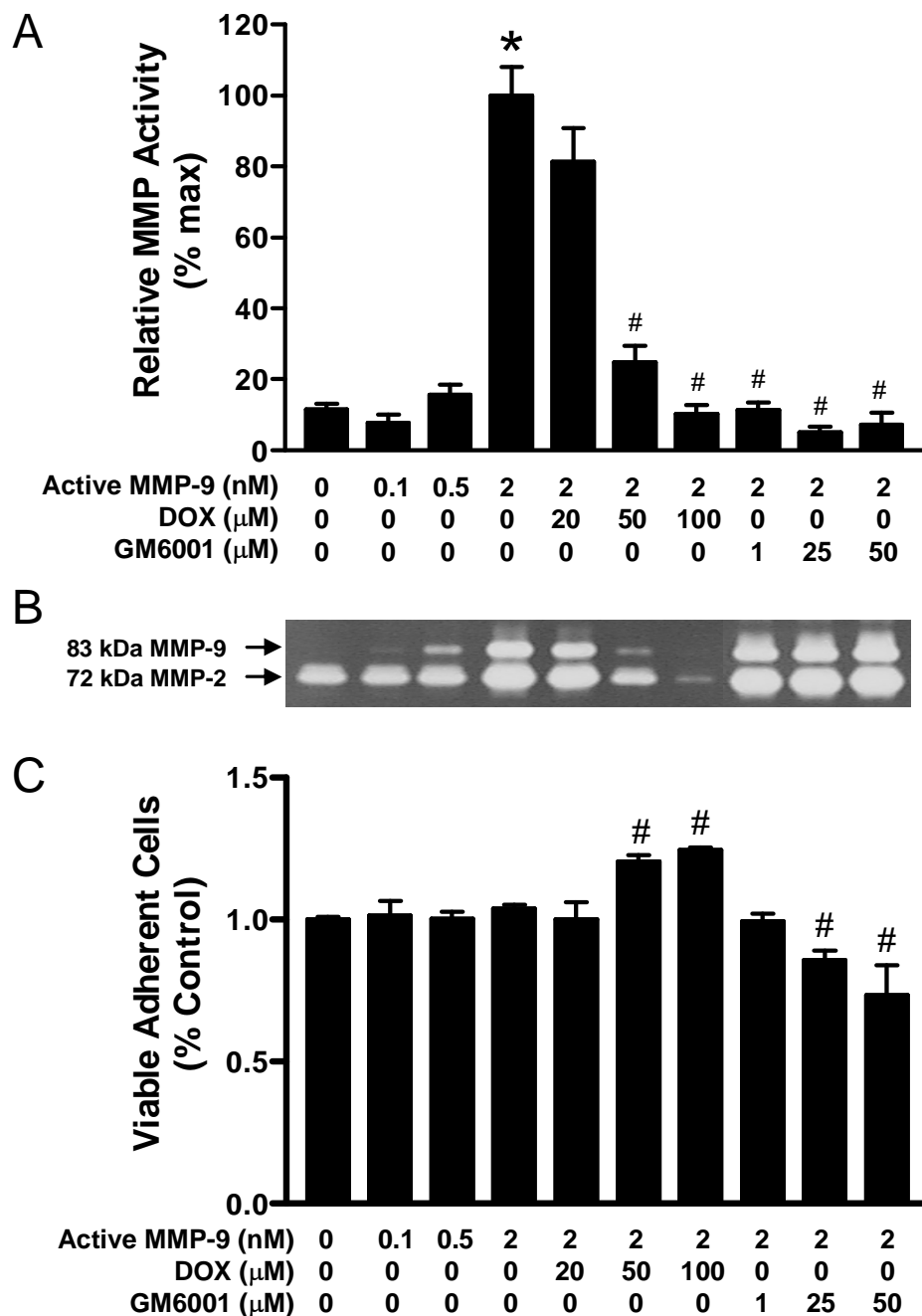


Figure 3-8. Effects of DOX co-treatment on MMP activity and cell detachment in cultures of NRVMs stimulated with 83 kDa active MMP-9 for 48 hr. **A**, Dose-dependent increase in MMP activity and inhibition by DOX and GM6001 as assessed by hydrolysis of a peptide substrate. Activities are expressed as the percentage of maximal activity. **B**, Representative gelatin zymogram following stimulation of NRVMs with 83 kDa MMP-9 in the presence or absence of inhibitors. Gel lanes correspond to columns in **A**. **C**, Remaining viable adherent cells as assessed by reduction of MTT. Values are normalized to unstimulated cells. Data are expressed as mean±SEM from experiments performed at least in triplicate from two different cell preparations. * $p \leq 0.05$ vs. unstimulated control. # $p \leq 0.05$ vs. 2 nM active MMP-9 stimulated only.

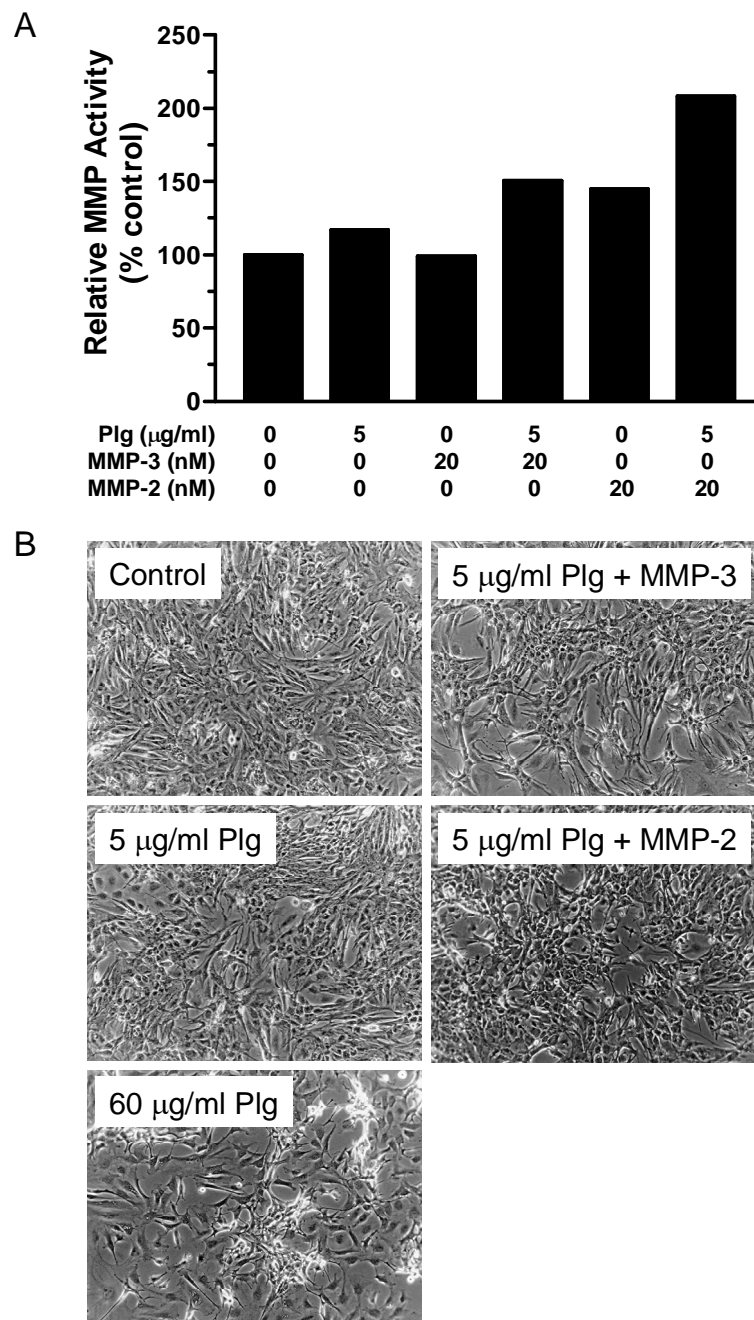


Figure 3-9. Effects of MMP stimulation on MMP activity and cell detachment in cultures of NRVMs. **A**, Increase in MMP activity in NRVMs co-stimulated with a low, catalytic concentration of plasminogen and either proMMP-3 or a proMMP-2/active MMP-2 mixture for 48 hr. **B**, Phase contrast microscopy images of unstimulated control NRVMs and NRVMs co-stimulated with plasminogen and either proMMP-3 (20 nM) or a proMMP-2/active MMP-2 mixture (20 nM) for 48 hr. Data are from a single experiment.

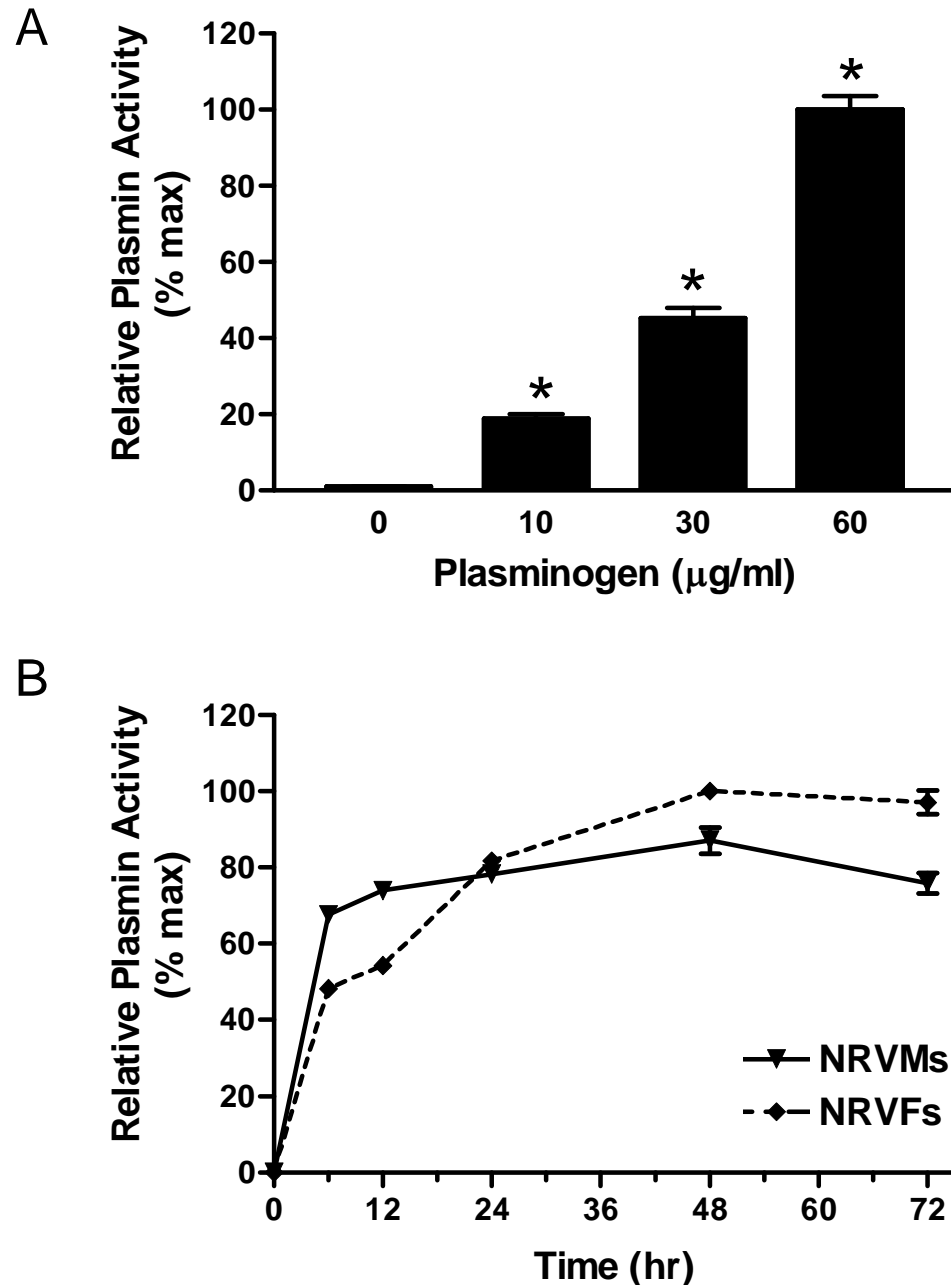


Figure 3-10. Effects of plasminogen treatment on plasmin activity in cultures of NRVMs and NRVFs as assessed by hydrolysis of a peptide substrate. **A**, Dose-dependent plasmin activity induced by 48 hr of plasminogen treatment in NRVMs. Data are mean±SEM from experiments performed at least in triplicate from two different cell preparations. **B**, Time-dependent plasmin activity induced by 60 μg/ml plasminogen in NRVMs and NRVFs. Data are mean±SEM from experiments performed at least in triplicate. * $p \leq 0.05$ vs unstimulated.

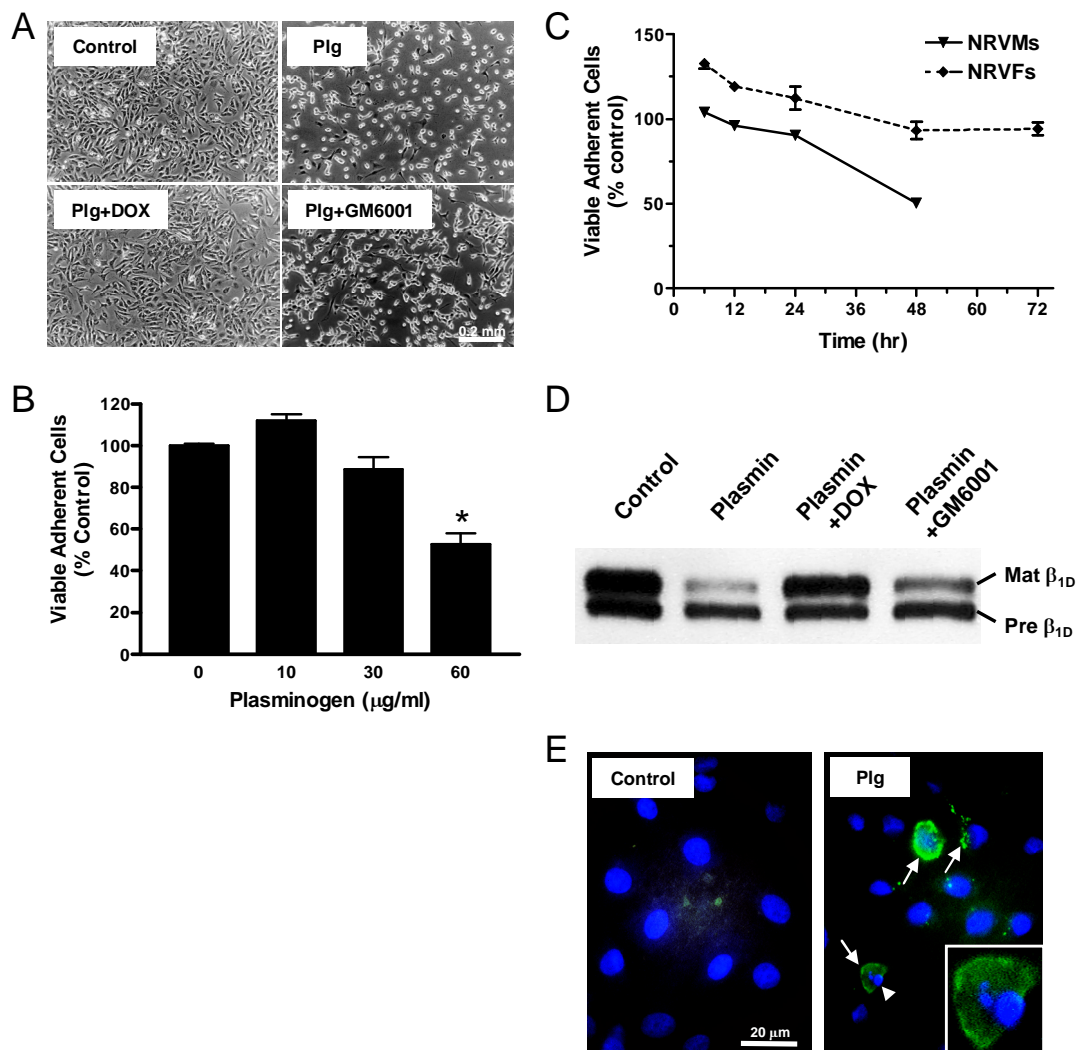


Figure 3-11. NRVM detachment and death following 48 hr of plasminogen stimulation. **A**, Representative phase contrast microscopy images of untreated NRVMs and NRVMs stimulated with plasminogen (60 $\mu\text{g/ml}$) with or without DOX (100 μM) or GM6001 (50 μM). **B**, Remaining viable adherent NRVMs following plasminogen (60 $\mu\text{g/ml}$) stimulation for 48 hr as assessed by reduction of MTT. Values are normalized to the unstimulated control. **C**, Remaining viable adherent NRVMs and NRVFs following plasminogen (60 $\mu\text{g/ml}$) stimulation as assessed by reduction of MTT. Values are normalized to unstimulated controls. **D**, Immunoblot of β_{1D} -integrin in cell lysate from NRVMs stimulated for 16 hr with plasmin (60 $\mu\text{g/ml}$) with or without DOX (100 μM) or GM6001 (50 μM). ‘Mat β_{1D} ’ and ‘Pre β_{1D} ’ indicate mature and precursor β_{1D} -integrin, respectively. **E**, Annexin V (green) and DAPI (blue) staining of NRVMs stimulated with plasminogen (60 $\mu\text{g/ml}$). Annexin V localized to the membrane of apoptotic cells (arrows). Many of the annexin V positive cells showed nuclear fragmentation (arrowhead, magnified view in inset). Cells were negative for propidium iodide staining. Data are mean \pm SEM from experiments performed at least in triplicate from two different cell preparations, except for **C** which was performed in triplicate from one cell preparation. * $p \leq 0.05$ vs. unstimulated.

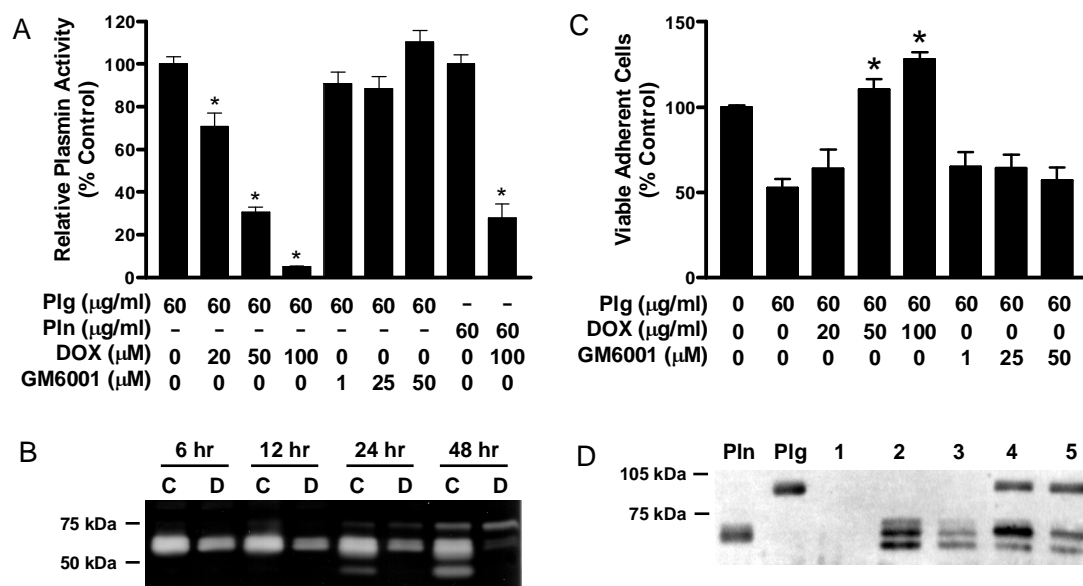


Figure 3-12. Effects of DOX co-treatment on plasmin activity and cell detachment in cultures of NRVMs. **A**, Inhibition of plasmin activity by DOX and GM6001 following 48 hr of plasminogen (Plg) stimulation or 16 hr of plasmin (Pln) stimulation as assessed by hydrolysis of a peptide substrate. Activity is expressed as the percentage of activity observed without inhibitors. **B**, Representative fibrin zymogram showing plasmin activity following stimulation with plasminogen (60 $\mu\text{g/ml}$) in the presence or absence of DOX (100 μM) for 6 to 48 hr. 'C' indicates control NRVMs receiving only plasminogen, and 'D' indicates NRVMs receiving plasminogen and DOX. **C**, Remaining viable adherent NRVMs following 48 hr of plasminogen (60 $\mu\text{g/ml}$) stimulation as assessed by reduction of MTT. Values are normalized to unstimulated cells. **D**, Representative immunoblot of media from NRVMs treated for 16 hr with 60 $\mu\text{g/ml}$ Pln (lane 2), 60 $\mu\text{g/ml}$ Pln + 100 μM DOX (lane 3), 60 $\mu\text{g/ml}$ Plg (lane 4), or 60 $\mu\text{g/ml}$ Plg + 100 μM DOX (lane 5). Lane 1 is untreated control. 'Pln' and 'Plg' indicate plasmin and plasminogen standard, respectively. Data are mean \pm SEM from experiments performed as least in triplicate (Plg) or duplicate (Pln) from two different cell preparations. * $p \leq 0.05$ vs. no inhibitor.

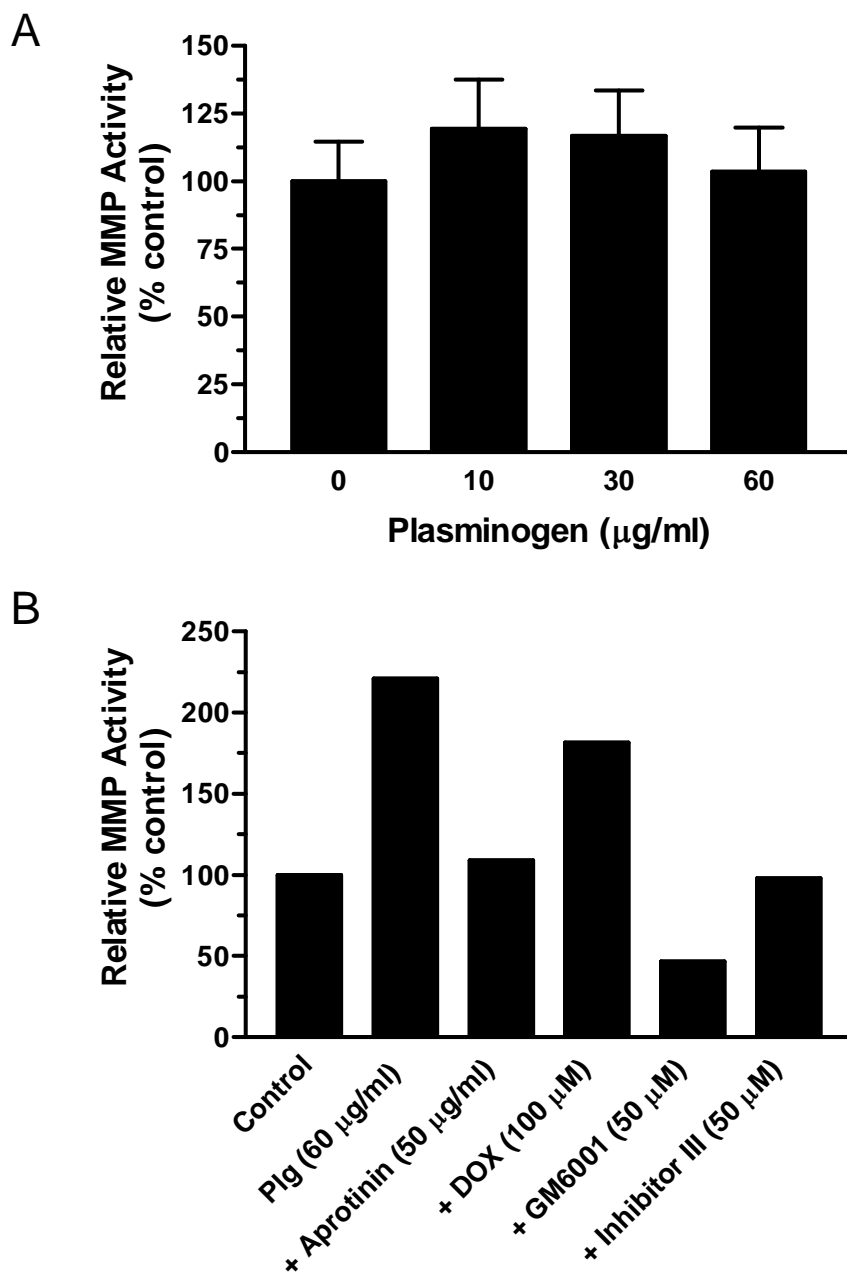


Figure 3-13. Effects of plasminogen treatment on MMP activity in culture as assessed by hydrolysis of a peptide substrate. **A**, MMP activity in NRVMs stimulated for 48 hr with plasminogen. Data are mean \pm SEM from experiments performed at least in triplicate from two different cell preparations. **B**, MMP activity in NRVM/NRVF co-cultures stimulated for 48 hr with plasminogen (Plg) in the presence or absence of inhibitors. Data are from a single experiment.

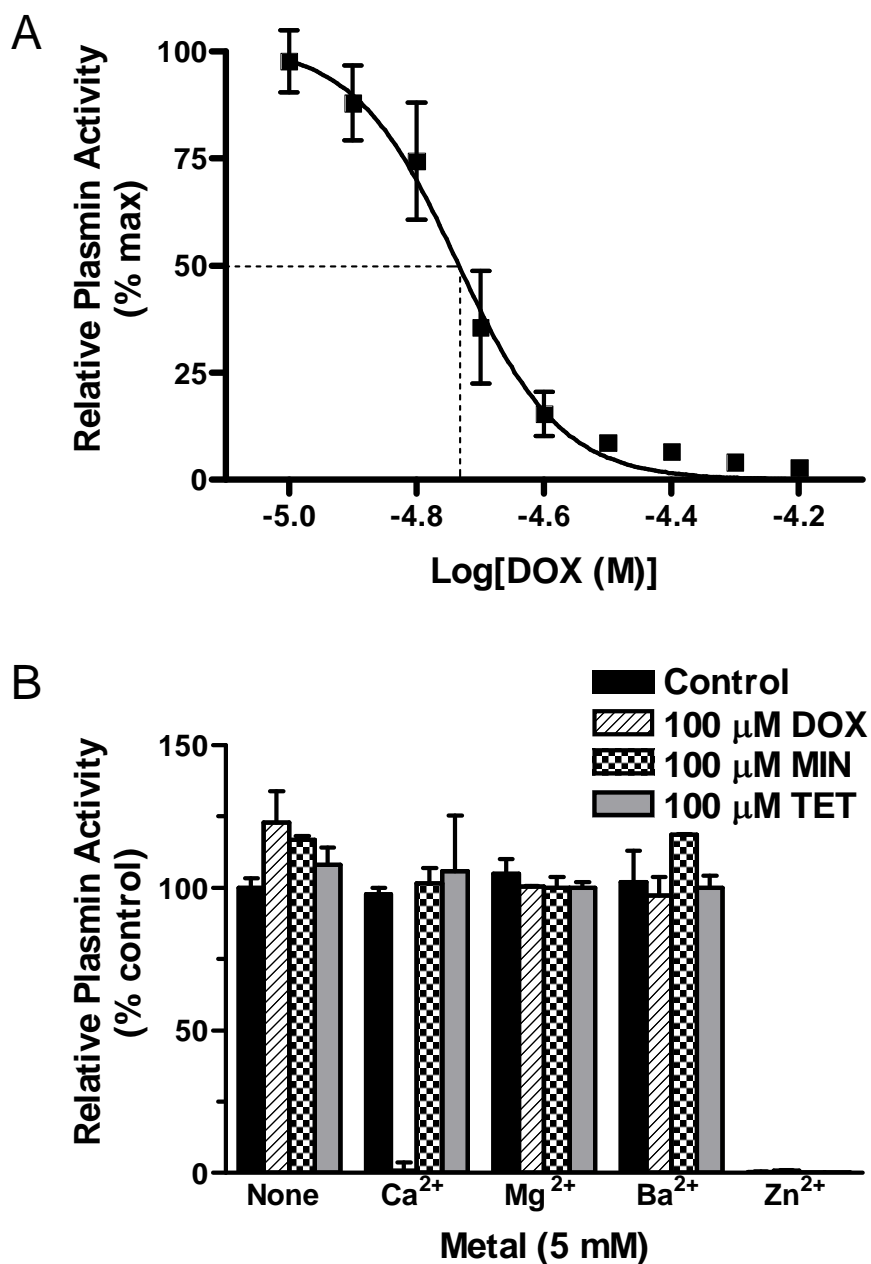


Figure 3-14. *In vitro* inhibition of human plasmin (100 nM) by the tetracyclines in the presence of divalent metals. **A**, Plasmin activity following preincubation with DOX in the presence of 5 mM Ca²⁺ for 1 hr. Data were fit to the sigmoidal Hill equation and the IC₅₀ determined to be 18.4 μ M. **B**, Plasmin activity following preincubation with DOX, minocycline (MIN), or tetracycline (TET) in the presence of divalent metals for 1 hr. Data points are shown as mean \pm SEM from experiments performed at least in duplicate.

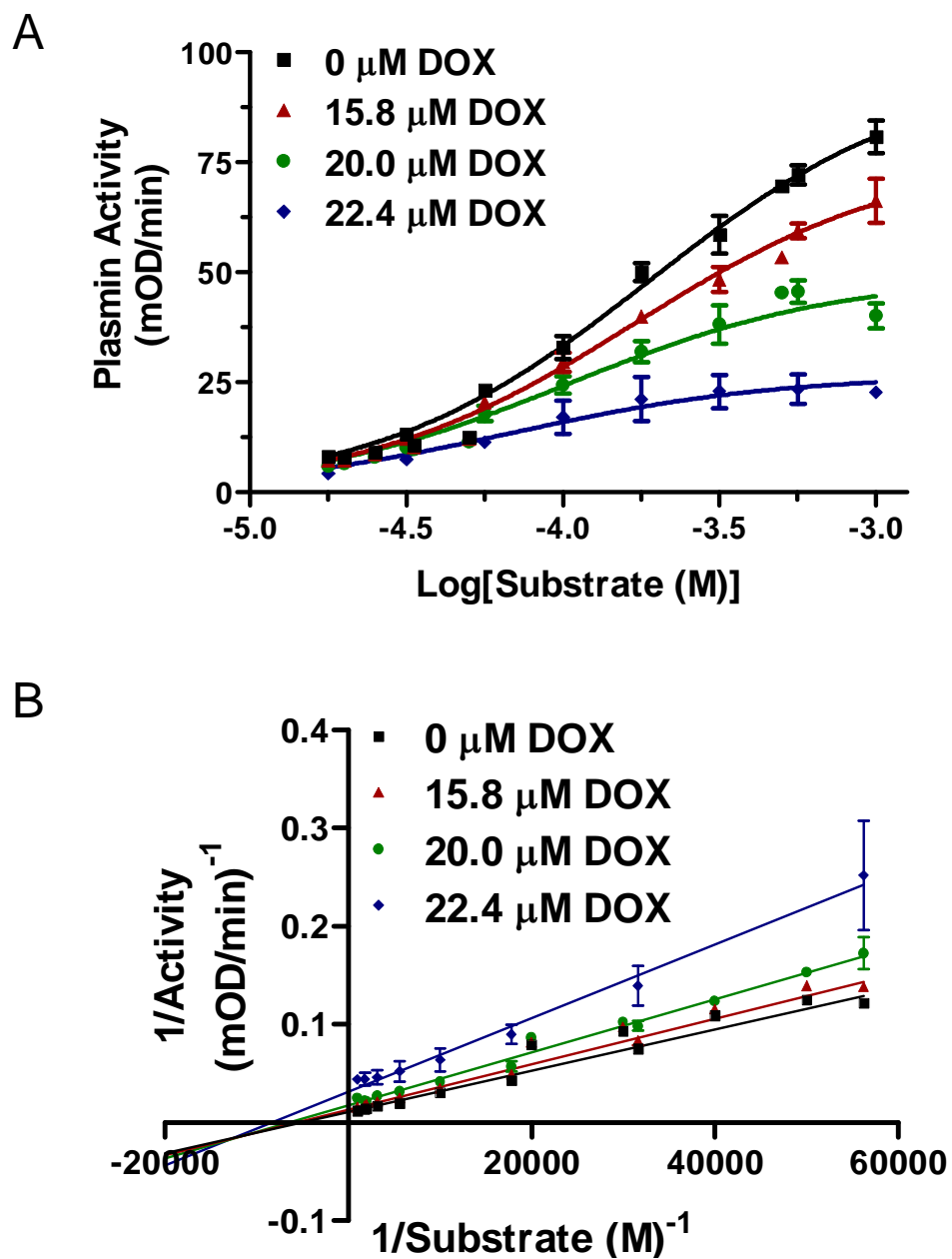


Figure 3-15. *In vitro* inhibitory effects of DOX on plasmin in the presence of Ca^{2+} . **A**, Plasmin activity was measured while holding the concentration of DOX constant at a fixed value and increasing the plasmin peptide substrate concentration. **B**, Lineweaver-Burk plot for inhibition of plasmin by DOX. The lines did not intersect on either axis. Values are mean \pm SEM from 3 experiments.

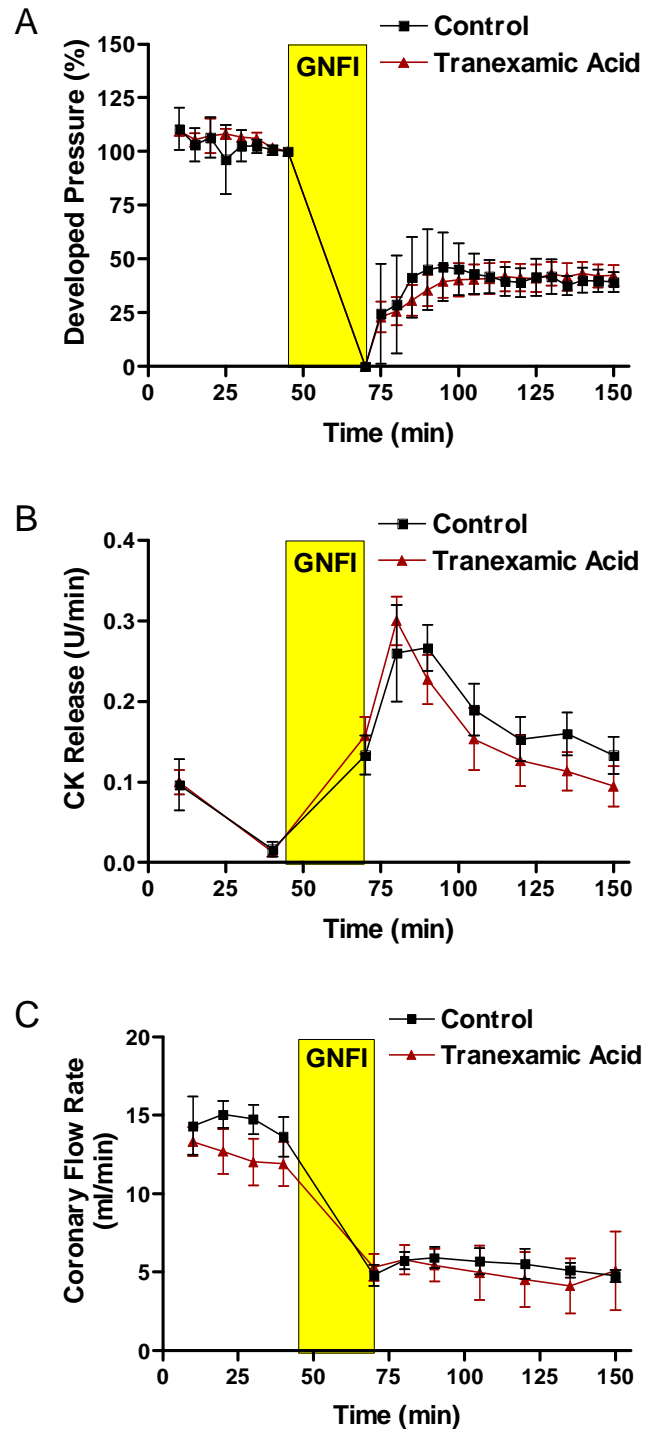


Figure 3-16. Effects of tranexamic acid on isolated, perfused rat hearts subjected to 25 min of global, no-flow ischemia (GNFI) and 80 min of reperfusion. TEA (1.3 mM) was infused from 30 min before GNFI until the end of the experiment. No differences between control ($n = 4$) and TEA-treated ($n = 3$) hearts were observed in left ventricular developed pressure (**A**), creatine kinase (CK) release from the myocardium into the effluent (**B**), or coronary flow rate (**C**). Data are mean \pm SEM.

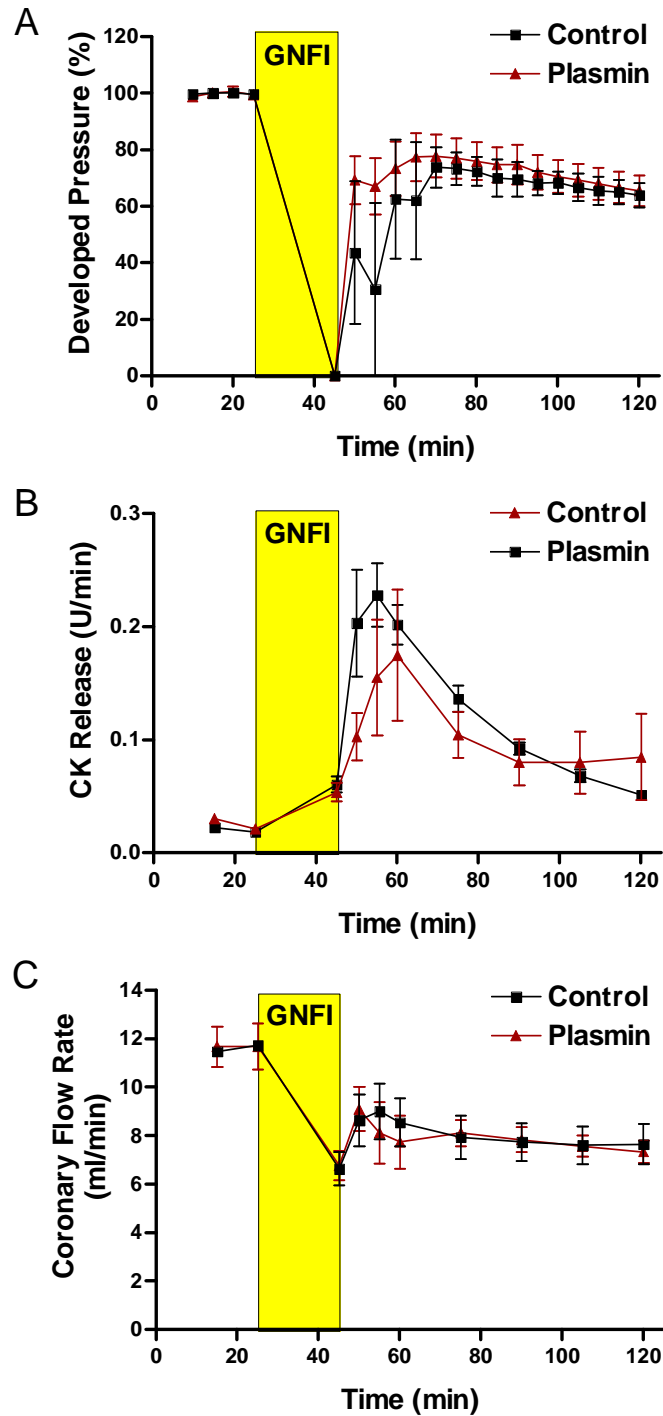


Figure 3-17. Effects of plasmin on isolated, perfused rat hearts subjected to 20 min of global, no-flow ischemia (GNFI) and 75 min of reperfusion. Plasmin (2.1 $\mu\text{g}/\text{ml}$) was infused during the last 5 min of aerobic perfusion and first 10 min of reperfusion. No differences between control ($n = 3$) and plasmin-treated ($n = 3$) hearts were observed in left ventricular developed pressure (**A**), creatine kinase (CK) release from the myocardium into the effluent (**B**), or coronary flow rate (**C**). Data are mean \pm SEM.

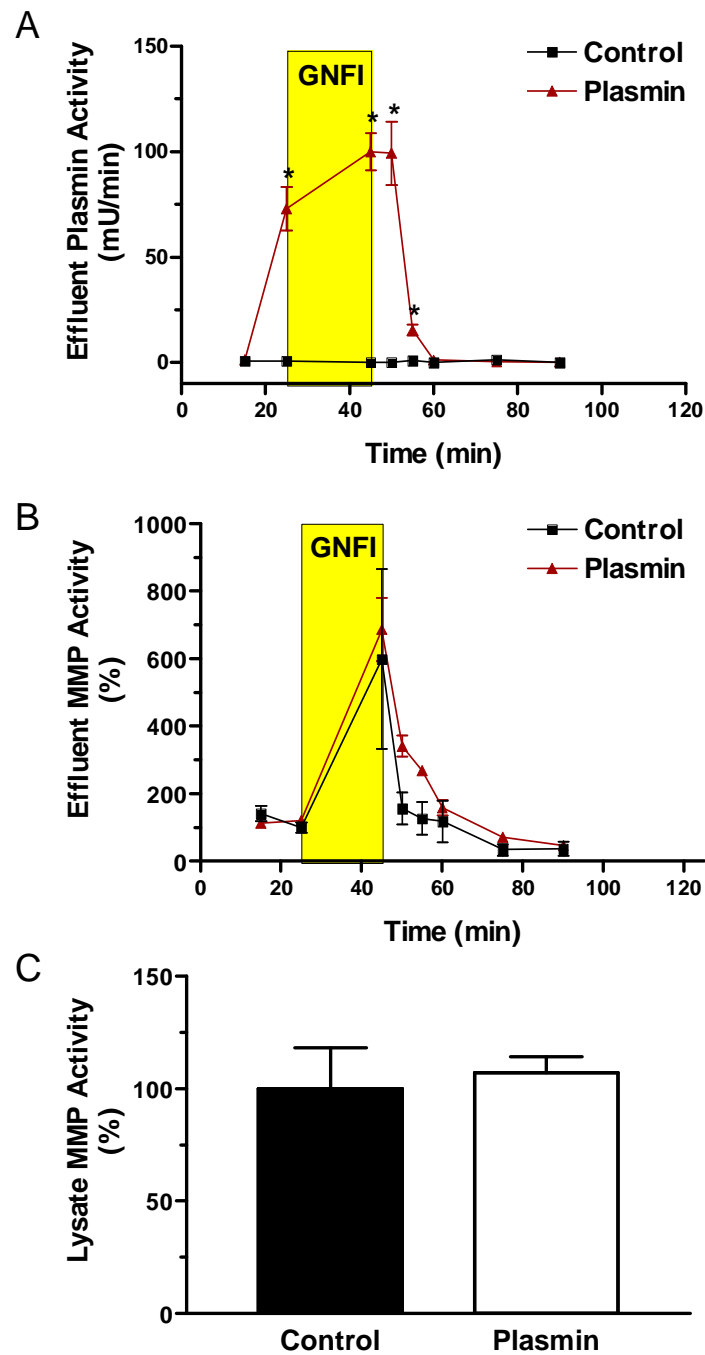


Figure 3-18. Effects of plasmin treatment on plasmin and MMP activities in isolated, perfused rat hearts subjected to 20 min of global, no-flow ischemia (GNFI) and 75 min of reperfusion. Plasmin (2.1 $\mu\text{g/ml}$) was infused during the last 5 min of aerobic perfusion and first 10 min of reperfusion. **A**, Plasmin activity and **B**, MMP activity in the coronary effluent as measured by hydrolysis of peptide substrates. **C**, MMP activity in the heart homogenates measured at the end of the experiment using a peptide substrate. Data are mean \pm SEM of 3 hearts. * $p \leq 0.05$ vs. control hearts.

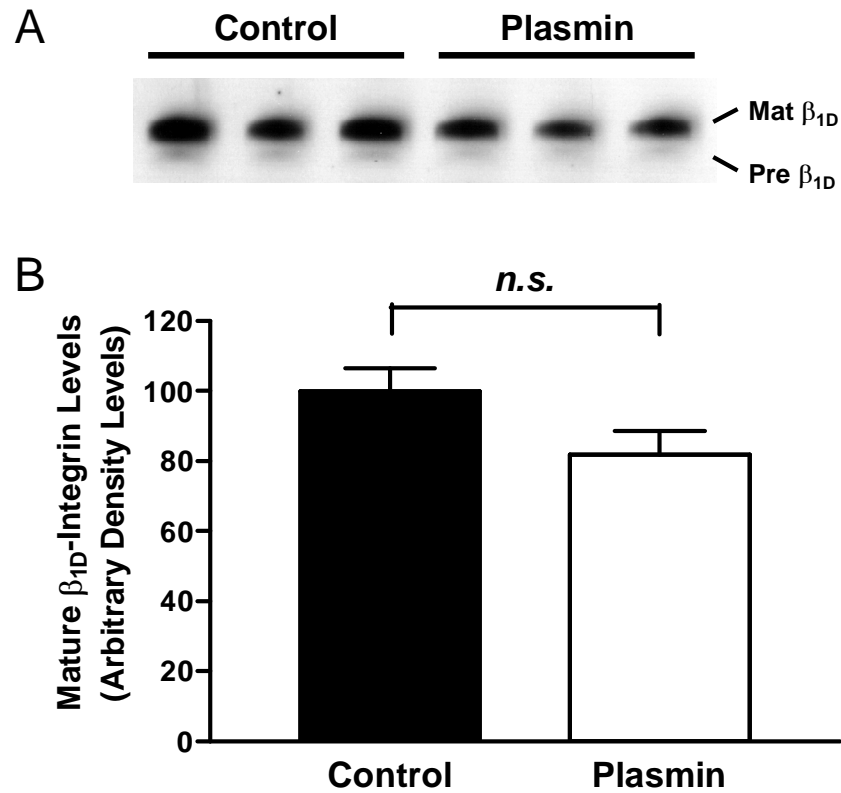


Figure 3-19. Effects of plasmin treatment on β_{1D} -integrin levels in isolated, perfused rat hearts subjected to 20 min of global, no-flow ischemia (GNFI) and 75 min of reperfusion. Plasmin (2.1 $\mu\text{g}/\text{ml}$) was infused during the last 5 min of aerobic perfusion and first 10 min of reperfusion. **A**, Immunoblot of β_{1D} -integrin in heart homogenates at the end of the perfusion protocol. 'Mat β_{1D} ' and 'Pre β_{1D} ' indicate mature and precursor β_{1D} -integrin, respectively. **B**, Densitometric analysis of mature β_{1D} -integrin levels in control ($n = 3$) and plasmin-treated ($n = 3$) hearts. No significant difference was observed between control and plasmin-treated hearts ($p = 0.13$). Values are mean \pm SEM. *n.s.* = not significant.

Chapter 4. Reduction of myocardial infarct size and stunning by minocycline

4.1. Abstract

It has previously been shown in isolated, perfused hearts subjected to I/R injury that MIN reduces myocardial infarct size by inhibiting the release of pro-apoptotic factors from the mitochondria and that DOX reduces stunning by inhibiting MMP-mediated proteolysis of troponin I (TnI). In this study, I investigated the ability of both MIN and DOX to protect the myocardium from I/R injury and stunning using an isolated, perfused heart model and myocyte cell cultures. In isolated, perfused rat hearts subjected to I/R, MIN treatment significantly reduced infarct size, reduced creatine kinase (CK) release, and improved the recovery of mechanical function compared with untreated controls. In contrast, DOX treatment had no protective effect. To examine whether DOX and MIN inhibited opening of the mitochondrial permeability transition pore (MPTP), isolated rat liver mitochondria were treated with calcium to induce opening of the MPTP in the presence or absence of DOX or MIN. Both MIN and DOX reduced MPTP opening as evidenced by reduced mitochondrial swelling, and DOX was a more potent inhibitor of the MPTP than MIN. MIN treatment also reduced the extent of stunning compared with untreated controls in isolated, perfused rat hearts subjected to brief I/R as measured by improved recovery of mechanical function and increased coronary flow. In these hearts, MIN treatment had no significant effect on MMP activity but tended toward reduced TnI release.

MIN treatment did not alter protein carbonyl content, a measure of oxidative stress, in heart homogenates at the end of the stunning protocol, and MIN significantly increased nitrotyrosine content, a measure of reactive nitrogen species production, in the heart homogenates. To further examine the mechanism of the potential protective effects of DOX and MIN directly on myocytes, cultures of neonatal rat ventricular myocytes were subjected to hypoxia-reoxygenation, chemical hypoxia with deoxyglucose and cyanide, or oxidative stress with hydrogen peroxide. Neither DOX nor MIN showed cytoprotection under these conditions as evidenced by no effect on cell viability or CK release. Likewise, cultures of adult rat ventricular myocytes subjected to hypoxia-reoxygenation were not protected by DOX or MIN. These results suggest that MIN, but not DOX, attenuates lethal I/R injury by acting directly on the myocardium and that MIN attenuates myocardial stunning independent of its ability to inhibit MMPs. In addition, the lack of efficacy of DOX and MIN in protecting myocyte cell cultures from hypoxic injury suggests that cell culture conditions may alter the expression and/or function of cellular targets of the tetracyclines, an important consideration for future studies.

4.2. Introduction

The tetracyclines are a family of broad-spectrum antibiotics that inhibit bacterial protein synthesis. In recent years, members of the tetracycline family, DOX and MIN, have been shown to have additional biological effects independent of their antimicrobial action (145). These effects appear to be mediated by several

mechanisms including inhibition of reactive oxygen species (ROS) (153), iNOS activity (150), apoptotic cell death pathways (114, 134), proteases such as the MMPs and plasmin (149, 198), and mitochondrial permeability (114). Numerous studies in rodents have demonstrated that MIN is protective against cerebral ischemic injury, such as global brain ischemia (110) and focal cerebral ischemia (199), and it is also protective against neurodegenerative diseases, such as Huntington's disease (115), amyotrophic lateral sclerosis (114), and Parkinson's disease (113). A single study has also reported a protective effect of MIN in a model of myocardial ischemic injury (134), and I and several others have demonstrated protective effects of DOX in models of myocardial I/R injury (198), stunning (73-75), and remodeling following infarction (68, 149, 200). While the tetracyclines have demonstrated efficacy in protecting the brain and heart from ischemic injury, the mechanisms by which these drugs exert their protective effects have not been completely elucidated.

The pathogenesis of myocardial I/R injury is incompletely understood and likely involves the interplay of several factors, including ROS, inflammation, protease activity, and other factors that ultimately lead to necrotic death or activation of the apoptosis cascade (9). I have previously demonstrated a role, at least in part, for the serine protease plasmin in mediating I/R injury in the heart (198). Plasmin circulates in the blood in its zymogen form, plasminogen, and becomes activated during thrombolysis. DOX treatment reduces infarct size in the rat *in vivo* and protects cultured myocytes from plasmin-mediated cell damage by inhibiting plasmin activity (198). However, whether DOX protects the heart from I/R injury via additional

mechanisms is unknown. Recently, it was demonstrated that MIN reduces infarct size in the isolated perfused rat heart, an I/R model devoid of blood, by attenuating the release of pro-apoptotic factors from the mitochondria and by reducing caspase expression and activity (134). Whether DOX is also capable of reducing infarct size in the blood-free isolated, perfused heart by these additional mechanisms remains to be determined.

Depending upon the length and severity of the ischemic period, I/R can lead to infarction or reversible contractile dysfunction in the absence of cell death, termed myocardial stunning. Reduced contractility during stunning has been shown to be due, at least in part, to intracellular MMP-2-mediated proteolysis of the sarcomeric proteins troponin I (TnI) and myosin light chain 1 (74, 75). DOX treatment has been shown to inhibit MMP-2 activity and preserve sarcomeric structure and function in an isolated, perfused rat heart model of stunning (74, 75). Like DOX, MIN is also capable of inhibiting MMPs (145). However, MIN is approximately twice as lipid soluble as DOX (32). Given the increased lipid solubility of MIN compared with DOX and its capacity to also inhibit MMPs, I hypothesized that MIN would have better access to the intracellular compartment than DOX and would therefore be a superior intracellular MMP inhibitor during myocardial stunning.

Therefore, the objectives of the present study were to (i) evaluate the cardioprotective effects of MIN and DOX on isolated, perfused rat hearts and cultured myocytes subjected to lethal I/R injury, and (ii) assess the effectiveness of MIN on

reducing injury and contractile dysfunction in isolated, perfused rat hearts subjected to stunning.

4.3. Experimental Methods

4.3.1. Isolated hearts

4.3.1.1. Langendorff method

Male Sprague-Dawley rats (Harlan, Indianapolis, IN) weighing 225-250 g were used. The animals were anesthetized by intraperitoneal injection of ketamine (100 mg/kg) and xylazine (10 mg/kg) coadministered with heparin (1000 U/kg), intubated, and positive-pressure ventilated with room air using a pressure-controlled ventilator (Kent Scientific, Torrington, CT). The heart was quickly excised and placed into a dish of ice-cold Krebs-Henseleit (K-H) buffer (118 mM NaCl, 4.7 mM KCl, 1.2 mM KH_2PO_4 , 1.2 mM MgSO_4 , 2.5 mM CaCl_2 , 0.5 mM EDTA, 11 mM glucose, 25 mM NaHCO_3). The aorta was quickly cannulated to a 14-gauge IV catheter connected to a Langendorff perfusion system. After cannulation, the heart was retrogradely perfused at a constant flow rate of 10 ml/min with K-H buffer, except the stunning experiments testing MIN were performed on hearts that were perfused at a constant pressure of 80 mmHg with K-H buffer. The K-H buffer was pre-filtered to 0.22 μm , continuously bubbled with 95% O_2 /5% CO_2 , and maintained at 37°C. The time from removal of the heart to perfusion was 1-2 min.

The left atrium was removed, and a water-filled balloon connected to a pressure transducer (Grass-Telefactor, West Warwick, RI) was inserted into the LV

through the mitral valve. The balloon volume was adjusted to achieve an end-diastolic pressure of 8-12 mmHg. Pacing leads attached to an electrical stimulator (Grass-Telefactor) were placed on the right atrium, and the heart was paced at 300 beats/min, except the stunning experiments testing MIN were performed on hearts that were not paced. Pacing was stopped during ischemia and resumed during reperfusion. LV pressure was digitally acquired (DataQ Instruments, Akron, OH) throughout the experiment. At various times coronary effluent was collected for determination of coronary flow rate. At the end of the protocol the hearts were removed and processed immediately for infarct size determination (see below) or flash frozen and stored at -80°C. Frozen tissue was homogenized on ice in lysis buffer (50 mM Tris pH 7.4, 150 mM NaCl, 5 mM CaCl₂, 0.2 mM NaN₃, 0.1% Triton X-100), except where indicated. Lysates were cleared by centrifugation at 12,000 g for 10 min at 4°C. Protein concentrations of the tissue extracts were determined using the Bio-Rad Protein Assay (Bio-Rad, Hercules, CA) with a BSA standard.

4.3.1.2. Minocycline treatment

For myocardial infarction studies, hearts were perfused under constant flow. Rats were pretreated with MIN or vehicle (water) for 3 days (90 mg/kg on day 1 and 45 mg/kg on days 2 and 3) by intraperitoneal injection. In addition, hearts were infused with MIN (1 µM) or vehicle (DMSO) throughout the experiment. Hearts were subjected to 35 min of global, no-flow ischemia (GNFI) by stopping the perfusion pump. The pump was then restarted and the hearts reperfused for 120 min.

For myocardial stunning studies, hearts were perfused under constant pressure. Hearts were subjected to 25 min of GNFI by clamping the perfusion line. The clamp was then released and the hearts reperfused for 30 min. MIN (0.5 μ M) or vehicle (DMSO) was infused into hearts throughout the experiment.

4.3.1.3. Doxycycline treatment

For myocardial infarction studies, hearts were perfused under constant flow. Rats were pretreated with DOX or vehicle (water) for 3 days (30 mg/kg per day) by intraperitoneal injection. In addition, hearts were infused with DOX (50 μ M) or vehicle (water) throughout the experiment. Hearts were subjected to 30 min of GNFI and 120 min of reperfusion.

In a separate group of hearts ischemic preconditioning was used as a positive control for cardioprotection. After 15 min of aerobic perfusion, hearts were subjected to 2 cycles of 5 min of GNFI and 5 min reperfusion followed by 30 min of GNFI and 120 min of reperfusion.

4.3.1.4. Creatine kinase (CK) release

Coronary effluent was collected on ice for measurement of CK activity before ischemia and during reperfusion. To each well of a microtiter plate was added 100 μ l of coronary effluent and 200 μ l of CK reagent (Pointe Scientific, Canton, MI). The rate of change in absorbance of NADH was determined spectrophotometrically at 340 nm for 15 min. The enzyme activity was calculated using the molar extinction coefficient of NADH ($\epsilon = 6.22$).

4.3.1.5. Determination of infarct size

The heart was sliced into 2-mm short-axis rings and stained with triphenyltetrazolium chloride (1%, Sigma) to identify viable myocardium. Apical and basal surfaces of each slice were photographed. The infarct area was determined by a blinded observer using computer-assisted planimetry (NIH Image).

4.3.1.6. Troponin I (TnI) release

Coronary effluent was analyzed for TnI content using a troponin I ELISA kit (Life Diagnostics, West Chester, PA) according to the manufacturer instructions.

4.3.1.7. MMP activity

A fluorescence-quenched peptide substrate probe was used to assess global MMP activity. Cleavage of the peptide results in release of the quencher and an increase in fluorescence. Tissue lysates or culture media were reacted with 10 μ M OmniMMP substrate (Mca-Pro-Leu-Gly-Leu-Dpa-Ala-Arg, BIOMOL Research Laboratories, Plymouth Meeting, PA) in assay buffer (50 mM Tris pH 7.5, 150 mM NaCl, 5 mM CaCl₂). Fluorescence (335 nm excitation, 405 nm emission) was monitored continuously at 37°C for 30 min using a fluorescence microplate reader (Bio-Tek Instruments, Winooski, VT).

4.3.1.8. Protein carbonyl assay

Protein carbonyl content within the tissue was measured using the Protein Carbonyl Assay kit per manufacturer instructions (Cayman Chemical, Ann Arbor, MI). This kit utilizes the reaction between 2,4-dinitrophenylhydrazine and protein carbonyls, which can be measured spectrophotometrically at 360 nm.

4.3.1.9. Nitrotyrosine immunoblot

Immunoblotting was performed as previously described (76). Tissue lysates were diluted 1:1 with 2X reducing sample buffer (17% glycerol, 8.7% β -ME, 5.2% SDS, 109 mM Tris pH 6.8), electrophoresed on 7.5% poly-acrylamide gels, and transferred to PVDF membranes (Millipore, Bedford, MA). Blots were probed with a rabbit polyclonal anti-nitrotyrosine antibody (1:5000, Calbiochem, San Diego, CA) followed by a horseradish peroxidase-conjugated secondary antibody (1:5000, Santa Cruz Biotechnology, Santa Cruz, CA). The immunoreactive proteins were detected using an enhanced chemiluminescence reaction kit (Amersham Biosciences, Piscataway, NJ). Blots were digitally scanned and band intensities were quantified (NIH Image).

4.3.2. Neonatal rat ventricular myocyte (NRVM) cultures

4.3.2.1. Isolation and culture

NRVMs were prepared as previously described (174). The hearts of 1-2 day old Sprague-Dawley rats were excised, minced, and digested with collagenase type 2 (80 U/ml, Worthington, Lakewood, NJ) and pancreatin (0.6 mg/ml, Sigma). The dispersed cells were applied to a discontinuous percoll density gradient, and the NRVMs and NRVMs were separated. The NRVMs were plated on 1% gelatin-coated tissue culture dishes to a density of 2.5×10^5 cells/cm² in plating media (68% DMEM, 17% M199, 10% horse serum, 5% FBS) and incubated at 37°C in a 5% CO₂ humidified environment. The NRVMs were cultured for 2 days in plating media, by which time the cells were spontaneously contracting. This purification protocol resulted in cultures of >95% myocytes as assessed by visual inspection of beating

cells and morphological characteristics. The media was then replaced with serum-free maintenance media (80% DMEM, 20% M199) until experimentation (1-2 days).

4.3.2.2. Hypoxia-reoxygenation

NRVMs were pretreated with DOX or MIN for 24 hours in maintenance media. The cells were made hypoxic by replacing the media with glucose-free DMEM containing DOX or MIN and using the BD GasPak EZ Anaerobic Chamber (BD Diagnostics, Franklin Lakes, NJ). This system provides an atmosphere of <1% O₂ within 2.5 hours. After 12 hours the cells were removed from the hypoxic chamber, the media replaced with maintenance media containing DOX or MIN, and the cells returned to the incubator for 24 hours.

4.3.2.3. Chemical hypoxia

NRVMs were pretreated with DOX or MIN for 24 hours in maintenance media. The cells were subjected to chemical hypoxia as previously described (201). Chemical hypoxia was induced by placing the cells into hypoxia buffer (106 mM NaCl, 4.4 mM KCl, 1.0 mM MgCl₂, 38 mM NaHCO₃, 2.5 mM CaCl₂, 20 mM 2-deoxyglucose, 1.0 mM NaCN, at pH 6.6) containing DOX or MIN for 4 hours.

Preliminary experiments established that 4 hours of chemical hypoxia resulted in ~50-60% cell viability when assessed 24 hours later. Control cells were incubated in the same buffer without 2-deoxyglucose or NaCN. The media was then replaced with maintenance media and the cells allowed to recover for 24 hours.

4.3.2.4. Oxidative stress

NRVMs were pretreated with DOX or MIN for 24 hours in maintenance media. The cells were then subjected to acute oxidative stress by the addition of 100 μM H_2O_2 for 24 hours. Preliminary experiments established that 100 μM H_2O_2 resulted in ~50-60% cell viability after 24 hours.

4.3.2.5. Cell viability

Cell viability was assessed using a methylthiazoletrazolium (MTT)-based *in vitro* toxicology assay kit (Sigma) per manufacturer instructions. Following treatment, cells were reacted with 0.5 mg/ml MTT for 2 hours. The reaction was stopped by the addition of solubilization solution (0.1 M HCl, 10% Triton X-100, 90% isopropanol). After mixing, the absorbance at 570 nm was measured.

4.3.2.6. CK release

Following treatment, culture media was removed and centrifuged at 200 g for 5 min to clear the media of any cells. CK activity in the media was determined as described above for coronary effluent.

4.3.3. Adult rat ventricular myocyte (ARVM) cultures

4.3.3.1. Isolation and culture

The isolation of calcium-tolerant adult rat ventricular myocytes was performed as previously described (202) with modifications. Briefly, adult male Sprague-Dawley rats weighing 225-250 g were anesthetized with ketamine (100 mg/kg) and xylazine (10 mg/kg) coadministered with heparin (1000 U/kg). The heart was quickly excised and mounted on a modified Langendorff perfusion system. The heart was perfused (10 ml/min) with a Ca^{2+} -free modified Tyrode's solution (126 mM NaCl, 4.4

mM KCl, 1.0 mM MgSO₄, 0.12 mM NaH₂PO₄, 10 mM HEPES, 5.5 mM glucose, 1.8 mM sodium pyruvate, 5.0 mM taurine, 4.0 mM NaHCO₃, 30 mM 2,3-butanedione monoxime [BDM], pH 7.3) at 37°C, bubbled with oxygen. After several minutes, the perfusate was switched to 25 μM Ca²⁺ Tyrode's solution containing collagenase type II (200 U/ml; Worthington Biochemical, Lakewood, NJ) for another 20 min. The ventricles were dissected free and minced. The tissue was then incubated in 25 mM Ca²⁺ Tyrode's solution containing collagenase type II (200 U/ml) and BSA (20 mg/ml) for an additional 20 min. The myocytes were gently dispersed and then passed through a 100 μm cell strainer to remove undigested tissue. Calcium was slowly reintroduced to the cells by serial washes with Tyrode's solution containing 100 μM Ca²⁺, 200 μM Ca²⁺, and 600 μM Ca²⁺. Myocytes were plated onto laminin-coated dishes (1 μg/cm²) at a concentration of 20,000 cells/cm² in modified Opti-MEM media (60% Opti-MEM [Invitrogen, Carlsbad, CA], 37% Ca²⁺-free Tyrodes solution without BDM, 3% FBS). After 2 hours the media was replaced and the myocytes used for experimentation.

4.3.3.2. Hypoxia-reoxygenation

ARVMs were pretreated with DOX or MIN for 1 hour in modified Opti-MEM media. The cells were made hypoxic by replacing the media with glucose-free DMEM containing DOX or MIN and placing the cells into the BD GasPak EZ Anaerobic Chamber. The cells were reoxygenated by removing them from the hypoxic chamber and replacing the media with fresh modified Opti-MEM containing DOX or MIN.

4.3.3.3. Apoptotic agents

Some ARVMs were treated with staurosporine (1 μ M) in modified Opti-MEM for up to 24 hours. Additional ARVMs were exposed to a germicidal UV light at a distance of 3 cm for 3 min. Both treatments resulted in microscopic evidence of membrane blebbing and cell shrinkage.

4.3.3.4. Viability assays

Cell viability was assessed by reaction with MTT as described above.

4.3.3.5. CK assay

CK release into the media was assessed as described above.

4.3.4. Mitochondria isolation and permeability assays

Mitochondria were isolated from rat livers by differential centrifugation. Briefly, rat livers were minced and then homogenized with a tissue tearer in buffer (250 mM sucrose, 5 mM HEPES pH 7.2, 1 mM EDTA) for 10 sec on ice. The homogenate was centrifuged at 500 g for 10 min at 4°C. The supernatant containing the mitochondria was collected and centrifuged at 9,400 g for 15 min at 4°C. The pellet containing the mitochondria was resuspended in buffer without EDTA and centrifuged at 9,400 g as before and repeated 3 more times. The final mitochondria pellet was stored on ice until experimentation. Protein concentration of the preparation was determined using the Bio-Rad Protein Assay. Mitochondria (50 μ g) were resuspended in 200 μ l swelling buffer (120 mM KCl, 10 mM Tris, 20 mM MOPS, 5 mM KH_2PO_4 , pH 7.4) in the presence or absence of DOX or MIN at room temperature for 5 min. Mitochondrial swelling was induced by the addition of CaCl_2 .

The amount of swelling was determined by monitoring the decrease in absorbance at 520 nm.

4.3.5. *In vitro* MMP inhibition by MIN

Human recombinant active MMP-9 (1.3 μ M; Calbiochem) or MMP-7 (1.7 μ M; Calbiochem) was incubated with various concentrations of MIN in assay buffer (50 mM Tris pH 7.5, 150 mM NaCl, 5 mM CaCl₂) 5 min at room temperature.

OmniMMP substrate was then added to a final concentration of 10 μ M and MMP activity determined as described above. The data were fit to the sigmoidal Hill equation: $Y = [MIN]^n / ([MIN]^n + k^n)$ (Prism, GraphPad Software, San Diego, CA). Y is the rate of substrate hydrolysis as a fraction of maximal substrate hydrolysis, n is the Hill coefficient, and k is the MIN concentration at which activity is half maximal (IC₅₀).

4.3.6. Statistical analysis

Results are expressed as mean \pm SEM. Comparisons between means were analyzed by student's t-test. A value of $p \leq 0.05$ was considered statistically significant.

4.4. Results

4.4.1. Minocycline, but not doxycycline, reduced infarct size following I/R injury

MIN and DOX were assessed for their abilities to protect against I/R injury in the isolated, perfused rat heart. In one experiment, rats were pretreated for 3 days with MIN (90 mg/kg on day 1 and 45 mg/kg on days 2 and 3) or vehicle (water). This dose

of MIN was previously shown to protect isolated hearts from I/R injury (134). Hearts were then subjected to 35 min of ischemia and 120 min of reperfusion. MIN (1 μ M) or vehicle (DMSO) was also infused through the heart throughout the experiment. MIN treatment resulted in a significant improvement in the recovery of contractile function as assessed by LV developed pressure and dP/dt (Figures 4-1A and B). MIN also reduced the amount of CK released during reperfusion (Figure 4-1C) and reduced infarct size by ~35% (Figure 4-1D).

In a second experiment, rats were pretreated for 3 days with DOX (30 mg/kg per day) or vehicle (water). This dose of DOX was previously shown to reduce infarct size in rats *in vivo* (198). Hearts were then subjected to 30 min of ischemia and 120 min of reperfusion. DOX (50 μ M) or vehicle (water) was also infused throughout the experiment. In this set of hearts, 35 min of ischemia resulted in no recovery of function, so the time of ischemia was reduced to 30 min. DOX treated hearts showed no difference in the recovery of LV developed pressure or dP/dt compared with controls (Figures 4-2A and B). Also, no difference was seen in the amount of CK released (Figure 4-2C). Ischemic preconditioning (2 cycles of 5 min ischemia and 5 min reperfusion prior to the 30 min of ischemia) was used as a positive control, and these hearts showed improved recovery of function (Figures 4-2A and B) and reduced CK release (Figure 4-2C).

4.4.2. Minocycline and doxycycline inhibited opening of the mitochondrial permeability transition pore

Since MIN has been shown to attenuate myocardial injury, at least in part, by inhibiting the release of pro-apoptotic factors from the mitochondria (134), I investigated the capacity of DOX and MIN to inhibit opening of the mitochondrial permeability transition pore (MPTP) in isolated mitochondria. MPTP opening was induced by the addition of calcium. The addition of increasing concentrations of calcium resulted in a dose-dependent increase in mitochondrial swelling, an indicator of MPTP opening, as measured by a decrease in absorbance at 520 nm (Figure 4-3A). Pretreatment with DOX resulted in a dose-dependent attenuation of swelling upon calcium stimulation (Figure 4-3B). Pretreatment with MIN reduced swelling only at a concentration of 200 μ M (Figure 4-3C). Therefore, both DOX and MIN inhibited Ca^{2+} -induced mitochondrial swelling, but surprisingly DOX showed a greater potency than MIN at inhibiting swelling.

4.4.3. Minocycline reduced myocardial stunning without inhibiting MMP activity

Since DOX has previously been shown to attenuate myocardial stunning via inhibition of intracellular MMP-mediated cleavage of troponin I (75), I also examined the capacity of MIN to reduce myocardial stunning given its increased lipophilicity compared with DOX and ability to penetrate cell membranes. Isolated, perfused rat hearts were subjected to 25 min of ischemia and 30 min of reperfusion in the presence or absence of MIN (0.5 μ M) infused throughout the experiment. In control hearts mechanical function recovered to ~60% of the pre-ischemia values as determined by the rate-pressure product. MIN treatment resulted in a significant increase in the

recovery of mechanical function compared with controls (Figure 4-4A). MIN also led to increased coronary flow rates during reperfusion, indicating improved vascular integrity (Figure 4-4B).

To determine if the protective effect of MIN was indeed due to MMP inhibition, MMP activity in the heart homogenates was measured at the end of the perfusion protocol. No difference in MMP activity was observed between the MIN-treated and the control hearts (Figure 4-5). Furthermore, the addition of MIN to purified MMP-9 (1.3 μM) or MMP-7 (1.7 μM) in buffer resulted in a dose-dependent inhibition of MMP activity with an IC_{50} of $135 \pm 35 \mu\text{M}$ for MMP-9 and $120 \pm 34 \mu\text{M}$ for MMP-7 as determined by hydrolysis of a peptide substrate. Therefore, the concentration of MIN infused into the isolated, perfused hearts (0.5 μM) was much lower than would be needed to inhibit MMPs.

Release of troponin I from the heart into the coronary effluent was also assessed. MIN-treated hearts tended toward reduced troponin I release, and this nearly reached statistical significance ($p = 0.06$) (Figure 4-6).

4.4.4. Minocycline increased peroxynitrite generation in stunned hearts

Since antioxidants have been shown to attenuate myocardial stunning by scavenging reactive oxygen species (79), stunned hearts were assessed for markers of oxidative stress. Tissue protein carbonyl content has previously been used as a marker of oxidative stress in isolated hearts (203). At the end of reperfusion, heart lysates were analyzed for protein carbonyl levels using a colorimetric kit. No significant difference in protein carbonyl content was seen between control and MIN-treated

hearts (Figure 4-7). Tissue nitrotyrosine content was measured by immunoblot as a second marker of oxidative stress. Peroxynitrite formed under conditions of oxidative stress can react with tyrosine residues on proteins to form nitrotyrosine. Several bands were observed on the immunoblot corresponding to proteins containing nitrotyrosine. Densitometric analysis of the sum of all bands revealed a significant increase in nitrotyrosine content within the MIN treated hearts compared with controls (Figure 4-8).

4.4.5. Minocycline and doxycycline did not preserve NRVM viability following hypoxia-reoxygenation

In order to further investigate mechanisms of actions of DOX and MIN in the protection against I/R injury, the drugs were assessed in cultures of NRVMs. NRVMs in the presence or absence of DOX or MIN were placed into a hypoxic chamber for 12 hours and then reoxygenated for 12 hours as a model of I/R injury. This procedure resulted in a 60% reduction in cell viability in untreated controls. Neither DOX nor MIN treatment resulted in improved cell survival as assessed by reduction of MTT, and 100 μ M MIN actually worsened cell survival (Figure 4-9A). Analysis of CK release into the culture media revealed an increase in CK after hypoxia but no increase in CK after reperfusion compared with normoxic controls (Figures 4-9B and C). These data indicate that hypoxia/reoxygenation in the NRVMs induced hypoxic injury but not reoxygenation injury. DOX and MIN did not reduce CK release, and 100 μ M MIN actually increased CK release (Figures 4-9B and C).

NRVMs were also subjected to chemical hypoxia followed by recovery as another model of I/R injury. Cells treated with various concentrations of DOX or MIN were incubated in 2-deoxyglucose and cyanide for 4 hours to inhibit oxidative respiration and then allowed to recover in normal media for 24 hours. This protocol resulted in ~40% reduction in cell viability. Neither DOX nor MIN improved cell survival under these conditions (Figure 4-10).

4.4.6. Minocycline and doxycycline did not preserve NRVM viability following oxidative stress

Since the generation of reactive oxygen species contributes to myocardial I/R injury (9), DOX and MIN were investigated for their abilities to protect NRVMs challenged with oxidative stress. NRVMs were incubated in 100 μ M H₂O₂ for 24 hours in the presence of varying concentrations of DOX or MIN. In the absence of any drug, H₂O₂ resulted in a 40% loss of cell viability as assessed by reduction of MTT. Neither DOX nor MIN improved cell survival, and 100 μ M DOX or MIN actually worsened survival (Figure 4-11).

4.4.7. Minocycline and doxycycline did not preserve ARVM viability following hypoxia-reoxygenation

Due to the lack of reperfusion injury with NRVMs, adult rat ventricular myocytes (ARVMs) were also tested to determine if they were a more suitable model of I/R injury. ARVMs were placed into a hypoxic chamber for 1 to 3 hours and then reoxygenated for up to 24 hours. CK release into the media increased upon reoxygenation, indicating additional injury to ARVMs upon reoxygenation.

Therefore, unlike NRVMs, reoxygenation injury was seen in ARVMs. CK release peaked at ~1 hour of reoxygenation and remained elevated for 8 hours (Figure 4-12). Viability in ARVMs pretreated with DOX or MIN was then assessed after 3 hours hypoxia and 2 hours reoxygenation. Hypoxia-reoxygenation resulted in ~60% loss in ARVM viability (Figure 4-13A) and ~4-fold increase in CK release into the media (Figure 4-13B). Neither DOX nor MIN protected against the loss of viability or release of CK. Cyclosporine A was used as a positive control for protection against reoxygenation injury since it has been shown to protect ARVMs from reoxygenation injury by preventing mitochondrial permeability pore opening (105). However, in this set of experiments cyclosporine A did not protect ARVMs (Figures 4-13A and B).

4.5. Discussion

In this study I demonstrated that MIN, but not DOX, improved the recovery of mechanical function and reduced infarct size in isolated, perfused rat hearts subjected to lethal I/R injury. The observed reduction in infarct size corroborate a recent report by Scarabelli et al. showing reduced infarct size in isolated, perfused rat hearts subjected to regional I/R (134), supporting the concept that MIN may be a novel cardioprotective agent. The cytoprotective capacity of MIN is an emerging area of research. MIN has previously been shown to improve survival in several models of neuronal cell injury (110-114). The mechanism by which MIN protects cells is thought to be due to its ability to inhibit caspase expression or to inhibit the mitochondrial apoptotic cascade. Zhu et al. demonstrated that MIN inhibits Ca^{2+} -

induced mitochondrial swelling and cytochrome c release in isolated mitochondria, indicating that the mitochondria, and perhaps the MPTP, are direct targets of MIN (114). The finding by Scarabelli et al. that MIN reduced cytochrome c translocation from the mitochondria to the cytosol in intact hearts following I/R (134) supports the idea that MIN causes mitochondrial stabilization in the heart.

The finding that DOX did not reduce infarct size in isolated hearts was somewhat surprising given that I have previously shown DOX to reduce infarct size *in vivo* (198). To explore the possibility that DOX lacked the mitochondrial-stabilizing properties of MIN, I compared the abilities of these two tetracyclines to inhibit MPTP opening in isolated mitochondria. I found that both DOX and MIN inhibited the Ca^{2+} -induced opening of the MPTP in a dose-dependent manner. However, DOX appeared a more potent inhibitor of the MPTP, displaying MPTP inhibition at 50 μM , whereas 200 μM MIN was required for inhibition. The concentration of MIN needed for inhibition is in agreement with the study by Zhu et al (114). Thus, these data show that DOX is an effective MPTP inhibitor and superior to MIN *in vitro*.

I propose that the disparity in protection by DOX and MIN in the isolated heart could be due to differences in subcellular distribution. MIN is a more lipophilic molecule, capable of penetrating tissues and crossing cell membranes as evidenced by its ability to cross the blood-brain barrier (32). DOX is of intermediate lipophilicity, and TET is the least lipophilic of the three and unable to penetrate the blood-brain barrier (32). Three previous studies support the idea of tissue penetration affecting their protective abilities. Yrjanheikki et al. showed that, in an *in vivo* model of brain

ischemia, MIN treatment resulted in the greatest reduction in infarct size, DOX showed an intermediate reduction, and TET had no effect (110). Baptiste et al. showed that MIN, but not TET, increased cell survival in retinal cell cultures subjected to cytotoxic stimuli (204). Finally, Scarabelli et al. showed that MIN, but not TET, reduced infarct size in isolated hearts (134). Thus, although DOX may be a superior inhibitor of MPTP opening compared with MIN *in vitro*, the ability of MIN to penetrate the cell membrane and reach the mitochondria may underlie its superior cytoprotective ability in intact cells.

I have previously reported that the ability of DOX to reduce infarct size *in vivo* may be due to its ability to inhibit plasmin (198). In the current study, DOX was not protective using an isolated, perfused heart model. The lack of protection in this *ex vivo*, blood-free system supports the idea that DOX protects the heart against a toxic blood-derived factor, which I believe to be plasmin. The ability of MIN to protect the heart in this model suggests that MIN is protective by a different mechanism than DOX, possibly by inhibiting MPTP opening. Taken together, these data suggest that DOX may exert its cardioprotective effect against I/R injury *in vivo* by targeting an extracellular, blood-derived factor (i.e., plasmin), while MIN protects by inhibiting MPTP-mediated apoptosis.

While MIN may in fact protect myocytes against cell death by inhibiting MPTP opening, MIN also has other effects, including its ability to inhibit MMPs (145) and scavenge ROS (82), that could protect against I/R injury. While a role for MMPs in contributing to adverse post-MI ventricular remodeling has been clearly established,

there remains some controversy as to whether MMPs may also contribute to myocyte death following I/R. In an *in vivo* rat model, Romanic et al. showed that MMP-9-deficient mice subjected to I/R had reduced infarct sizes compared with wild-type controls, suggesting MMP-9 contributes to myocyte injury (76). A previous study from my lab showed that DOX treatment reduced infarct size, and this correlated with reduced MMP-9 activity (198). However, when I assessed the ability of MMPs to directly compromise myocyte viability in culture, I found that physiological concentrations of MMPs were not cytotoxic (198).

Because of the potential, but uncertain, role for MMPs in inducing cell death in the heart, I decided to evaluate the capacity of MIN to inhibit MMPs in the heart using a model of myocardial stunning. In contrast to their uncertain role in mediating lethal I/R injury, MMPs, and MMP-2 in particular, have been clearly demonstrated to contribute to the loss of myocardial contractile activity following I/R (i.e., stunning) (73-75). It has been shown that MMP-2 activity is increased in isolated, perfused rat hearts following I/R, and inhibiting MMP-2 activity with an MMP-2 neutralizing antibody or with DOX improves the recovery of contractile function (73). It appears MMP-2 contributes to stunning by proteolyzing troponin I and myosin light chain intracellularly (74, 75). It is unclear how MMP-2 enters the myocyte during I/R. It has been shown that myocytes can undergo reversible membrane wounding, with transient cytosolic uptake of albumin in response to acute pressure overload (205). Therefore, one can speculate that myocyte membranes are reversibly wounded during I/R, allowing entry of MMPs.

Since Cheung et al. showed that DOX inhibited MMP-2 activity during myocardial stunning and improved functional recovery (73), I decided to use this model to test for the capacity of MIN to protect the heart by inhibiting MMPs. I infused the hearts with 0.5 μM MIN, the same concentration that reduced infarct size during lethal I/R. My results showed that MIN did improve the recovery of mechanical function during the first 30 minutes of reperfusion, and this was associated with improved coronary blood flow during reperfusion. However, MIN had no effect on MMP activity within the heart homogenates at the end of the 30 minute reperfusion period. Since I found the IC_{50} values for inhibition of MMP-9 and MMP-7 by MIN *in vitro* to be 135 μM and 120 μM , respectively, it is not surprising that the concentration of MIN infused into the heart (0.5 μM) did not inhibit MMP activity. Thus, these data suggest that MIN attenuated stunning by a mechanism independent of MMP inhibition.

I also evaluated the effect of MIN on markers of oxidative stress in the hearts following the stunning protocol. The generation of ROS during I/R is thought to be an important mediator of stunning (206), and MIN has been shown to be an effective ROS scavenger (82). Although MIN had no effect on protein carbonyl content, MIN actually increased protein nitrotyrosine content in the heart homogenates. Nitrotyrosine forms as a consequence of peroxynitrite generation from superoxide and nitric oxide (NO). Controversy exists within the literature as to whether peroxynitrite is cytotoxic or cytoprotective (207). The cytotoxic effects of peroxynitrite observed in some studies are attributed to oxidation of proteins, lipids, and DNA, leading to

interference of critical cellular functions. The cytoprotective effects of peroxynitrite observed in other studies are attributed to its ability to react with thiols, such as glutathione, and form NO-donor compounds (208). Indeed, infusion of peroxynitrite reduces infarct size and preserves coronary vascular function following I/R in cats (209). Therefore, it appears that MIN may attenuate myocardial stunning by augmenting peroxynitrite formation following I/R, as indicated by the increased nitrotyrosine content, leading to improved coronary artery flow via the formation of NO donor compounds.

In order to further explore the possibilities that MIN may protect the myocardium from I/R injury via inhibition of the MPTP or modulation of oxidative stress and NO, I explored the effects of DOX and MIN on cultured NRVMs subjected to hypoxia-reoxygenation injury. Surprisingly, I found that neither DOX nor MIN improved myocyte survival or reduced CK release. This is in contrast to the study by Scarabelli et al. showing MIN reduced apoptosis and necrosis of cultured NRVMs following hypoxia-reoxygenation (134). This discrepancy may be explained by inability of my culture conditions and hypoxia-reoxygenation protocol to induce reoxygenation injury in the NRVMs. I determined that reoxygenation injury was not occurring with this protocol due to the lack of additional CK release upon reoxygenation; CK was released only following the ischemic period. NRVMs were also subjected to two other insults, chemical hypoxia-reoxygenation and oxidative stress with H₂O₂. However, neither drug was cytoprotective using either of these

insults. Thus, these data show that, in my hands, DOX and MIN do not directly protect NRVMs from hypoxia-reoxygenation injury or oxidative stress.

I also assessed DOX and MIN in cultures of adult myocytes subjected to hypoxia-reoxygenation. Cultured ARVMs are more dependent upon oxidative respiration than NRVMs and, therefore, are a closer representation of the myocytes present within intact heart. ARVMs were appropriately more sensitive to hypoxia than NRVMs, with ~50% cell death within 1 hour of hypoxia versus 12 hours for NRVMs. In addition, ARVMs released additional CK into the media upon reoxygenation, demonstrating that reoxygenation injury was occurring. The amount of CK release upon reoxygenation was directly proportional to the time of ischemia. Therefore, cultured ARVM death in response to hypoxia-reoxygenation paralleled what is commonly observed in the intact organ, suggesting the ARVM culture model was an appropriate representation of the intact heart. However, again, DOX and MIN elicited no cytoprotection during hypoxia-reoxygenation. In addition, cyclosporine A, which has been shown to reduce infarct size in isolated hearts by inhibiting MPTP opening (131), did not improve survival.

It is interesting that MIN did not improve survival in the NRVM and ARVM cultures despite showing a clear reduction in myocyte cell death in the isolated, perfused heart. Cultures of NRVMs and ARVMs are used extensively as simplified models for investigating the effects of hypoxia and hypoxia-reoxygenation on the heart. However, it must be remembered that culture environment is profoundly different from the environment of the intact heart. The lack of three-dimensional

structure, supporting fibroblasts, mechanical stress, and electrical activity in addition to the altered extracellular matrix and cell-cell and cell-matrix interactions likely has significant effects on the expression and/or function of cellular targets of the tetracyclines. Thus, the lack of cytoprotection by DOX and MIN in culture does not take away from or invalidate the protective effects observed both in the isolated heart and *in vivo*.

In conclusion, MIN, but not DOX, reduced infarct size in isolated, perfused rat hearts subjected to I/R injury. The lack of protection by DOX supports my previous study demonstrating that DOX is cardioprotective by its ability to inhibit plasmin, a blood-borne protease. The protection by MIN in the absence of blood indicates acts by a different mechanism, likely inhibition of the MPTP given its ability to penetrate into the cell. MIN may also preserve coronary artery function via increasing NO levels. Taken together, these studies provide insight into the mechanisms by which the tetracyclines protect the heart from I/R injury, furthering our understanding of a potentially useful class of novel cardioprotective agents.

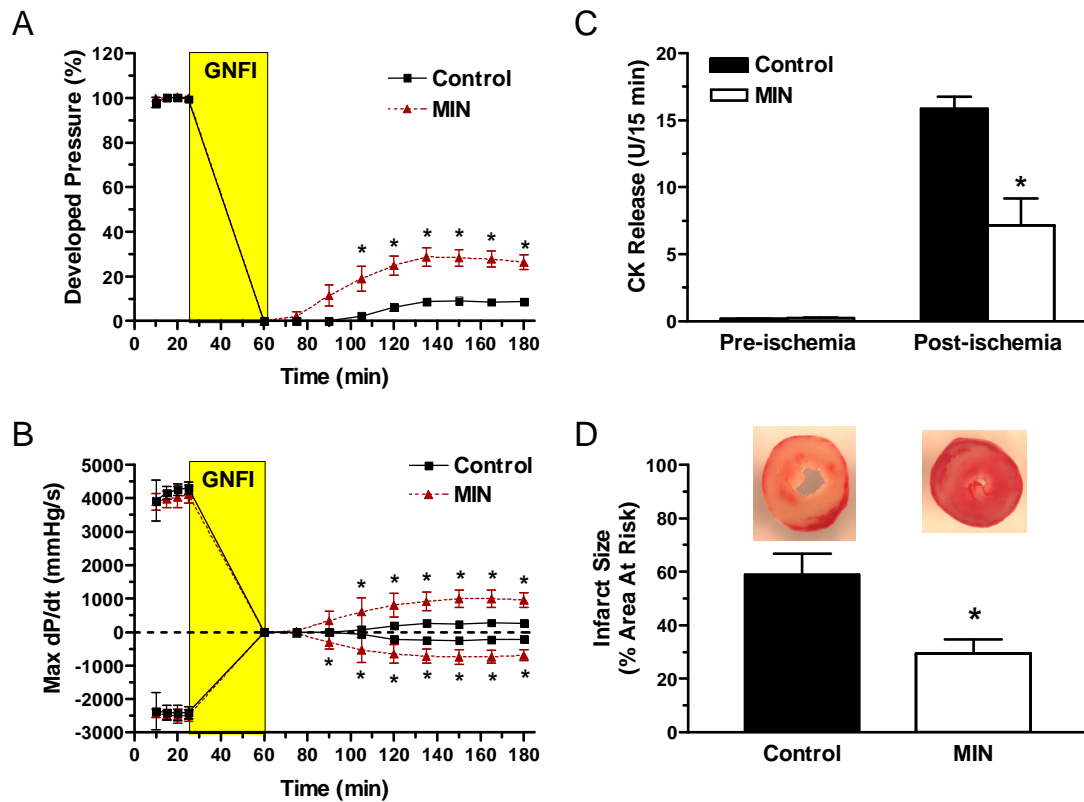


Figure 4-1. Effects of MIN treatment on isolated, perfused rat hearts subjected to 35 min of global, no-flow ischemia (GNFI) and 120 min of reperfusion. Rats were pretreated with MIN (90 mg/kg on day 1 and 45 mg/kg on days 2 & 3) prior to experimentation. MIN (1 μ M) was also infused during the perfusion. Recovery of LV developed pressure (**A**) and maximum dP/dt (**B**) during reperfusion were greater in the MIN-treated animals compared with controls. **C**, CK released during the 15 min before ischemia (Pre-ischemia) and the 15 min after ischemia (Post-ischemia). **D**, Infarct size in control and MIN-treated hearts. Images above the graph are representative TTC-stained sections used in the analysis of infarct size. Data are expressed as mean \pm SEM for control (n = 4) and MIN-treated (n = 4) hearts. * $p \leq 0.05$.

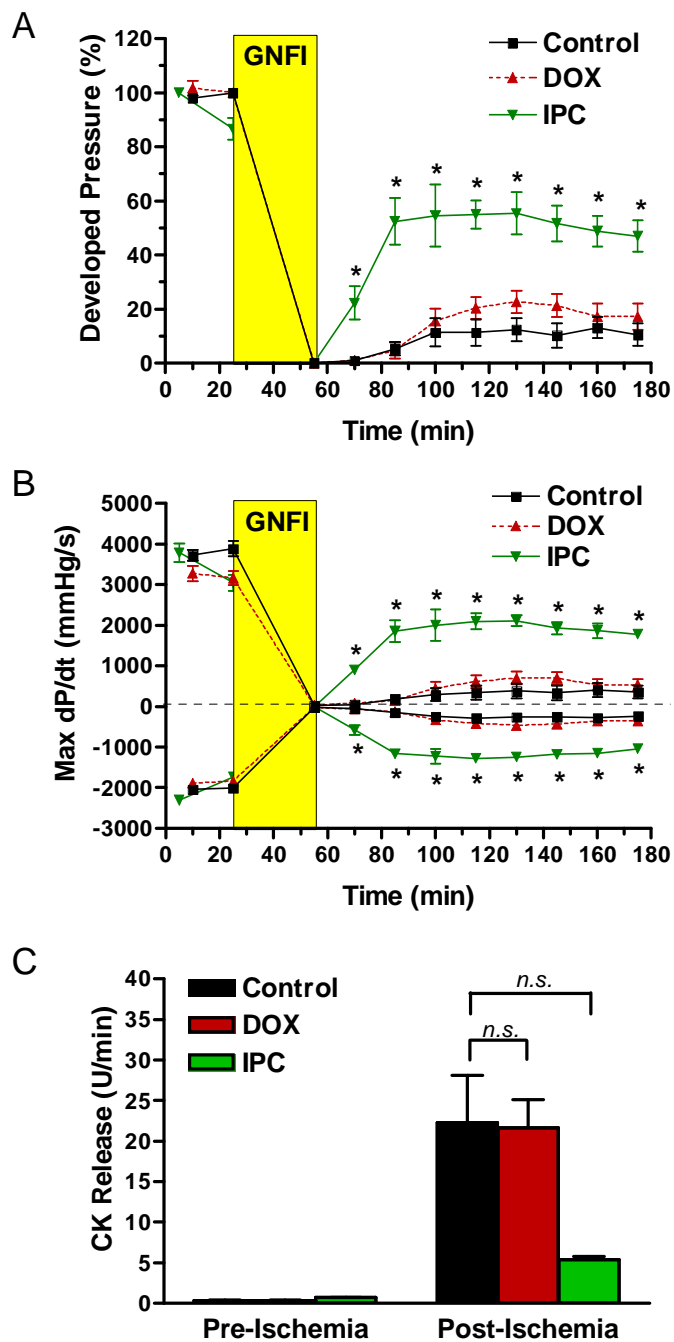


Figure 4-2. Effects of DOX treatment on isolated, perfused rat hearts subjected to 30 min of global, no-flow ischemia (GNFI) and 120 min of reperfusion. Rats were pretreated with DOX (30 mg/kg per day orally) for 3 days prior to experimentation, and hearts were also infused with DOX (50 μ M) throughout the perfusion. Ischemic preconditioning (IPC) (2 cycles of 5 min ischemia and 5 min reperfusion) was used as a positive control. Recovery of LV developed pressure (A) and maximum dP/dt (B) during reperfusion were similar between the DOX-treated and control hearts and improved by IPC. C, CK released during the 15 min before ischemia (Pre-ischemia) and the 15 min after ischemia (Post-ischemia). Data are expressed as mean \pm SEM for control (n = 7), DOX-treated (n = 7), and IPC (n = 2) hearts. n.s. = not significant. * $p \leq 0.05$.

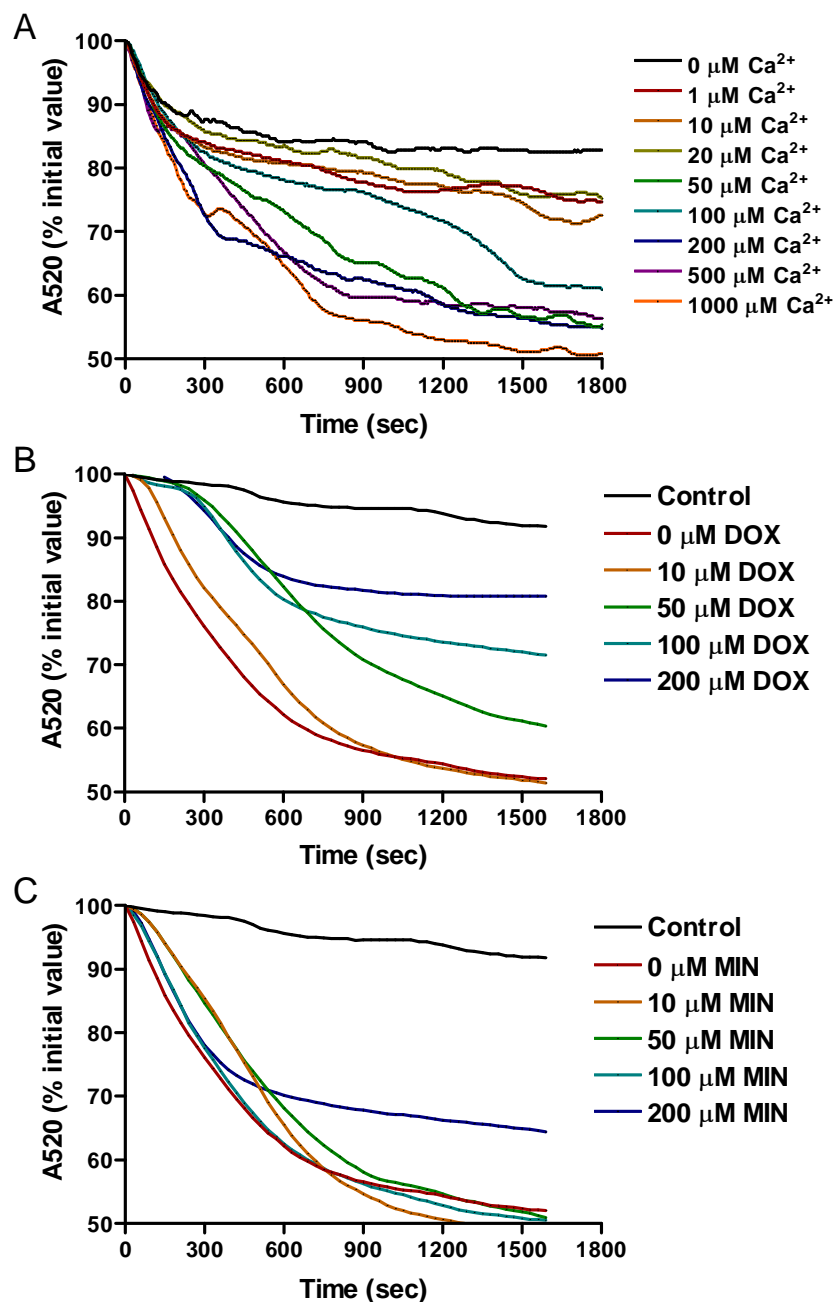


Figure 4-3. Effects of DOX and MIN on mitochondrial swelling under conditions associated with permeability transition pore opening in diluted rat liver mitochondria. **A**, Decrease in light absorbance following a pulse of varying Ca^{2+} concentrations. **B**, Decrease in light absorbance following a pulse of 500 $\mu\text{M Ca}^{2+}$ in the presence of varying DOX concentrations. **C**, Decrease in light absorbance following a pulse of 500 $\mu\text{M Ca}^{2+}$ in the presence of varying MIN concentrations. Absorbances were normalized to the absorbance immediately prior to the Ca^{2+} pulse. Traces are the mean of experiments performed from two different mitochondria preparations.

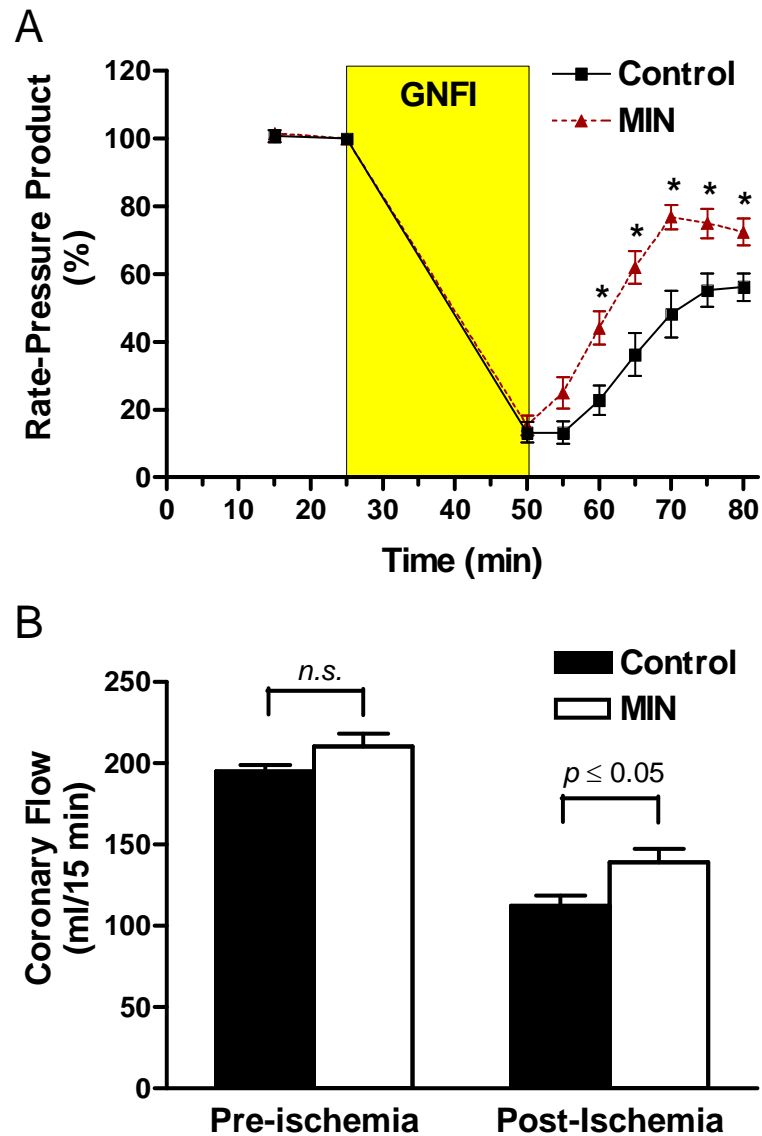


Figure 4-4. Effects of MIN on the recovery of mechanical function and coronary flow rate after 25 min of global, no-flow ischemia (GNFI). **A**, Recovery of rate-pressure product in control ($n = 8$) and MIN-treated ($n = 8$) hearts. **B**, Average coronary flow rates in control ($n = 8$) and MIN-treated ($n = 8$) hearts during the 15 min before (Pre-ischemia) and after (Post-ischemia) GNFI. Data are mean \pm SEM. * $p \leq 0.05$.

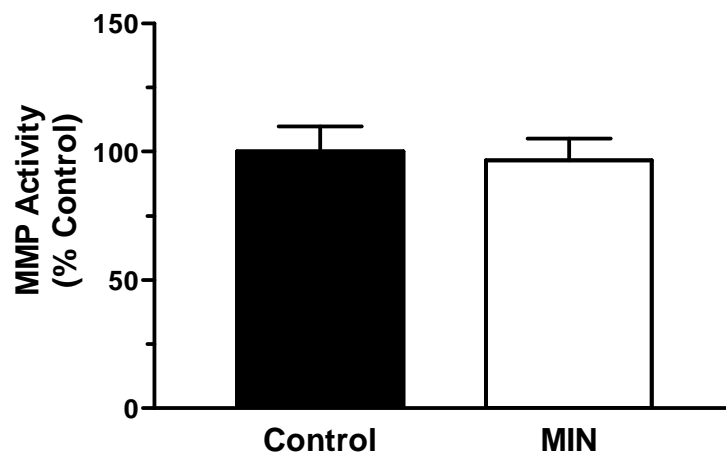


Figure 4-5. MMP activity in heart homogenates from control (n = 8) and MIN-treated (n = 8) hearts after 25 min of global, no-flow ischemia and 30 min of reperfusion as assessed by hydrolysis of a peptide substrate. Data are mean \pm SEM.

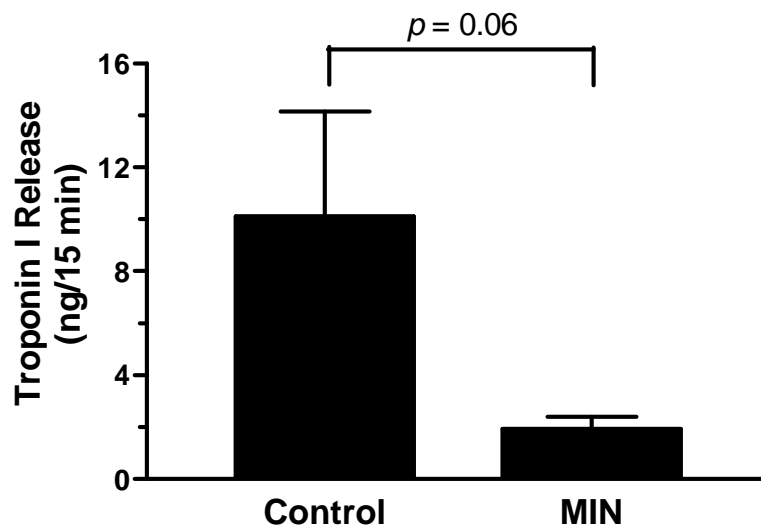


Figure 4-6. Effects of MIN on troponin I release following 25 min of global, no-flow ischemia. Troponin I released into the effluent during the first 15 min of reperfusion was collected and measured by ELISA. Data are mean \pm SEM for 8 hearts per group.

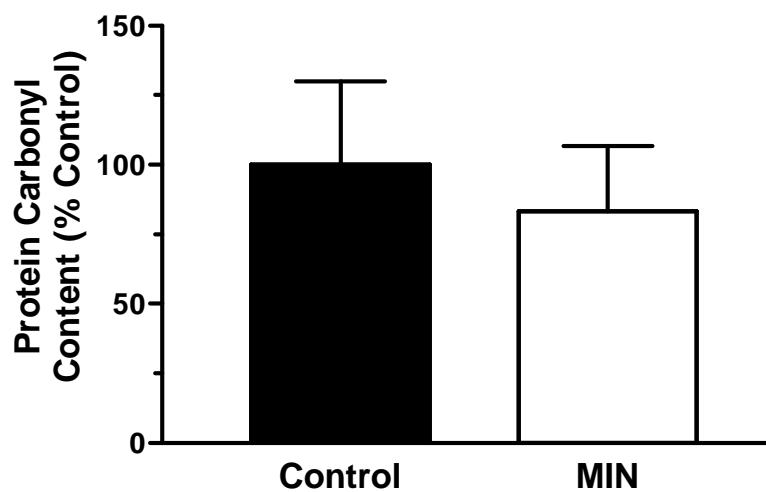


Figure 4-7. Protein carbonyl content in the homogenates of control (n = 8) and MIN-treated (n = 8) hearts following 25 min of global, no-flow ischemia and 30 min of reperfusion. No significant difference was found. Data are mean \pm SEM.

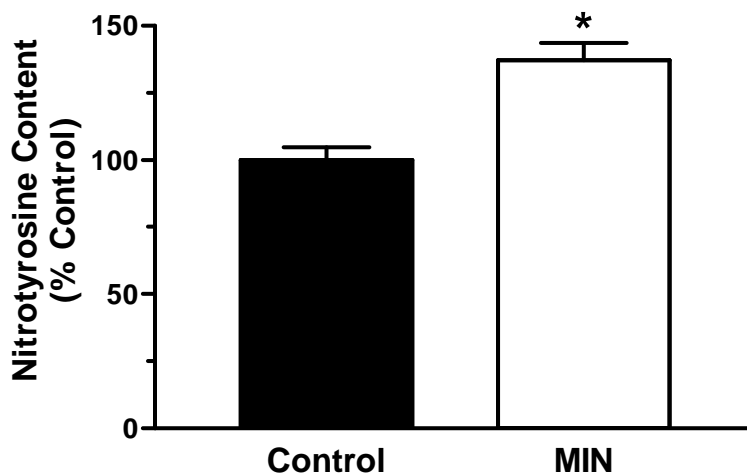


Figure 4-8. Nitrotyrosine content in the homogenates of control (n = 8) and MIN-treated (n = 8) hearts following 25 min of global, no-flow ischemia and 30 min of reperfusion. Data are mean \pm SEM. * $p \leq 0.05$.

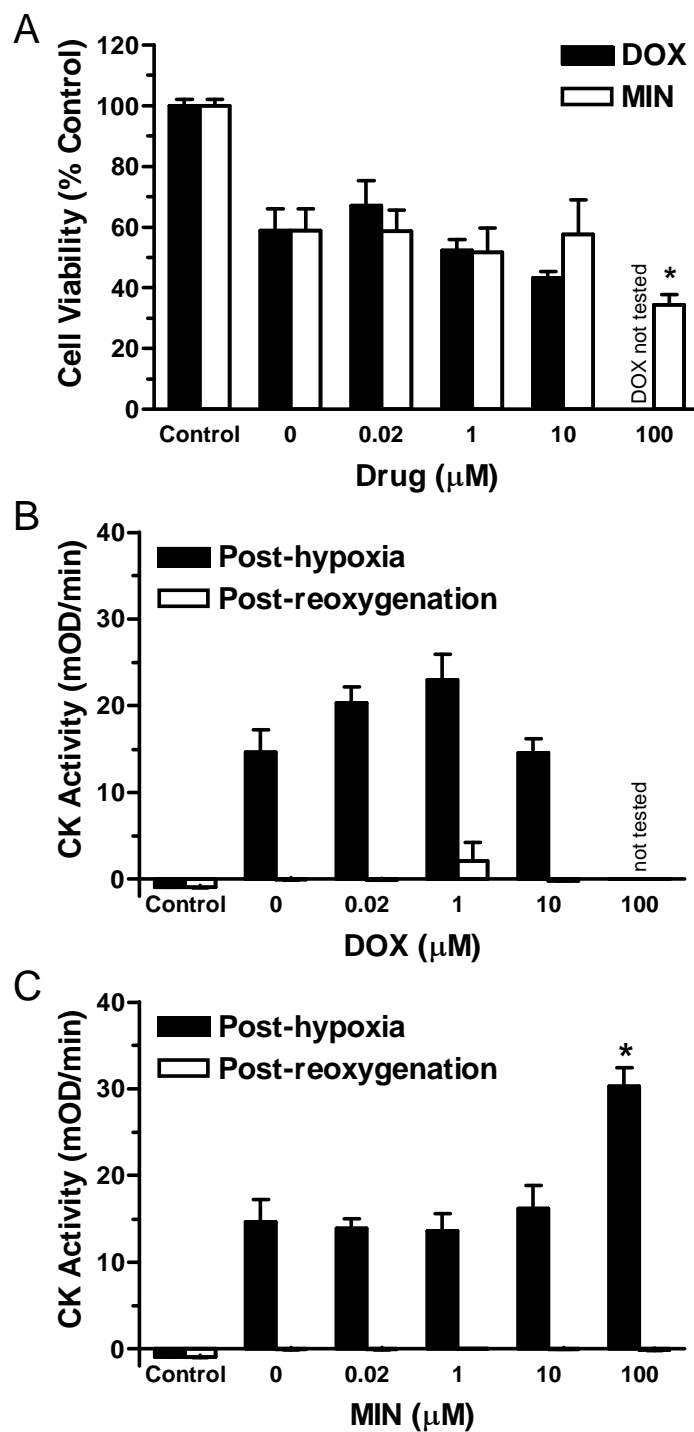


Figure 4-9. Effects of DOX and MIN on neonatal rat ventricular myocyte survival following 12 hr of hypoxia and 24 hr reoxygenation. **A**, Cell viability as assessed by reduction of MTT after reoxygenation. Values are normalized to normoxic controls. **B**, CK activity in the media of cells treated with varying concentrations of DOX. **C**, CK activity in the media of cells treated with varying concentrations of MIN. Data are mean \pm SEM for 3 replicates. * $p \leq 0.05$ versus 0 μM drug.

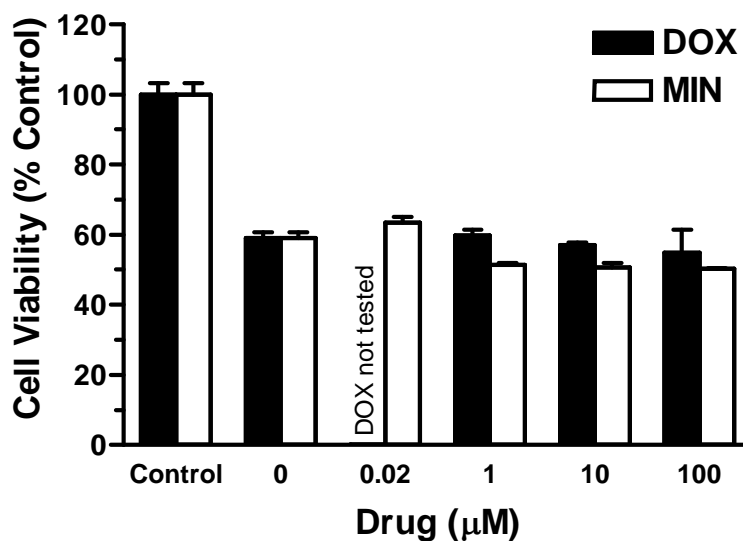


Figure 4-10. Effects of DOX and MIN on neonatal rat ventricular myocyte survival following 4 hr of chemical hypoxia and 24 hr of recovery. Values are normalized to normoxic controls. Data are mean \pm SEM for 3 replicates.

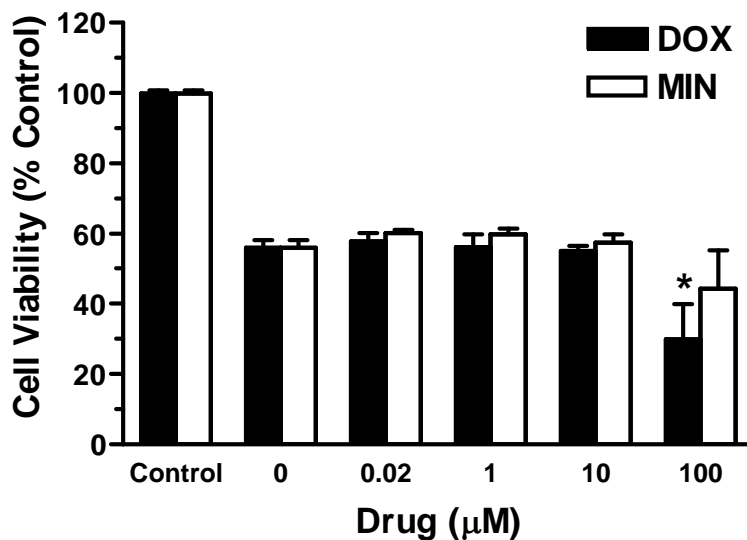


Figure 4-11. Effects of DOX and MIN on neonatal rat ventricular myocyte survival following incubation in 100 μ M H₂O₂ for 24hr. Values are normalized to normoxic controls. Data are mean \pm SEM for at least 6 replicates. * $p \leq 0.05$ versus 0 μ M drug.

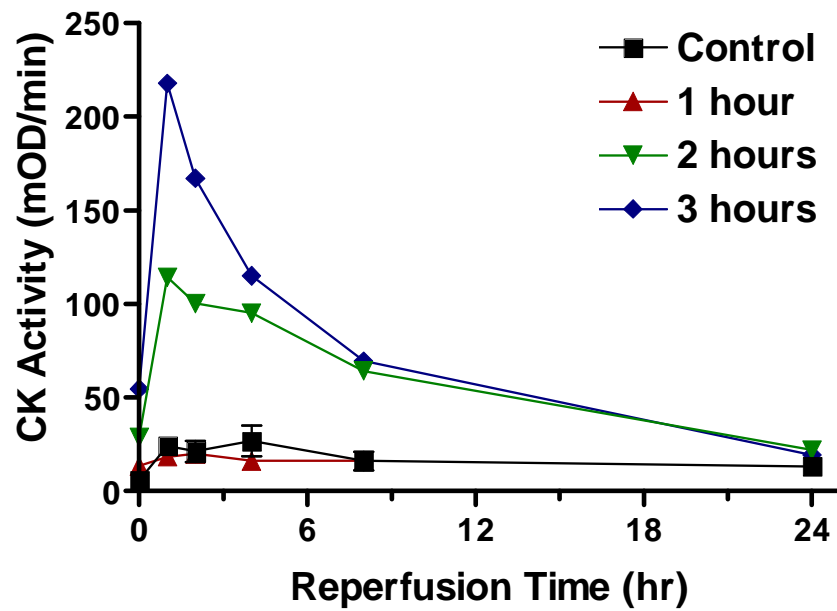


Figure 4-12. Increase in CK release upon reoxygenation in adult rat ventricular myocytes (ARVMs) previously made hypoxic. ARVMs were subjected to hypoxia for 1 to 3 hr and reoxygenation for up to 24 hr. CK activity in the media was assessed. Data are from a single experiment.

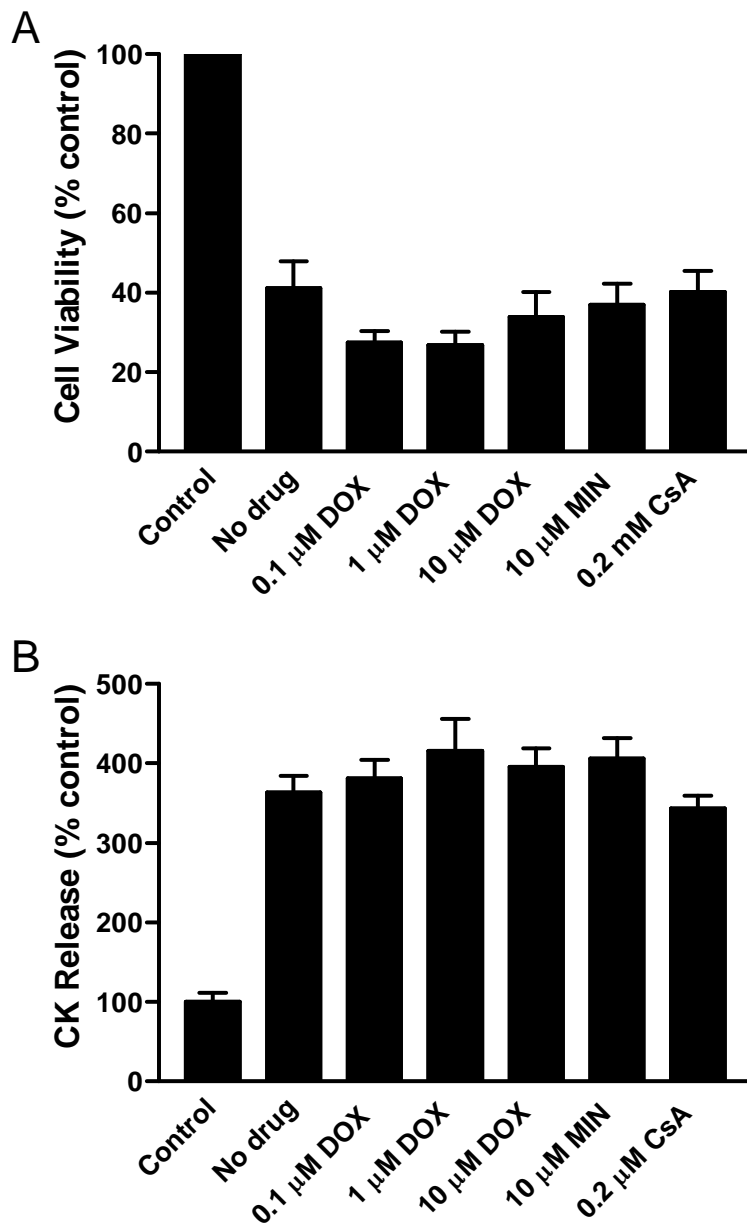


Figure 4-13. Effects of DOX and MIN on adult rat ventricular myocyte (ARVM) survival following 1 hr of hypoxia and 2 hr of reoxygenation. **A**, Cell viability as assessed by reduction of MTT. **B**, CK release into the media. Data are mean \pm SEM of experiments performed at least in duplicate from 4-6 cell preparations. CsA indicates cyclosporine A.

Chapter 5. Summary and Future Directions

The overall goal of this work was to examine the utility of the tetracyclines for use as novel cardioprotective agents in the setting of myocardial ischemic injury and to explore the potential mechanisms for their protective effects. Tetracyclines had previously been shown in other disease processes to have properties that held the potential to target important processes in the pathogenesis of adverse post-MI ventricular remodeling and I/R injury. In particular, the tetracyclines were known to inhibit MMPs, scavenge ROS, and inhibit the apoptotic cascade, all of which were known to contribute to cardiac remodeling or I/R injury. Thus, I undertook a systematic approach to examine these putative protective actions in the heart.

First, I demonstrated that DOX inhibited MMP activation and release post-MI, clarifying the mechanism by which DOX attenuated the adverse post-MI ventricular remodeling seen in a previous study from our laboratory. The concept of inhibiting MMPs to prevent remodeling was not new, however the hydroxamate-based drugs utilized in many of these previous studies have been evaluated in clinical trials and found to be either ineffective or discontinued due to intolerable side effects. My finding that DOX was an effective MMP inhibitor in the heart shed light upon a new class of MMP inhibitors with a long history of safe use in humans. Along these lines, I also evaluated the potency of novel zinc-binding groups developed by my colleagues for development into another new class of MMP inhibitors. I found that several members of this new class of compounds were up to 100-fold more potent than hydroxamate at inhibiting MMP activity in cultured cardiac fibroblasts. Therefore,

these new compounds hold promise for development into a novel class MMP inhibitors with the potential to be orders of magnitude more potent than hydroxamate-based MMP inhibitors. However, whether these compounds can be developed into MMP inhibitors with the same safety profile in humans as the tetracyclines or whether they follow in the footsteps of so many hydroxamate-based inhibitors before them remains to be seen.

Secondly, I demonstrated that DOX reduced infarct size following I/R in the rat *in vivo*. While I initially thought that DOX would be exerting this effect again by MMP inhibition, the results proved surprising. I found that MMPs did not compromise myocyte viability, but rather the plasmin that was being used to activate the MMPs was in fact killing myocytes, likely by proteolyzing β_{1D} -integrin and disrupting myocyte-matrix interactions. Through experiments performed both in culture and *in vitro*, I found that DOX, but not MIN or TET, was capable of inhibiting plasmin and preserving myocyte viability. It had previously been shown that tetracyclines could inhibit serine protease activity indirectly by preventing the MMP-mediated destruction of serine protease inhibitors. However, I found that the inhibition of plasmin by DOX was independent of its ability to inhibit MMPs and was actually due to direct inhibition of the plasmin enzyme. Thus, these experiments not only demonstrated a novel non-antimicrobial action for DOX but also set forth the possibility that plasmin can contribute to I/R injury.

To specifically examine the role of plasmin in I/R injury, I attempted to demonstrate that the addition of exogenous plasmin enhanced injury in isolated,

perfused hearts subjected to I/R. However, given the high concentration of endogenous plasmin/plasminogen in the blood, it was not economically feasible to perform the experiments with a physiological concentration of plasmin. Therefore, while I did not observe any additional injury with a sub-physiological concentration of plasmin, these results do not rule out a role for plasmin in I/R injury. Thus, continued investigation into this potential role of plasmin is warranted. Two approaches could be used to explore this: 1) infusion of physiological amounts of plasmin into isolated, perfused hearts (i.e., break the bank), or 2) *in vivo* I/R studies using a myocyte-specific anti-plasmin-overexpressing mouse.

Thirdly, I showed that MIN, but not DOX, reduced infarct size and improved the recovery of contractile function in isolated, perfused hearts subjected to I/R injury. The protective effect of MIN could be attributed to inhibition of the mitochondrial apoptosis pathway, since MIN directly inhibited MPTP opening. However, DOX was a more potent inhibitor of the MPTP, suggesting that other differences between these two tetracyclines must contribute to the discrepancy in their protective effects. I propose that the greater lipophilicity of MIN compared with DOX gives it greater ability to penetrate into tissues and cross cell membranes, thereby achieving higher intracellular concentrations. Future studies characterizing the subcellular distributions of DOX and MIN would help clarify this issue.

Fourthly, I demonstrated that MIN reduced the degree of myocardial stunning in isolated, perfused hearts as evidenced by improved recovery of contractile function and improved coronary artery flow. MMP-mediated proteolysis of intracellular

sarcomeric proteins was previously shown to contribute to myocardial stunning in isolated hearts, and, therefore, it provided a good model to examine whether a component of the cardioprotective action of MIN involved MMP inhibition. Results from these experiments showed that the reduction in stunning by MIN was not associated with a reduction in MMP activity. It was, however, associated with an increase in peroxynitrite generation. The role of peroxynitrite is a controversial in the literature, with some studies showing it is a cardiotoxic compound and others showing it is a cardioprotective compound. The cardioprotective actions are thought to be due to its ability to interact with thiols, such as glutathione, and generate NO-donor compounds. The elevated NO production causes vasodilation or contributes to the preconditioning effect. Since I observed improved coronary artery flow in the MIN-treated hearts, it is likely that MIN increases NO formation in the hearts, thereby causing vasodilation and improving post-ischemic delivery of oxygen. Additional studies are needed to validate this mechanism of action. Specifically, quantification of NO production in a similar set of experiments would verify that the MIN-induced increase in peroxynitrite does in fact generate NO.

Taken together, these studies demonstrate that, although the tetracyclines share many properties, they are sufficiently different to target different biochemical process involved in the pathogenesis of myocardial I/R injury and remodeling. The lipophilic nature of MIN allows it to have greater impact on intracellular processes, such as inhibiting MPTP opening and increasing peroxynitrite generation. The less lipophilic

nature of DOX confines its actions to the extracellular environment, with plasmin and MMP inhibition among its major effects.

In conclusion, the tetracyclines have a proven safety record in humans, are well tolerated, and possess disease-modifying capabilities. These characteristics justify continued research into their potential utility as adjuvant therapies in the treatment of myocardial I/R injury and post-MI remodeling.

REFERENCES

1. Braunwald, E. 1997. Shattuck lecture--cardiovascular medicine at the turn of the millennium: triumphs, concerns, and opportunities. *N Engl J Med* 337:1360-1369.
2. Thom, T., Haase, N., Rosamond, W., Howard, V.J., Rumsfeld, J., Manolio, T., Zheng, Z.J., Flegal, K., O'Donnell, C., Kittner, S., et al. 2006. Heart disease and stroke statistics--2006 update: a report from the American Heart Association Statistics Committee and Stroke Statistics Subcommittee. *Circulation* 113:e85-151.
3. Muller, J.E., Tofler, G.H., and Stone, P.H. 1989. Circadian variation and triggers of onset of acute cardiovascular disease. *Circulation* 79:733-743.
4. Virmani, R., Kolodgie, F.D., Burke, A.P., Farb, A., and Schwartz, S.M. 2000. Lessons from sudden coronary death: a comprehensive morphological classification scheme for atherosclerotic lesions. *Arterioscler Thromb Vasc Biol* 20:1262-1275.
5. Saraste, A., Pulkki, K., Kallajoki, M., Henriksen, K., Parvinen, M., and Voipio-Pulkki, L.M. 1997. Apoptosis in human acute myocardial infarction. *Circulation* 95:320-323.
6. Kloner, R.A., and Rezkalla, S.H. 2004. Cardiac protection during acute myocardial infarction: where do we stand in 2004? *J Am Coll Cardiol* 44:276-286.
7. Braunwald, E. 1989. Myocardial reperfusion, limitation of infarct size, reduction of left ventricular dysfunction, and improved survival. Should the paradigm be expanded? *Circulation* 79:441-444.
8. Boersma, E., Maas, A.C., Deckers, J.W., and Simoons, M.L. 1996. Early thrombolytic treatment in acute myocardial infarction: reappraisal of the golden hour. *Lancet* 348:771-775.
9. Park, J.L., and Lucchesi, B.R. 1999. Mechanisms of myocardial reperfusion injury. *Ann Thorac Surg* 68:1905-1912.
10. Pfeffer, M.A., and Braunwald, E. 1990. Ventricular remodeling after myocardial infarction. Experimental observations and clinical implications. *Circulation* 81:1161-1172.
11. Duggar, B.M. 1948. Aureomycin. *Ann N Y Acad Sci* 51:177-181.

12. Hash, J.H., Wishnick, M., and Miller, P.A. 1964. On the Mode of Action of the Tetracycline Antibiotics in *Staphylococcus Aureus*. *J Biol Chem* 239:2070-2078.
13. Tritton, T.R. 1977. Ribosome-tetracycline interactions. *Biochemistry* 16:4133-4138.
14. Semenkov Yu, P., Makarov, E.M., Makhno, V.I., and Kirillov, S.V. 1982. Kinetic aspects of tetracycline action on the acceptor (A) site of *Escherichia coli* ribosomes. *FEBS Lett* 144:125-129.
15. Levy, S.B., and McMurry, L. 1974. Detection of an inducible membrane protein associated with R-factor-mediated tetracycline resistance. *Biochem Biophys Res Commun* 56:1060-1068.
16. Yamaguchi, A., Udagawa, T., and Sawai, T. 1990. Transport of divalent cations with tetracycline as mediated by the transposon Tn10-encoded tetracycline resistance protein. *J Biol Chem* 265:4809-4813.
17. Hinrichs, W., Kisker, C., Duvel, M., Muller, A., Tovar, K., Hillen, W., and Saenger, W. 1994. Structure of the Tet repressor-tetracycline complex and regulation of antibiotic resistance. *Science* 264:418-420.
18. Gossen, M., and Bujard, H. 1992. Tight control of gene expression in mammalian cells by tetracycline-responsive promoters. *Proc Natl Acad Sci U S A* 89:5547-5551.
19. McNamara, T.F., Golub, L.M., D'Angelo, G., and Ramamurthy, N.S. 1986. The synthesis and characterization of non-antimicrobial chemically-modified tetracycline (CMT). *J Dent Res* 65 (Spec. Iss.):IADR Abstr. no. 515.
20. Golub, L.M., McNamara, T.F., D'Angelo, G., Greenwald, R.A., and Ramamurthy, N.S. 1987. A non-antibacterial chemically-modified tetracycline inhibits mammalian collagenase activity. *J Dent Res* 66:1310-1314.
21. Golub, L.M., Ramamurthy, N.S., McNamara, T.F., Greenwald, R.A., and Rifkin, B.R. 1991. Tetracyclines inhibit connective tissue breakdown: new therapeutic implications for an old family of drugs. *Crit Rev Oral Biol Med* 2:297-321.
22. Takahashi, M., Altschmied, L., and Hillen, W. 1986. Kinetic and equilibrium characterization of the Tet repressor-tetracycline complex by fluorescence measurements. Evidence for divalent metal ion requirement and energy transfer. *J Mol Biol* 187:341-348.

23. Ryan, M.E., Usman, A., Ramamurthy, N.S., Golub, L.M., and Greenwald, R.A. 2001. Excessive matrix metalloproteinase activity in diabetes: inhibition by tetracycline analogues with zinc reactivity. *Curr Med Chem* 8:305-316.
24. Goldman, R.A., Hasan, T., Hall, C.C., Strycharz, W.A., and Cooperman, B.S. 1983. Photoincorporation of tetracycline into *Escherichia coli* ribosomes. Identification of the major proteins photolabeled by native tetracycline and tetracycline photoproducts and implications for the inhibitory action of tetracycline on protein synthesis. *Biochemistry* 22:359-368.
25. Nelson, M.L. 1998. Chemical and biological dynamics of tetracyclines. *Adv Dent Res* 12:5-11.
26. Berthon, G., Brion, M., and Lambs, L. 1983. Metal ion-tetracycline interactions in biological fluids. 2. Potentiometric study of magnesium complexes with tetracycline, oxytetracycline, doxycycline, and minocycline, and discussion of their possible influence on the bioavailability of these antibiotics in blood plasma. *J Inorg Biochem* 19:1-18.
27. Lambs, L., Brion, M., and Berthon, G. 1984. Metal ion-tetracycline interactions in biological fluids. Part 3. Formation of mixed-metal ternary complexes of tetracycline, oxytetracycline, doxycycline and minocycline with calcium and magnesium, and their involvement in the bioavailability of these antibiotics in blood plasma. *Agents Actions* 14:743-750.
28. Brion, M., Lambs, L., and Berthon, G. 1985. Metal ion-tetracycline interactions in biological fluids. Part 5. Formation of zinc complexes with tetracycline and some of its derivatives and assessment of their biological significance. *Agents Actions* 17:229-242.
29. Burns, F.R., Stack, M.S., Gray, R.D., and Paterson, C.A. 1989. Inhibition of purified collagenase from alkali-burned rabbit corneas. *Invest Ophthalmol Vis Sci* 30:1569-1575.
30. Colaizzi, J.L., and Klink, P.R. 1969. pH-Partition behavior of tetracyclines. *J Pharm Sci* 58:1184-1189.
31. Blackwood, R.K., and English, A.R. 1970. Structure-activity relationships in the tetracycline series. *Adv Appl Microbiol* 13:237-266.
32. Barza, M., Brown, R.B., Shanks, C., Gamble, C., and Weinstein, L. 1975. Relation between lipophilicity and pharmacological behavior of minocycline, doxycycline, tetracycline, and oxytetracycline in dogs. *Antimicrob Agents Chemother* 8:713-720.

33. Yang, Q., Nakkula, R.J., and Walters, J.D. 2002. Accumulation of ciprofloxacin and minocycline by cultured human gingival fibroblasts. *J Dent Res* 81:836-840.
34. Walters, J.D., Nakkula, R.J., and Maney, P. 2005. Modulation of gingival fibroblast minocycline accumulation by biological mediators. *J Dent Res* 84:320-323.
35. Walters, J.D. 2006. Characterization of minocycline transport by human neutrophils. *J Periodontol* 77:1964-1968.
36. Holman, B.L., Idoine, J., Fliegel, C.P., Davis, M.A., Treves, S., Eldh, P., and Dewanjee, M.K. 1973. Detection and localization of experimental myocardial infarction with ^{99m}Tc-tetracycline. *J Nucl Med* 14:595-599.
37. Schelbert, H.R., Ingwall, J.S., Sybers, H.D., and Ashburn, W.L. 1976. Uptake of infarct-imaging agents in reversibly and irreversibly injured myocardium in cultured fetal mouse heart. *Circ Res* 39:860-868.
38. Nagase, H., and Woessner, J.F., Jr. 1999. Matrix metalloproteinases. *J Biol Chem* 274:21491-21494.
39. Spinale, F.G. 2002. Matrix metalloproteinases: regulation and dysregulation in the failing heart. *Circ Res* 90:520-530.
40. d'Ortho, M.P., Will, H., Atkinson, S., Butler, G., Messent, A., Gavrilovic, J., Smith, B., Timpl, R., Zardi, L., and Murphy, G. 1997. Membrane-type matrix metalloproteinases 1 and 2 exhibit broad-spectrum proteolytic capacities comparable to many matrix metalloproteinases. *Eur J Biochem* 250:751-757.
41. Mauviel, A. 1993. Cytokine regulation of metalloproteinase gene expression. *J Cell Biochem* 53:288-295.
42. Jones, C.B., Sane, D.C., and Herrington, D.M. 2003. Matrix metalloproteinases: a review of their structure and role in acute coronary syndrome. *Cardiovasc Res* 59:812-823.
43. Van Wart, H.E., and Birkedal-Hansen, H. 1990. The cysteine switch: a principle of regulation of metalloproteinase activity with potential applicability to the entire matrix metalloproteinase gene family. *Proc Natl Acad Sci U S A* 87:5578-5582.
44. Desrochers, P.E., Mookhtiar, K., Van Wart, H.E., Hasty, K.A., and Weiss, S.J. 1992. Proteolytic inactivation of alpha 1-proteinase inhibitor and alpha 1-antichymotrypsin by oxidatively activated human neutrophil metalloproteinases. *J Biol Chem* 267:5005-5012.

45. Michaelis, J., Vissers, M.C., and Winterbourn, C.C. 1990. Human neutrophil collagenase cleaves alpha 1-antitrypsin. *Biochem J* 270:809-814.
46. Nagase, H., Visse, R., and Murphy, G. 2006. Structure and function of matrix metalloproteinases and TIMPs. *Cardiovasc Res* 69:562-573.
47. Rohde, L.E., Ducharme, A., Arroyo, L.H., Aikawa, M., Sukhova, G.H., Lopez-Anaya, A., McClure, K.F., Mitchell, P.G., Libby, P., and Lee, R.T. 1999. Matrix metalloproteinase inhibition attenuates early left ventricular enlargement after experimental myocardial infarction in mice. *Circulation* 99:3063-3070.
48. Peterson, J.T. 2004. Matrix metalloproteinase inhibitor development and the remodeling of drug discovery. *Heart Fail Rev* 9:63-79.
49. Golub, L.M., Lee, H.M., Lehrer, G., Nemiroff, A., McNamara, T.F., Kaplan, R., and Ramamurthy, N.S. 1983. Minocycline reduces gingival collagenolytic activity during diabetes. Preliminary observations and a proposed new mechanism of action. *J Periodontal Res* 18:516-526.
50. Yu, L.P., Jr., Smith, G.N., Jr., Hasty, K.A., and Brandt, K.D. 1991. Doxycycline inhibits type XI collagenolytic activity of extracts from human osteoarthritic cartilage and of gelatinase. *J Rheumatol* 18:1450-1452.
51. Smith, G.N., Jr., Mickler, E.A., Hasty, K.A., and Brandt, K.D. 1999. Specificity of inhibition of matrix metalloproteinase activity by doxycycline: relationship to structure of the enzyme. *Arthritis Rheum* 42:1140-1146.
52. Garcia, R.A., Pantazatos, D.P., Gessner, C.R., Go, K.V., Woods, V.L., Jr., and Villarreal, F.J. 2005. Molecular interactions between matrilysin and the matrix metalloproteinase inhibitor doxycycline investigated by deuterium exchange mass spectrometry. *Mol Pharmacol* 67:1128-1136.
53. Greenwald, R.A., Golub, L.M., Ramamurthy, N.S., Chowdhury, M., Moak, S.A., and Sorsa, T. 1998. In vitro sensitivity of the three mammalian collagenases to tetracycline inhibition: relationship to bone and cartilage degradation. *Bone* 22:33-38.
54. Golub, L.M., Sorsa, T., Lee, H.M., Ciancio, S., Sorbi, D., Ramamurthy, N.S., Gruber, B., Salo, T., and Kontinen, Y.T. 1995. Doxycycline inhibits neutrophil (PMN)-type matrix metalloproteinases in human adult periodontitis gingiva. *J Clin Periodontol* 22:100-109.
55. Sorsa, T., Ding, Y., Salo, T., Lauhio, A., Teronen, O., Ingman, T., Ohtani, H., Andoh, N., Takeha, S., and Kontinen, Y.T. 1994. Effects of tetracyclines on

- neutrophil, gingival, and salivary collagenases. A functional and western-blot assessment with special reference to their cellular sources in periodontal diseases. *Ann N Y Acad Sci* 732:112-131.
56. Smith, G.N., Jr., Brandt, K.D., Mickler, E.A., and Hasty, K.A. 1997. Inhibition of recombinant human neutrophil collagenase by doxycycline is pH dependent. *J Rheumatol* 24:1769-1773.
 57. Hanemaaijer, R., Sorsa, T., Konttinen, Y.T., Ding, Y., Sutinen, M., Visser, H., van Hinsbergh, V.W., Helaakoski, T., Kainulainen, T., Ronka, H., et al. 1997. Matrix metalloproteinase-8 is expressed in rheumatoid synovial fibroblasts and endothelial cells. Regulation by tumor necrosis factor-alpha and doxycycline. *J Biol Chem* 272:31504-31509.
 58. Jonat, C., Chung, F.Z., and Baragi, V.M. 1996. Transcriptional downregulation of stromelysin by tetracycline. *J Cell Biochem* 60:341-347.
 59. Creemers, E.E., Cleutjens, J.P., Smits, J.F., and Daemen, M.J. 2001. Matrix metalloproteinase inhibition after myocardial infarction: a new approach to prevent heart failure? *Circ Res* 89:201-210.
 60. Sorsa, T., Lindy, O., Konttinen, Y.T., Suomalainen, K., Ingman, T., Saari, H., Halinen, S., Lee, H.M., Golub, L.M., Hall, J., et al. 1993. Doxycycline in the protection of serum alpha-1-antitrypsin from human neutrophil collagenase and gelatinase. *Antimicrob Agents Chemother* 37:592-594.
 61. Sorsa, T., Konttinen, Y.T., Lindy, O., Suomalainen, K., Ingman, T., Saari, H., Halinen, S., Lee, H.M., Golub, L.M., Hall, J., et al. 1993. Doxycycline protects serum alpha-1-antitrypsin from human neutrophil collagenase. *Agents Actions Suppl* 39:225-229.
 62. Golub, L.M., Evans, R.T., McNamara, T.F., Lee, H.M., and Ramamurthy, N.S. 1994. A non-antimicrobial tetracycline inhibits gingival matrix metalloproteinases and bone loss in *Porphyromonas gingivalis*-induced periodontitis in rats. *Ann N Y Acad Sci* 732:96-111.
 63. Crout, R.J., Lee, H.M., Schroeder, K., Crout, H., Ramamurthy, N.S., Wiener, M., and Golub, L.M. 1996. The "cyclic" regimen of low-dose doxycycline for adult periodontitis: a preliminary study. *J Periodontol* 67:506-514.
 64. Grenier, D., Plamondon, P., Sorsa, T., Lee, H.M., McNamara, T., Ramamurthy, N.S., Golub, L.M., Teronen, O., and Mayrand, D. 2002. Inhibition of proteolytic, serpinolytic, and progelatinase-b activation activities of periodontopathogens by doxycycline and the non-antimicrobial chemically modified tetracycline derivatives. *J Periodontol* 73:79-85.

65. Etoh, T., Joffs, C., Deschamps, A.M., Davis, J., Dowdy, K., Hendrick, J., Baicu, S., Mukherjee, R., Manhaini, M., and Spinale, F.G. 2001. Myocardial and interstitial matrix metalloproteinase activity after acute myocardial infarction in pigs. *Am J Physiol Heart Circ Physiol* 281:H987-994.
66. Romanic, A.M., Burns-Kurtis, C.L., Gout, B., Berrebi-Bertrand, I., and Ohlstein, E.H. 2001. Matrix metalloproteinase expression in cardiac myocytes following myocardial infarction in the rabbit. *Life Sci* 68:799-814.
67. Danielsen, C.C., Wiggers, H., and Andersen, H.R. 1998. Increased amounts of collagenase and gelatinase in porcine myocardium following ischemia and reperfusion. *J Mol Cell Cardiol* 30:1431-1442.
68. Villarreal, F., Omens, J., Dillmann, W., Risteli, J., Nguyen, J., and Covell, J. 2004. Early degradation and serum appearance of type I collagen fragments after myocardial infarction. *J Mol Cell Cardiol* 36:597-601.
69. Heymans, S., Luttun, A., Nuyens, D., Theilmeier, G., Creemers, E., Moons, L., Dyspersin, G.D., Cleutjens, J.P., Shipley, M., Angellilo, A., et al. 1999. Inhibition of plasminogen activators or matrix metalloproteinases prevents cardiac rupture but impairs therapeutic angiogenesis and causes cardiac failure. *Nat Med* 5:1135-1142.
70. Ducharme, A., Frantz, S., Aikawa, M., Rabkin, E., Lindsey, M., Rohde, L.E., Schoen, F.J., Kelly, R.A., Werb, Z., Libby, P., et al. 2000. Targeted deletion of matrix metalloproteinase-9 attenuates left ventricular enlargement and collagen accumulation after experimental myocardial infarction. *J Clin Invest* 106:55-62.
71. Hayashidani, S., Tsutsui, H., Ikeuchi, M., Shiomi, T., Matsusaka, H., Kubota, T., Imanaka-Yoshida, K., Itoh, T., and Takeshita, A. 2003. Targeted deletion of MMP-2 attenuates early LV rupture and late remodeling after experimental myocardial infarction. *Am J Physiol Heart Circ Physiol* 285:H1229-1235.
72. Matsumura, S., Iwanaga, S., Mochizuki, S., Okamoto, H., Ogawa, S., and Okada, Y. 2005. Targeted deletion or pharmacological inhibition of MMP-2 prevents cardiac rupture after myocardial infarction in mice. *J Clin Invest* 115:599-609.
73. Cheung, P.Y., Sawicki, G., Wozniak, M., Wang, W., Radomski, M.W., and Schulz, R. 2000. Matrix metalloproteinase-2 contributes to ischemia-reperfusion injury in the heart. *Circulation* 101:1833-1839.
74. Sawicki, G., Leon, H., Sawicka, J., Sariahmetoglu, M., Schulze, C.J., Scott, P.G., Szczesna-Cordary, D., and Schulz, R. 2005. Degradation of myosin light

- chain in isolated rat hearts subjected to ischemia-reperfusion injury: a new intracellular target for matrix metalloproteinase-2. *Circulation* 112:544-552.
75. Wang, W., Schulze, C.J., Suarez-Pinzon, W.L., Dyck, J.R., Sawicki, G., and Schulz, R. 2002. Intracellular action of matrix metalloproteinase-2 accounts for acute myocardial ischemia and reperfusion injury. *Circulation* 106:1543-1549.
 76. Romanic, A.M., Harrison, S.M., Bao, W., Burns-Kurtis, C.L., Pickering, S., Gu, J., Grau, E., Mao, J., Sathe, G.M., Ohlstein, E.H., et al. 2002. Myocardial protection from ischemia/reperfusion injury by targeted deletion of matrix metalloproteinase-9. *Cardiovasc Res* 54:549-558.
 77. Sabri, A., Alcott, S.G., Elouardighi, H., Pak, E., Derian, C., Andrade-Gordon, P., Kinnally, K., and Steinberg, S.F. 2003. Neutrophil cathepsin G promotes detachment-induced cardiomyocyte apoptosis via a protease-activated receptor-independent mechanism. *J Biol Chem* 278:23944-23954.
 78. Ding, B., Price, R.L., Goldsmith, E.C., Borg, T.K., Yan, X., Douglas, P.S., Weinberg, E.O., Bartunek, J., Thielen, T., Didenko, V.V., et al. 2000. Left ventricular hypertrophy in ascending aortic stenosis mice: anoikis and the progression to early failure. *Circulation* 101:2854-2862.
 79. Bolli, R., and Marban, E. 1999. Molecular and cellular mechanisms of myocardial stunning. *Physiol Rev* 79:609-634.
 80. Duilio, C., Ambrosio, G., Kuppusamy, P., DiPaula, A., Becker, L.C., and Zweier, J.L. 2001. Neutrophils are primary source of O₂ radicals during reperfusion after prolonged myocardial ischemia. *Am J Physiol Heart Circ Physiol* 280:H2649-2657.
 81. Wang, P., and Zweier, J.L. 1996. Measurement of nitric oxide and peroxynitrite generation in the postischemic heart. Evidence for peroxynitrite-mediated reperfusion injury. *J Biol Chem* 271:29223-29230.
 82. Kraus, R.L., Pasieczny, R., Lariosa-Willingham, K., Turner, M.S., Jiang, A., and Trauger, J.W. 2005. Antioxidant properties of minocycline: neuroprotection in an oxidative stress assay and direct radical-scavenging activity. *J Neurochem* 94:819-827.
 83. Hoeben, D., Burvenich, C., and Heyneman, R. 1998. Antibiotics commonly used to treat mastitis and respiratory burst of bovine polymorphonuclear leukocytes. *J Dairy Sci* 81:403-410.

84. Ramamurthy, N.S., Vernillo, A.T., Greenwald, R.A., Lee, H.M., Sorsa, T., Golub, L.M., and Rifkin, B.R. 1993. Reactive oxygen species activate and tetracyclines inhibit rat osteoblast collagenase. *J Bone Miner Res* 8:1247-1253.
85. Becker, L.B., vanden Hoek, T.L., Shao, Z.H., Li, C.Q., and Schumacker, P.T. 1999. Generation of superoxide in cardiomyocytes during ischemia before reperfusion. *Am J Physiol* 277:H2240-2246.
86. Zweier, J.L., Flaherty, J.T., and Weisfeldt, M.L. 1987. Direct measurement of free radical generation following reperfusion of ischemic myocardium. *Proc Natl Acad Sci U S A* 84:1404-1407.
87. Zweier, J.L., Kuppusamy, P., and Lutty, G.A. 1988. Measurement of endothelial cell free radical generation: evidence for a central mechanism of free radical injury in postischemic tissues. *Proc Natl Acad Sci U S A* 85:4046-4050.
88. Thompson-Gorman, S.L., and Zweier, J.L. 1990. Evaluation of the role of xanthine oxidase in myocardial reperfusion injury. *J Biol Chem* 265:6656-6663.
89. Chen, Z., Siu, B., Ho, Y.S., Vincent, R., Chua, C.C., Hamdy, R.C., and Chua, B.H. 1998. Overexpression of MnSOD protects against myocardial ischemia/reperfusion injury in transgenic mice. *J Mol Cell Cardiol* 30:2281-2289.
90. Wang, P., Chen, H., Qin, H., Sankarapandi, S., Becher, M.W., Wong, P.C., and Zweier, J.L. 1998. Overexpression of human copper, zinc-superoxide dismutase (SOD1) prevents postischemic injury. *Proc Natl Acad Sci U S A* 95:4556-4560.
91. Yoshida, T., Watanabe, M., Engelman, D.T., Engelman, R.M., Schley, J.A., Maulik, N., Ho, Y.S., Oberley, T.D., and Das, D.K. 1996. Transgenic mice overexpressing glutathione peroxidase are resistant to myocardial ischemia reperfusion injury. *J Mol Cell Cardiol* 28:1759-1767.
92. Jolly, S.R., Kane, W.J., Bailie, M.B., Abrams, G.D., and Lucchesi, B.R. 1984. Canine myocardial reperfusion injury. Its reduction by the combined administration of superoxide dismutase and catalase. *Circ Res* 54:277-285.
93. Ambrosio, G., Becker, L.C., Hutchins, G.M., Weisman, H.F., and Weisfeldt, M.L. 1986. Reduction in experimental infarct size by recombinant human superoxide dismutase: insights into the pathophysiology of reperfusion injury. *Circulation* 74:1424-1433.

94. Naslund, U., Haggmark, S., Johansson, G., Marklund, S.L., Reiz, S., and Oberg, A. 1986. Superoxide dismutase and catalase reduce infarct size in a porcine myocardial occlusion-reperfusion model. *J Mol Cell Cardiol* 18:1077-1084.
95. Tanonaka, K., Iwai, T., Motegi, K., and Takeo, S. 2003. Effects of N-(2-mercaptopropionyl)-glycine on mitochondrial function in ischemic-reperfused heart. *Cardiovasc Res* 57:416-425.
96. Yagi, H., Horinaka, S., and Matsuoka, H. 2005. Edaravone prevented deteriorated cardiac function after myocardial ischemia-reperfusion via inhibiting lipid peroxidation in rat. *J Cardiovasc Pharmacol* 46:46-51.
97. McDonald, M.C., Zacharowski, K., Bowes, J., Cuzzocrea, S., and Thiernemann, C. 1999. Tempol reduces infarct size in rodent models of regional myocardial ischemia and reperfusion. *Free Radic Biol Med* 27:493-503.
98. Massey, K.D., and Burton, K.P. 1989. alpha-Tocopherol attenuates myocardial membrane-related alterations resulting from ischemia and reperfusion. *Am J Physiol* 256:H1192-1199.
99. Flaherty, J.T., Pitt, B., Gruber, J.W., Heuser, R.R., Rothbaum, D.A., Burwell, L.R., George, B.S., Kereiakes, D.J., Deitchman, D., Gustafson, N., et al. 1994. Recombinant human superoxide dismutase (h-SOD) fails to improve recovery of ventricular function in patients undergoing coronary angioplasty for acute myocardial infarction. *Circulation* 89:1982-1991.
100. Yau, T.M., Weisel, R.D., Mickle, D.A., Burton, G.W., Ingold, K.U., Ivanov, J., Mohabeer, M.K., Tumiati, L., and Carson, S. 1994. Vitamin E for coronary bypass operations. A prospective, double-blind, randomized trial. *J Thorac Cardiovasc Surg* 108:302-310.
101. Lassnigg, A., Punz, A., Barker, R., Keznickl, P., Manhart, N., Roth, E., and Hiesmayr, M. 2003. Influence of intravenous vitamin E supplementation in cardiac surgery on oxidative stress: a double-blinded, randomized, controlled study. *Br J Anaesth* 90:148-154.
102. Fischer, U., Janicke, R.U., and Schulze-Osthoff, K. 2003. Many cuts to ruin: a comprehensive update of caspase substrates. *Cell Death Differ* 10:76-100.
103. Thorburn, A. 2004. Death receptor-induced cell killing. *Cell Signal* 16:139-144.

104. Saelens, X., Festjens, N., Vande Walle, L., van Gurp, M., van Loo, G., and Vandenameele, P. 2004. Toxic proteins released from mitochondria in cell death. *Oncogene* 23:2861-2874.
105. Halestrap, A.P., Clarke, S.J., and Javadov, S.A. 2004. Mitochondrial permeability transition pore opening during myocardial reperfusion--a target for cardioprotection. *Cardiovasc Res* 61:372-385.
106. Jiang, X., and Wang, X. 2004. Cytochrome C-mediated apoptosis. *Annu Rev Biochem* 73:87-106.
107. Nagata, S., Nagase, H., Kawane, K., Mukae, N., and Fukuyama, H. 2003. Degradation of chromosomal DNA during apoptosis. *Cell Death Differ* 10:108-116.
108. Susin, S.A., Lorenzo, H.K., Zamzami, N., Marzo, I., Snow, B.E., Brothers, G.M., Mangion, J., Jacotot, E., Costantini, P., Loeffler, M., et al. 1999. Molecular characterization of mitochondrial apoptosis-inducing factor. *Nature* 397:441-446.
109. Cory, S., and Adams, J.M. 2002. The Bcl2 family: regulators of the cellular life-or-death switch. *Nat Rev Cancer* 2:647-656.
110. Yrjanheikki, J., Keinanen, R., Pellikka, M., Hokfelt, T., and Koistinaho, J. 1998. Tetracyclines inhibit microglial activation and are neuroprotective in global brain ischemia. *Proc Natl Acad Sci U S A* 95:15769-15774.
111. Chen, M., Ona, V.O., Li, M., Ferrante, R.J., Fink, K.B., Zhu, S., Bian, J., Guo, L., Farrell, L.A., Hersch, S.M., et al. 2000. Minocycline inhibits caspase-1 and caspase-3 expression and delays mortality in a transgenic mouse model of Huntington disease. *Nat Med* 6:797-801.
112. Sanchez Mejia, R.O., Ona, V.O., Li, M., and Friedlander, R.M. 2001. Minocycline reduces traumatic brain injury-mediated caspase-1 activation, tissue damage, and neurological dysfunction. *Neurosurgery* 48:1393-1399; discussion 1399-1401.
113. Du, Y., Ma, Z., Lin, S., Dodel, R.C., Gao, F., Bales, K.R., Triarhou, L.C., Chernet, E., Perry, K.W., Nelson, D.L., et al. 2001. Minocycline prevents nigrostriatal dopaminergic neurodegeneration in the MPTP model of Parkinson's disease. *Proc Natl Acad Sci U S A* 98:14669-14674.
114. Zhu, S., Stavrovskaya, I.G., Drozda, M., Kim, B.Y., Ona, V., Li, M., Sarang, S., Liu, A.S., Hartley, D.M., Wu du, C., et al. 2002. Minocycline inhibits

cytochrome c release and delays progression of amyotrophic lateral sclerosis in mice. *Nature* 417:74-78.

115. Wang, X., Zhu, S., Drozda, M., Zhang, W., Stavrovskaya, I.G., Cattaneo, E., Ferrante, R.J., Kristal, B.S., and Friedlander, R.M. 2003. Minocycline inhibits caspase-independent and -dependent mitochondrial cell death pathways in models of Huntington's disease. *Proc Natl Acad Sci U S A* 100:10483-10487.
116. Wang, J., Wei, Q., Wang, C.Y., Hill, W.D., Hess, D.C., and Dong, Z. 2004. Minocycline up-regulates Bcl-2 and protects against cell death in mitochondria. *J Biol Chem* 279:19948-19954.
117. Olivetti, G., Quaini, F., Sala, R., Lagrasta, C., Corradi, D., Bonacina, E., Gambert, S.R., Cigola, E., and Anversa, P. 1996. Acute myocardial infarction in humans is associated with activation of programmed myocyte cell death in the surviving portion of the heart. *J Mol Cell Cardiol* 28:2005-2016.
118. Kajstura, J., Cheng, W., Reiss, K., Clark, W.A., Sonnenblick, E.H., Krajewski, S., Reed, J.C., Olivetti, G., and Anversa, P. 1996. Apoptotic and necrotic myocyte cell deaths are independent contributing variables of infarct size in rats. *Lab Invest* 74:86-107.
119. Bialik, S., Geenen, D.L., Sasson, I.E., Cheng, R., Horner, J.W., Evans, S.M., Lord, E.M., Koch, C.J., and Kitsis, R.N. 1997. Myocyte apoptosis during acute myocardial infarction in the mouse localizes to hypoxic regions but occurs independently of p53. *J Clin Invest* 100:1363-1372.
120. Palojoki, E., Saraste, A., Eriksson, A., Pulkki, K., Kallajoki, M., Voipio-Pulkki, L.M., and Tikkanen, I. 2001. Cardiomyocyte apoptosis and ventricular remodeling after myocardial infarction in rats. *Am J Physiol Heart Circ Physiol* 280:H2726-2731.
121. Tanaka, M., Ito, H., Adachi, S., Akimoto, H., Nishikawa, T., Kasajima, T., Marumo, F., and Hiroe, M. 1994. Hypoxia induces apoptosis with enhanced expression of Fas antigen messenger RNA in cultured neonatal rat cardiomyocytes. *Circ Res* 75:426-433.
122. Kang, P.M., Haunstetter, A., Aoki, H., Usheva, A., and Izumo, S. 2000. Morphological and molecular characterization of adult cardiomyocyte apoptosis during hypoxia and reoxygenation. *Circ Res* 87:118-125.
123. Webster, K.A., Discher, D.J., Kaiser, S., Hernandez, O., Sato, B., and Bishopric, N.H. 1999. Hypoxia-activated apoptosis of cardiac myocytes requires reoxygenation or a pH shift and is independent of p53. *J Clin Invest* 104:239-252.

124. von Harsdorf, R., Li, P.F., and Dietz, R. 1999. Signaling pathways in reactive oxygen species-induced cardiomyocyte apoptosis. *Circulation* 99:2934-2941.
125. Cheng, W., Li, B., Kajstura, J., Li, P., Wolin, M.S., Sonnenblick, E.H., Hintze, T.H., Olivetti, G., and Anversa, P. 1995. Stretch-induced programmed myocyte cell death. *J Clin Invest* 96:2247-2259.
126. Heidkamp, M.C., Bayer, A.L., Kalina, J.A., Eble, D.M., and Samarel, A.M. 2002. GFP-FRNK disrupts focal adhesions and induces anoikis in neonatal rat ventricular myocytes. *Circ Res* 90:1282-1289.
127. Krown, K.A., Page, M.T., Nguyen, C., Zechner, D., Gutierrez, V., Comstock, K.L., Glembotski, C.C., Quintana, P.J., and Sabbadini, R.A. 1996. Tumor necrosis factor alpha-induced apoptosis in cardiac myocytes. Involvement of the sphingolipid signaling cascade in cardiac cell death. *J Clin Invest* 98:2854-2865.
128. Jeremias, I., Kupatt, C., Martin-Villalba, A., Habazettl, H., Schenkel, J., Boekstegers, P., and Debatin, K.M. 2000. Involvement of CD95/Apo1/Fas in cell death after myocardial ischemia. *Circulation* 102:915-920.
129. Yaoita, H., Ogawa, K., Maehara, K., and Maruyama, Y. 1998. Attenuation of ischemia/reperfusion injury in rats by a caspase inhibitor. *Circulation* 97:276-281.
130. Okamura, T., Miura, T., Takemura, G., Fujiwara, H., Iwamoto, H., Kawamura, S., Kimura, M., Ikeda, Y., Iwatate, M., and Matsuzaki, M. 2000. Effect of caspase inhibitors on myocardial infarct size and myocyte DNA fragmentation in the ischemia-reperfused rat heart. *Cardiovasc Res* 45:642-650.
131. Halestrap, A.P., Connern, C.P., Griffiths, E.J., and Kerr, P.M. 1997. Cyclosporin A binding to mitochondrial cyclophilin inhibits the permeability transition pore and protects hearts from ischaemia/reperfusion injury. *Mol Cell Biochem* 174:167-172.
132. Argaud, L., Gateau-Roesch, O., Muntean, D., Chalabreysse, L., Loufouat, J., Robert, D., and Ovize, M. 2005. Specific inhibition of the mitochondrial permeability transition prevents lethal reperfusion injury. *J Mol Cell Cardiol* 38:367-374.
133. Chen, Z., Chua, C.C., Ho, Y.S., Hamdy, R.C., and Chua, B.H. 2001. Overexpression of Bcl-2 attenuates apoptosis and protects against myocardial I/R injury in transgenic mice. *Am J Physiol Heart Circ Physiol* 280:H2313-2320.

134. Scarabelli, T.M., Stephanou, A., Pasini, E., Gitti, G., Townsend, P., Lawrence, K., Chen-Scarabelli, C., Saravolatz, L., Latchman, D., Knight, R., et al. 2004. Minocycline inhibits caspase activation and reactivation, increases the ratio of XIAP to smac/DIABLO, and reduces the mitochondrial leakage of cytochrome C and smac/DIABLO. *J Am Coll Cardiol* 43:865-874.
135. Takahashi, S., Barry, A.C., and Factor, S.M. 1990. Collagen degradation in ischaemic rat hearts. *Biochem J* 265:233-241.
136. Sato, S., Ashraf, M., Millard, R.W., Fujiwara, H., and Schwartz, A. 1983. Connective tissue changes in early ischemia of porcine myocardium: an ultrastructural study. *J Mol Cell Cardiol* 15:261-275.
137. Caulfield, J.B., and Borg, T.K. 1979. The collagen network of the heart. *Lab Invest* 40:364-372.
138. Thompson, M.M., and Squire, I.B. 2002. Matrix metalloproteinase-9 expression after myocardial infarction: physiological or pathological? *Cardiovasc Res* 54:495-498.
139. Kelley, S.T., Malekan, R., Gorman, J.H., 3rd, Jackson, B.M., Gorman, R.C., Suzuki, Y., Plappert, T., Bogen, D.K., Sutton, M.G., and Edmunds, L.H., Jr. 1999. Restraining infarct expansion preserves left ventricular geometry and function after acute anteroapical infarction. *Circulation* 99:135-142.
140. Lalu, M.M., Csonka, C., Giricz, Z., Csont, T., Schulz, R., and Ferdinandy, P. 2002. Preconditioning decreases ischemia/reperfusion-induced release and activation of matrix metalloproteinase-2. *Biochem Biophys Res Commun* 296:937-941.
141. Jugdutt, B.I. 1993. Prevention of ventricular remodelling post myocardial infarction: timing and duration of therapy. *Can J Cardiol* 9:103-114.
142. Kovacs, E.J., and DiPietro, L.A. 1994. Fibrogenic cytokines and connective tissue production. *Faseb J* 8:854-861.
143. Witte, M.B., and Barbul, A. 1997. General principles of wound healing. *Surg Clin North Am* 77:509-528.
144. Heath, E.I., and Grochow, L.B. 2000. Clinical potential of matrix metalloprotease inhibitors in cancer therapy. *Drugs* 59:1043-1055.
145. Golub, L.M., Lee, H.M., Ryan, M.E., Giannobile, W.V., Payne, J., and Sorsa, T. 1998. Tetracyclines inhibit connective tissue breakdown by multiple non-antimicrobial mechanisms. *Adv Dent Res* 12:12-26.

146. Curci, J.A., Mao, D., Bohner, D.G., Allen, B.T., Rubin, B.G., Reilly, J.M., Sicard, G.A., and Thompson, R.W. 2000. Preoperative treatment with doxycycline reduces aortic wall expression and activation of matrix metalloproteinases in patients with abdominal aortic aneurysms. *J Vasc Surg* 31:325-342.
147. Baxter, B.T., Pearce, W.H., Waltke, E.A., Littooy, F.N., Hallett, J.W., Jr., Kent, K.C., Upchurch, G.R., Jr., Chaikof, E.L., Mills, J.L., Fleckten, B., et al. 2002. Prolonged administration of doxycycline in patients with small asymptomatic abdominal aortic aneurysms: report of a prospective (Phase II) multicenter study. *J Vasc Surg* 36:1-12.
148. Prall, A.K., Longo, G.M., Mayhan, W.G., Waltke, E.A., Fleckten, B., Thompson, R.W., and Baxter, B.T. 2002. Doxycycline in patients with abdominal aortic aneurysms and in mice: comparison of serum levels and effect on aneurysm growth in mice. *J Vasc Surg* 35:923-929.
149. Villarreal, F.J., Griffin, M., Omens, J., Dillmann, W., Nguyen, J., and Covell, J. 2003. Early short-term treatment with doxycycline modulates postinfarction left ventricular remodeling. *Circulation* 108:1487-1492.
150. Amin, A.R., Patel, R.N., Thakker, G.D., Lowenstein, C.J., Attur, M.G., and Abramson, S.B. 1997. Post-transcriptional regulation of inducible nitric oxide synthase mRNA in murine macrophages by doxycycline and chemically modified tetracyclines. *FEBS Lett* 410:259-264.
151. Pruzanski, W., Greenwald, R.A., Street, I.P., Laliberte, F., Stefanski, E., and Vadas, P. 1992. Inhibition of enzymatic activity of phospholipases A2 by minocycline and doxycycline. *Biochem Pharmacol* 44:1165-1170.
152. Meli, D.N., Coimbra, R.S., Erhart, D.G., Loquet, G., Bellac, C.L., Tauber, M.G., Neumann, U., and Leib, S.L. 2006. Doxycycline reduces mortality and injury to the brain and cochlea in experimental pneumococcal meningitis. *Infect Immun* 74:3890-3896.
153. Firatli, E., Unal, T., Onan, U., and Sandalli, P. 1994. Antioxidative activities of some chemotherapeutics. A possible mechanism in reducing gingival inflammation. *J Clin Periodontol* 21:680-683.
154. Attur, M.G., Patel, R.N., Patel, P.D., Abramson, S.B., and Amin, A.R. 1999. Tetracycline up-regulates COX-2 expression and prostaglandin E2 production independent of its effect on nitric oxide. *J Immunol* 162:3160-3167.
155. Puerta, D.T., Griffin, M.O., Lewis, J.A., Romero-Perez, D., Garcia, R., Villarreal, F.J., and Cohen, S.M. 2006. Heterocyclic zinc-binding groups for

- use in next-generation matrix metalloproteinase inhibitors: potency, toxicity, and reactivity. *J Biol Inorg Chem* 11:131-138.
156. Puerta, D.T., Lewis, J.A., and Cohen, S.M. 2004. New beginnings for matrix metalloproteinase inhibitors: identification of high-affinity zinc-binding groups. *J Am Chem Soc* 126:8388-8389.
 157. Hawkes, S.P., Li, H., and Taniguchi, G.T. 2001. Zymography and reverse zymography for detecting MMPs, and TIMPs. *Methods Mol Biol* 151:399-410.
 158. Villarreal, F.J., Kim, N.N., Ungab, G.D., Printz, M.P., and Dillmann, W.H. 1993. Identification of functional angiotensin II receptors on rat cardiac fibroblasts. *Circulation* 88:2849-2861.
 159. Hajduk, P.J., Shuker, S.B., Nettesheim, D.G., Craig, R., Augeri, D.J., Betebenner, D., Albert, D.H., Guo, Y., Meadows, R.P., Xu, L., et al. 2002. NMR-based modification of matrix metalloproteinase inhibitors with improved bioavailability. *J Med Chem* 45:5628-5639.
 160. Farkas, E., Katz, Y., Bhusare, S., Reich, R., Roschenthaler, G.V., Konigsmann, M., and Breuer, E. 2004. Carbamoylphosphonate-based matrix metalloproteinase inhibitor metal complexes: solution studies and stability constants. Towards a zinc-selective binding group. *J Biol Inorg Chem* 9:307-315.
 161. Xie, Z., Singh, M., and Singh, K. 2004. Differential regulation of matrix metalloproteinase-2 and -9 expression and activity in adult rat cardiac fibroblasts in response to interleukin-1beta. *J Biol Chem* 279:39513-39519.
 162. Tyagi, S.C., Lewis, K., Pikes, D., Marcello, A., Mujumdar, V.S., Smiley, L.M., and Moore, C.K. 1998. Stretch-induced membrane type matrix metalloproteinase and tissue plasminogen activator in cardiac fibroblast cells. *J Cell Physiol* 176:374-382.
 163. Festuccia, C., Dolo, V., Guerra, F., Violini, S., Muzi, P., Pavan, A., and Bologna, M. 1998. Plasminogen activator system modulates invasive capacity and proliferation in prostatic tumor cells. *Clin Exp Metastasis* 16:513-528.
 164. Parsa, C.J., Kim, J., Riel, R.U., Pascal, L.S., Thompson, R.B., Petrofski, J.A., Matsumoto, A., Stamler, J.S., and Koch, W.J. 2004. Cardioprotective effects of erythropoietin in the reperfused ischemic heart: a potential role for cardiac fibroblasts. *J Biol Chem* 279:20655-20662.
 165. Stadler, B., Phillips, J., Toyoda, Y., Federman, M., Levitsky, S., and McCully, J.D. 2001. Adenosine-enhanced ischemic preconditioning modulates necrosis

- and apoptosis: effects of stunning and ischemia-reperfusion. *Ann Thorac Surg* 72:555-563; discussion 563-554.
166. Wakiyama, H., Cowan, D.B., Toyoda, Y., Federman, M., Levitsky, S., and McCully, J.D. 2002. Selective opening of mitochondrial ATP-sensitive potassium channels during surgically induced myocardial ischemia decreases necrosis and apoptosis. *Eur J Cardiothorac Surg* 21:424-433.
 167. Collen, D. 2001. Ham-Wasserman lecture: role of the plasminogen system in fibrin-homeostasis and tissue remodeling. *Hematology (Am Soc Hematol Educ Program)*:1-9.
 168. Knoepfler, P.S., Bloor, C.M., and Carroll, S.M. 1995. Urokinase plasminogen activator activity is increased in the myocardium during coronary artery occlusion. *J Mol Cell Cardiol* 27:1317-1324.
 169. Gurevitch, J., Barak, J., Hochhauser, E., Paz, Y., and Yakirevich, V. 1994. Aprotinin improves myocardial recovery after ischemia and reperfusion. Effects of the drug on isolated rat hearts. *J Thorac Cardiovasc Surg* 108:109-118.
 170. McCarthy, R.J., Tuman, K.J., O'Connor, C., and Ivankovich, A.D. 1999. Aprotinin pretreatment diminishes postischemic myocardial contractile dysfunction in dogs. *Anesth Analg* 89:1096-1100.
 171. Imamura, T., Matsushita, K., Travis, J., and Potempa, J. 2001. Inhibition of trypsin-like cysteine proteinases (gingipains) from *Porphyromonas gingivalis* by tetracycline and its analogues. *Antimicrob Agents Chemother* 45:2871-2876.
 172. Curci, J.A., Petrincec, D., Liao, S., Golub, L.M., and Thompson, R.W. 1998. Pharmacologic suppression of experimental abdominal aortic aneurysms: a comparison of doxycycline and four chemically modified tetracyclines. *J Vasc Surg* 28:1082-1093.
 173. Lamparter, S., Slight, S.H., and Weber, K.T. 2002. Doxycycline and tissue repair in rats. *J Lab Clin Med* 139:295-302.
 174. Iwaki, K., Sukhatme, V.P., Shubeita, H.E., and Chien, K.R. 1990. Alpha- and beta-adrenergic stimulation induces distinct patterns of immediate early gene expression in neonatal rat myocardial cells. fos/jun expression is associated with sarcomere assembly; Egr-1 induction is primarily an alpha 1-mediated response. *J Biol Chem* 265:13809-13817.

175. Meilhac, O., Ho-Tin-Noe, B., Houard, X., Philippe, M., Michel, J.B., and Angles-Cano, E. 2003. Pericellular plasmin induces smooth muscle cell anoikis. *Faseb J* 17:1301-1303.
176. Choi, N.-S., Yoon, K.-S., Lee, J.-Y., Han, K.-Y., and Kim, S.-H. 2001. Comparison of three substrates (casein, fibrin, and gelatin) in zymographic gel. *J Biochem Mol Biol* 34:531-536.
177. Pozzi, A., Moberg, P.E., Miles, L.A., Wagner, S., Soloway, P., and Gardner, H.A. 2000. Elevated matrix metalloprotease and angiostatin levels in integrin alpha 1 knockout mice cause reduced tumor vascularization. *Proc Natl Acad Sci U S A* 97:2202-2207.
178. Pham, C.G., Harpf, A.E., Keller, R.S., Vu, H.T., Shai, S.Y., Loftus, J.C., and Ross, R.S. 2000. Striated muscle-specific beta(1D)-integrin and FAK are involved in cardiac myocyte hypertrophic response pathway. *Am J Physiol Heart Circ Physiol* 279:H2916-2926.
179. Lindsey, M., Wedin, K., Brown, M.D., Keller, C., Evans, A.J., Smolen, J., Burns, A.R., Rossen, R.D., Michael, L., and Entman, M. 2001. Matrix-dependent mechanism of neutrophil-mediated release and activation of matrix metalloproteinase 9 in myocardial ischemia/reperfusion. *Circulation* 103:2181-2187.
180. Griswold, D.E., Hillegass, L.M., Hill, D.E., Egan, J.W., and Smith, E.F., 3rd. 1988. Method for quantification of myocardial infarction and inflammatory cell infiltration in rat cardiac tissue. *J Pharmacol Methods* 20:225-235.
181. Kaden, J.J., Dempfle, C.E., Sueselbeck, T., Brueckmann, M., Poerner, T.C., Haghi, D., Haase, K.K., and Borggreffe, M. 2003. Time-dependent changes in the plasma concentration of matrix metalloproteinase 9 after acute myocardial infarction. *Cardiology* 99:140-144.
182. Ross, R.S., and Borg, T.K. 2001. Integrins and the myocardium. *Circ Res* 88:1112-1119.
183. Hoover-Plow, J.L., Miles, L.A., Fless, G.M., Scanu, A.M., and Plow, E.F. 1993. Comparison of the lysine binding functions of lipoprotein(a) and plasminogen. *Biochemistry* 32:13681-13687.
184. Smith, E.F., 3rd, Egan, J.W., Bugelski, P.J., Hillegass, L.M., Hill, D.E., and Griswold, D.E. 1988. Temporal relation between neutrophil accumulation and myocardial reperfusion injury. *Am J Physiol* 255:H1060-1068.

185. Kaito, K., Urayama, H., and Watanabe, G. 2003. Doxycycline treatment in a model of early abdominal aortic aneurysm. *Surg Today* 33:426-433.
186. Beckman, J.S., Beckman, T.W., Chen, J., Marshall, P.A., and Freeman, B.A. 1990. Apparent hydroxyl radical production by peroxynitrite: implications for endothelial injury from nitric oxide and superoxide. *Proc Natl Acad Sci U S A* 87:1620-1624.
187. van der Vliet, A., Eiserich, J.P., O'Neill, C.A., Halliwell, B., and Cross, C.E. 1995. Tyrosine modification by reactive nitrogen species: a closer look. *Arch Biochem Biophys* 319:341-349.
188. Liu, P., Hock, C.E., Nagele, R., and Wong, P.Y. 1997. Formation of nitric oxide, superoxide, and peroxynitrite in myocardial ischemia-reperfusion injury in rats. *Am J Physiol* 272:H2327-2336.
189. Owens, M.R., and Cimino, C.D. 1985. Biosynthesis of plasminogen by the perfused rat liver. *J Lab Clin Med* 105:368-373.
190. Creemers, E., Cleutjens, J., Smits, J., Heymans, S., Moons, L., Collen, D., Daemen, M., and Carmeliet, P. 2000. Disruption of the plasminogen gene in mice abolishes wound healing after myocardial infarction. *Am J Pathol* 156:1865-1873.
191. Reinartz, J., Schafer, B., Batrla, R., Klein, C.E., and Kramer, M.D. 1995. Plasmin abrogates alpha v beta 5-mediated adhesion of a human keratinocyte cell line (HaCaT) to vitronectin. *Exp Cell Res* 220:274-282.
192. Rossignol, P., Ho-Tin-Noe, B., Vranckx, R., Bouton, M.C., Meilhac, O., Lijnen, H.R., Guillin, M.C., Michel, J.B., and Angles-Cano, E. 2004. Protease nexin-1 inhibits plasminogen activation-induced apoptosis of adherent cells. *J Biol Chem* 279:10346-10356.
193. Gately, S., Twardowski, P., Stack, M.S., Cundiff, D.L., Grella, D., Castellino, F.J., Enghild, J., Kwaan, H.C., Lee, F., Kramer, R.A., et al. 1997. The mechanism of cancer-mediated conversion of plasminogen to the angiogenesis inhibitor angiostatin. *Proc Natl Acad Sci U S A* 94:10868-10872.
194. Strickland, D.K., Kounnas, M.Z., and Argraves, W.S. 1995. LDL receptor-related protein: a multiligand receptor for lipoprotein and proteinase catabolism. *Faseb J* 9:890-898.
195. Kisker, C., Hinrichs, W., Tovar, K., Hillen, W., and Saenger, W. 1995. The complex formed between Tet repressor and tetracycline-Mg²⁺ reveals mechanism of antibiotic resistance. *J Mol Biol* 247:260-280.

196. Khan, M.A., Muzammil, S., and Musarrat, J. 2002. Differential binding of tetracyclines with serum albumin and induced structural alterations in drug-bound protein. *Int J Biol Macromol* 30:243-249.
197. Baicu, C.F., Stroud, J.D., Livesay, V.A., Hapke, E., Holder, J., Spinale, F.G., and Zile, M.R. 2003. Changes in extracellular collagen matrix alter myocardial systolic performance. *Am J Physiol Heart Circ Physiol* 284:H122-132.
198. Griffin, M.O., Jinno, M., Miles, L.A., and Villarreal, F.J. 2005. Reduction of myocardial infarct size by doxycycline: a role for plasmin inhibition. *Mol Cell Biochem* 270:1-11.
199. Yrjanheikki, J., Tikka, T., Keinanen, R., Goldsteins, G., Chan, P.H., and Koistinaho, J. 1999. A tetracycline derivative, minocycline, reduces inflammation and protects against focal cerebral ischemia with a wide therapeutic window. *Proc Natl Acad Sci U S A* 96:13496-13500.
200. Camp, T.M., Tyagi, S.C., Aru, G.M., Hayden, M.R., and Mehta, J.L. 2004. Doxycycline ameliorates ischemic and border-zone remodeling and endothelial dysfunction after myocardial infarction in rats. *J Heart Lung Transplant* 23:729-736.
201. Gottlieb, R.A., Gruol, D.L., Zhu, J.Y., and Engler, R.L. 1996. Preconditioning rabbit cardiomyocytes: role of pH, vacuolar proton ATPase, and apoptosis. *J Clin Invest* 97:2391-2398.
202. Lew, W.Y., Lee, M., Yasuda, S., and Bayna, E. 1997. Depyrogenation of digestive enzymes reduces lipopolysaccharide tolerance in isolated cardiac myocytes. *J Mol Cell Cardiol* 29:1985-1990.
203. Canton, M., Neverova, I., Menabo, R., Van Eyk, J., and Di Lisa, F. 2004. Evidence of myofibrillar protein oxidation induced by postischemic reperfusion in isolated rat hearts. *Am J Physiol Heart Circ Physiol* 286:H870-877.
204. Baptiste, D.C., Hartwick, A.T., Jollimore, C.A., Baldrige, W.H., Seigel, G.M., and Kelly, M.E. 2004. An investigation of the neuroprotective effects of tetracycline derivatives in experimental models of retinal cell death. *Mol Pharmacol* 66:1113-1122.
205. Fischer, T.A., McNeil, P.L., Khakee, R., Finn, P., Kelly, R.A., Pfeffer, M.A., and Pfeffer, J.M. 1997. Cardiac myocyte membrane wounding in the abruptly pressure-overloaded rat heart under high wall stress. *Hypertension* 30:1041-1046.

206. Kim, S.J., Depre, C., and Vatner, S.F. 2003. Novel mechanisms mediating stunned myocardium. *Heart Fail Rev* 8:143-153.
207. Ferdinandy, P., and Schulz, R. 2003. Nitric oxide, superoxide, and peroxynitrite in myocardial ischaemia-reperfusion injury and preconditioning. *Br J Pharmacol* 138:532-543.
208. Villa, L.M., Salas, E., Darley-USmar, V.M., Radomski, M.W., and Moncada, S. 1994. Peroxynitrite induces both vasodilatation and impaired vascular relaxation in the isolated perfused rat heart. *Proc Natl Acad Sci U S A* 91:12383-12387.
209. Nossuli, T.O., Hayward, R., Scalia, R., and Lefer, A.M. 1997. Peroxynitrite reduces myocardial infarct size and preserves coronary endothelium after ischemia and reperfusion in cats. *Circulation* 96:2317-2324.